Annual Report FY 2004

平成 16 年度活動報告

Institute for Geothermal Sciences

Graduate School of Science

Kyoto University

京都大学

大学院理学研究科

附属地球熱学研究施設

Institute for Geothermal Sciences
Graduate School of Science, Kyoto University

京都大学大学院理学研究科
附属地球熱学研究施設

Beppu Geothermal Research Laboratory
Noguchibaru, Beppu, Oita 874-0903, Japan
Telephone: +81-977-22-0713
Facsimile: +81-977-22-0965

別府
〒874-0903 大分県別府市野口原
電話: 0977-22-0713
ファックス: 0977-22-0965
Homepage: http://www.vgs.kyoto-u.ac.jp

Aso Volcanological Laboratory
Minamiaso, Kumamoto 869-1404, Japan
Telephone: +81-9676-7-0022
Facsimile: +81-9676-7-2153

阿蘇（火山研究センター）
〒896-1404 熊本県阿蘇郡南阿蘇村河陽 5280
電話: 0967-67-0022
ファックス: 0967-67-2153
Homepage: http://www.aso.vgs.kyoto-u.ac.jp/

Front Cover Image:
A strombolian explosion in the 1st crater of Mt. Nakadake, Aso volcano in October 1979. (Photo by M. Sako)
表紙の写真
1979 年 10 月の阿蘇中岳第一火口のストロンボリ噴火の様子（迫幹夫撮影）

Editional compilation by J. Yamamoto
Printed in Japan by Touka Shobo

目次　Contents

序

地球熱学研究施設では、地球上で最大規模の火山・地熱温泉活動域のひとつである中部九州地域を巨大な実験装置とみなして、野外観測や室内実験などを中心に、造構運動・火山活動・地熱温泉活動など地球の熱的活動に関する総合的な地球科学の研究を推進させ、地殻の表層からマントルにいたる熱構造と熱現象に関する地球熱学の学問体系の構築を目指している。この基本理念に立脚して、平成９年に火山研究施設（阿蘇）と地球物理学研究施設(別府)が統合された。専門分野の異なる研究者が弾力的に協力できるよう、大部門制を採り、以下の 5 つの研究分野が置かれている。それらは地熱流体論研究分野、地熱テクトニクス研究分野、火山構造論研究分野、火山活動論研究分野、地球熱学情報研究分野（外国人客員）である。平成９年の改組以来早くも 8 年の歳月が経過した。平成１６年度には京都大学が法人化され、研究教育の効率化さらには定員削減を余儀なくされる状況にある。阿蘇と別府の有機的な連携を強化する努力が必要である。

法人化に伴い、経費執行について旅費枠の制約がなくなるなど自由になった面もあるが、施設運営交付金全体は減額されており、競争的資金の確保が重要になっている。他方、施設の管理や運営面では専任の教授・助教授に同数の教授会が選出する委員を加えた施設運営協議会が設置される事となった。このような中で、研究教育面での地球熱学研究施設の位置づけを明確にするとともに、主に地球惑星専攻との連携を深める必要がある。

平成１6 年度には雷害や台風被害が多発したが当局の支援を得て復旧させることが出来た。火山研究センターでは懸案であった建物模様替えが実施され、図書・資料室が１階に移動し、３階には研究室が整備された。

人事面では、4 月に井上寛之技官が阿蘇に着任し、9 月には火山活動論研究分野に鍵山恒臣教授が着任した。9 月末には外国人客員の Jianguo Du 氏が離任し、「東アジアのマントル捕獲岩とエクロジャイトに包有される流体の研究～プレートの沈み込み過程とマントル流体の進化～」をテーマに頼勇氏が別府に着任した。11月には機関研究員の北田直人氏が離任、西村光史が２１ＣＯＥに移籍し、後任として斉藤武士・杉本健両博士が別府に着任した。森健彦博士は産業総合研究所に移動した。

２１世紀ＣＯＥでは別府シンポジウムが開催された。夏期実習が開催され多くの学生や教官が阿蘇および別府を訪問した。地球物理学教室、別府、阿蘇を結ぶＴＶ会議システムが設置されセミナー等に活用されつつある。京都キャンパスとの連携の強化、遠隔地のリスク解消に役立つことを期待している。

平成 17 年 5 月
平成 16 年度地球熱学研究施設長
田中良和

Preface

We regard central Kyushu, one of the largest volcanic and geothermal fields in the world, as a natural experimental facility. The Institute for Geothermal Sciences is promoting a comprehensive research into volcanism, geothermics and tectonics mainly by fieldwork, laboratory experiments, and theory. Based on the fundamental scope of our research covers the thermal structure and the dynamics of the Earth's interior. A variety of research works can flexibly cooperate within this interdisciplinary Geothermal Science research system. We have the following five research sections, for geothermal fluids, for geothermal tectonics, for volcanic structure, for volcano-dynamics and Geothermal intelligence section (from abroad). It was passed 8 years since the last reorganization. In 2004 financial year, Kyoto University was reformed to juridical personalization of national universities. The situation puts us under pressure to do efficient education with limited staff. We must make effort to intensify the essential cooperative studies on Aso and Beppu.

Associated with the personalization, limitation of the travel budget is removed and we can go and back to Kyoto campus freely. This is a merit of the reformation, however, total revenue is decreased and it forced us to get other competitive fund. On the management, a steering committee is forced , witch composed with professors, associate professors of our laboratory and 8 other members elected by the faculty meeting. In this situation, we must make our position clear for education and research work, more over it will be important to reinforce with the earth-planet subject stuff in Kyoto. In this year, we met many disasters by lightning and typhoon, however many damaged devices were restored with financial support. In building of Aso, the library and reference room was repaired to the first floor and three private research rooms were formed 3rd floor.

In personnel affairs, Mr. Hiroyuki Inoue arrived as a technical professional at Aso in April, Dr. Tsuneomi Kagiyama arrived as professor of research section for volcano-dynamics in September. As a visiting faculty, Dr. Jianguo Du left at the end of September, and Dr. Yong LAI arrived at Beppu. As postdoctoral associate, Dr. Naoto Kitada left to a trainee of Kyoto University in November, and Dr. Koshi Nishimura transferred to 21COE, and Dr. Takeshi Saito and Dr. Takeshi Sugimoto replaced at Beppu. Dr. Takehiko Mori left to Geological Survey of Japan, AIST, at the end of March.

The 2nd KAGI21 International Symposium witch organized by the Kyoto University Active Geosphere Investigations for the 21st Century Centers of Excellence program, was held at Beppu in October 31-November 4, and new multi-disciplinary approaches for the Active Geosphere were discussed. In the end of July, observational geophysical field exercise for undergraduate was opened at Aso and Beppu. These events contributed to understand our laboratories. In the end of financial year, TV meeting systems were introduced at Aso and Beppu, and connected to Kyoto campus. We expect effective use of these devices.

Aso, May 2005

Yoshikazu Tanaka, Professor/ Director

構 成 員　Members

教授　　*Professors*

鍵山恒臣　Tsuneomi Kagiyama
（2004 年着任）
竹村恵二　Keiji Takemura
田中良和 (施設長)　Yoshikazu Tanaka (Director)

助教授　　*Associate Professors*

大倉敬宏　Takahiro Ohkura
大沢信二　Shinji Ohsawa
須藤靖明　Yasuaki Sudo
古川善紹　Yoshitsugu Furukawa

助手　　*Assistant Professors*

宇津木充　Mitsuru Utsugi
川本竜彦　Tatsuhiko Kawamoto
柴田知之　Tomoyuki Shibata
山本順司　Junji Yamamoto

外国人客員　　*Visiting Faculty*

頼　勇　Lai Yong
2004 年 10 月着任
杜　建国　Jianguo Du
2004 年 9 月退職

技術職員　　*Technical Professionals*

井上寛之　Hiroyuki Inoue
（2004 年着任）
馬渡秀夫　Hideo Mawatari
吉川　慎　Shin Yoshikawa

教務補佐員　　*Research Assistant*

芳川雅子　Masako Yoshikawa

研究機関研究員　　*Research Associates*

網田和宏　Amita Kazuhiro
井上（北田）直人　Naoto Inoue (Kitada)
2004 年 11 月転出
後藤秀作　Shusaku Goto
齋藤武士　Takeshi Saito
2004 年 12 月着任
杉本健　Takeshi Sugimoto
2005 年 1 月着任
西村光史　Koshi Nishimura
2004 年 10 月から COE 研究員
森健彦　Takehiko Mori

研修員　　**Reseach Fellow**

長谷英彰　Hideaki Hase
吉川美由紀　Miyuki Yoshikawa

研究生　　*Research Student*

中坊真　Makoto Nakaboh

COE 研究員　　*Research Assosiate (COE)*

西村光史　Koshi Nishimura
2004 年 10 月着任

大学院生　　*Graduate Student*

山田誠　Makoto Yamada

研究支援推進員　*Technical Assistant*

藤岡寿美　Hisami Fujioka
2004 年 11 月着任

事務補佐員　　*Secretaries*

今村町子　Matiko Imamura
後藤君子　Kimiko Goto
土屋寿子　Hisako Tsutiya

臨時用務員　　*Supply Janitor*

山崎咲代　Sakiyo Yamasaki

研究活動　Research Activities

機関内共同研究　Insider Colaboration

Origin of Arima-type deep thermal water from hot spring wells in Oita plain, eastern Kyushu, Japan

Amita, K., Ohsawa, S., Du, J., Yamada, M.

Chemical and isotopic compositions (concentrations of major dissolved constituents, δD and $\delta^{18}O$ of water and $\delta^{13}C$ of dissolved inorganic carbon) were determined for 11 hot and cold spring waters of Na−Cl, HCO_3 type especially which have high salinity collected from deep wells and natural springs in the Oita plain, eastern Kyushu, Japan. On $\delta^{18}O$ and δD diagram, most data points of the sampled hot and cold spring waters are plotted near local meteoric water line and this shows that these waters come from local precipitation. However, two of them with very high Cl concentration (24000mg/L and 19000 mg/L) have extremely high δD and $\delta^{18}O$ values (−22.2‰, −27.1‰ and +2.7‰, +1.9‰, respectively) and it can be classified into the "Arima-type deep thermal water". We thought that such high values in water isotope composition imply that these saline waters are originated from andesitic magmatic steam or metamorphic water. Linear relationship between reciprocal of concentration and stable carbon isotope ratio ($\delta^{13}C$) of dissolved inorganic carbon (DIC) of the sampled waters shows that DIC in the hot and cold spring waters laid under the Oita plain is the mixture of soil CO_2 and magmatic or mantle-derived CO_2. Concentration and $\delta^{13}C$ of DIC in the foregoing heavy waters are 24000mg/L, 19000mg/L and −3.8‰, −3.2‰, respectively and these accord with the deep-originated end-member of the mixing relation as shown before. Therefore, it is appropriate that the Arima-type deep thermal water found in the Oita plain this time is derived from the Earth's interior. Furthermore, formation of this deep-originated thermal water should have no relation to magma generation, because the Oita plain is located in fore-arc region. Linear relationships between δD versus Li concentration and δD vs. B concentration of the sampled hot and cold spring waters also show that these waters are a mixture of two end-members: one is subsurface water of meteoric origin having low δD and low Li and B concentrations and the other is deep-originated thermal water having high δD and high Li and B concentrations.

The latter would be the fluid devolatilized from the subducting oceanic plate. In addition, good liner relations between Li and Cl concentration and B and Cl concentrations of the sampled hot and cold spring waters suggest that Cl as major constituent of these waters of Na−Cl, HCO_3 type in the Oita plain is also derived from the devolatilized fluid of the slab.

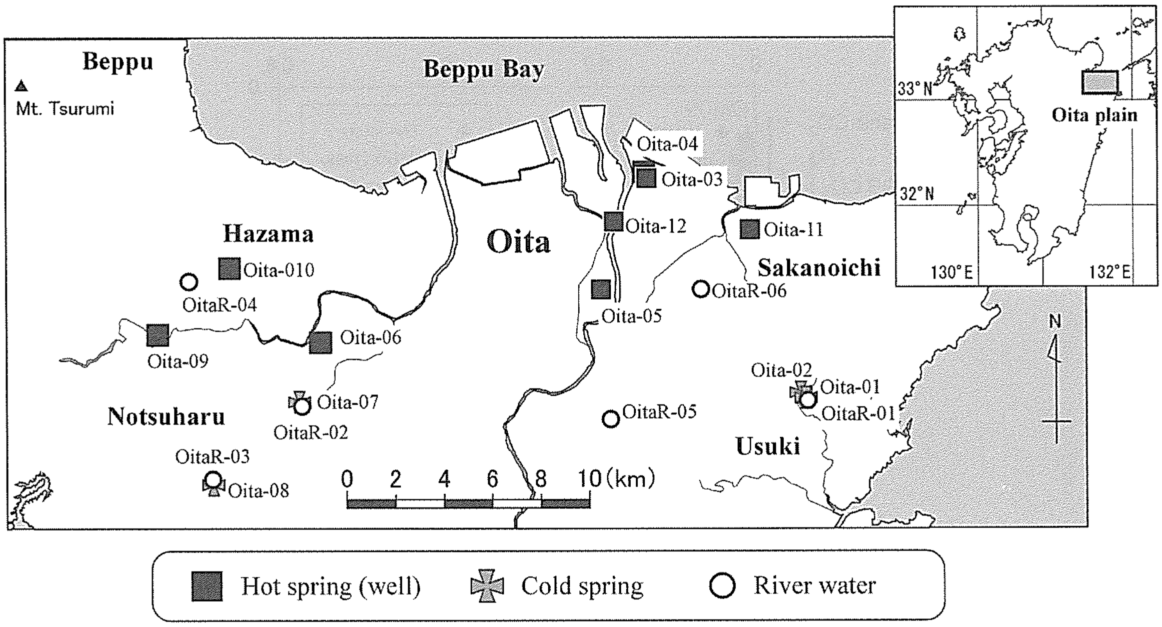

Fig. 1. Map of sample locations in the Oita plain. Solid squares, gray hatched crosses and open circles show sampling points at hot spring (well), cold spring and river, respectively.

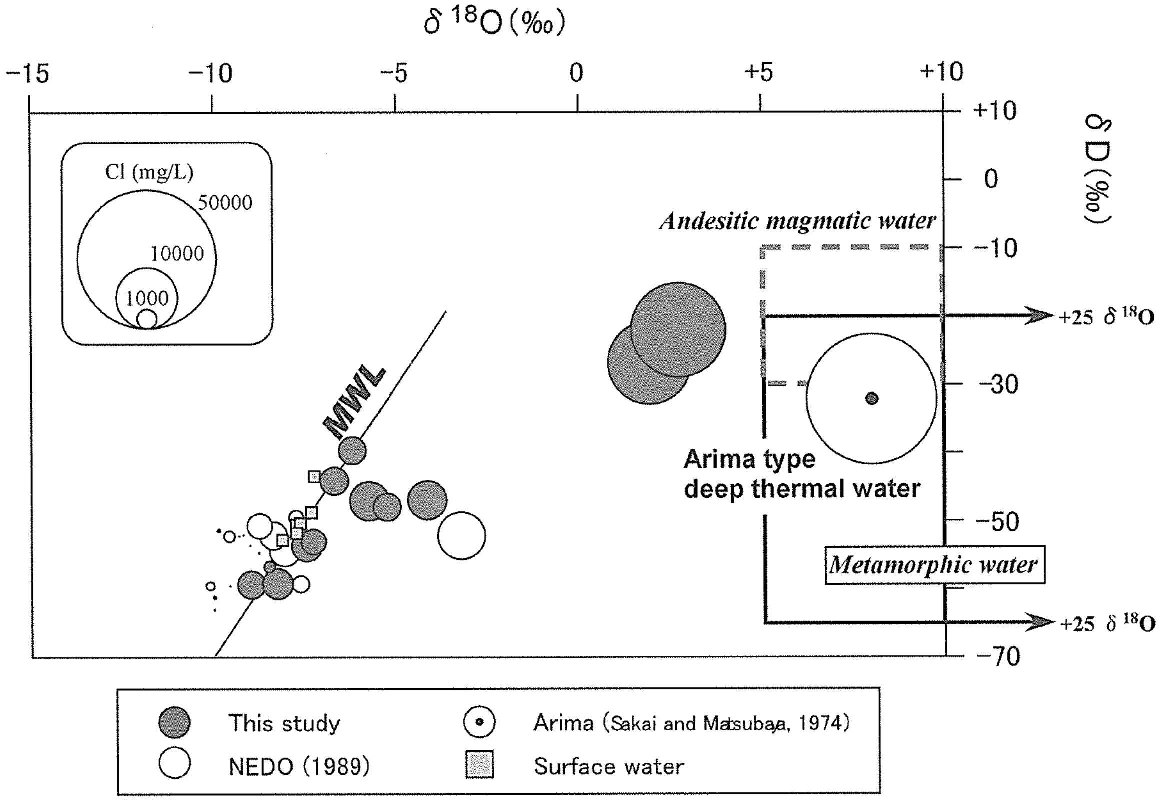

Fig. 2. δD− δ^{18}O plots of water samples from hot and cold springs (solid circles) and from rivers (gray squares) collected in this study. Open circles show hot spring water samples collected and measured by NEDO (1989). Open circle with dot in center indicates the Arima-type deep thermal water (Sakai and Matsubatya, 1974). Dashed line box shows the range of δD and δ^{18}O values of andesitic magmatic steam (Giggenbach, 1992). Bold line box shows the range of δ-values of "metamorphic water" (Sasaki, 1977). Solid straight line labeled with MWL expresses meteoric water line： $\delta D = 8 \times \delta^{18}O + 10$.

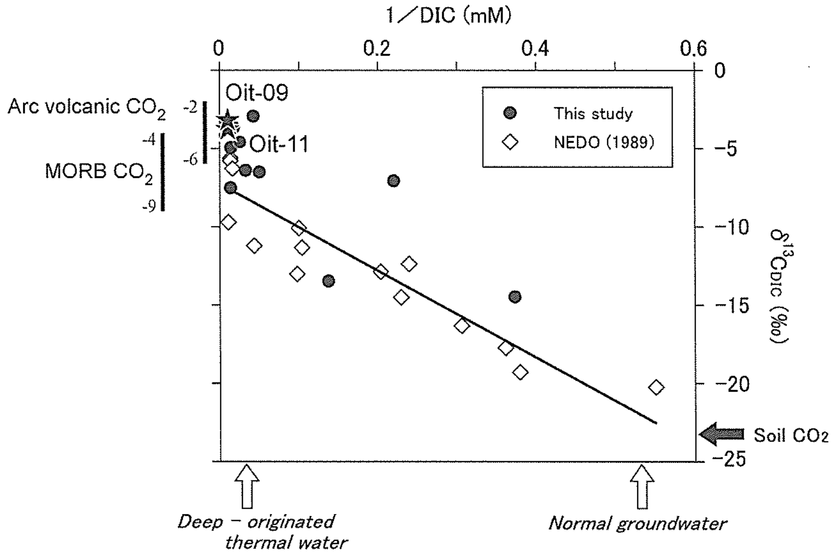

Fig. 3. Diagram of $\delta^{13}C$ versus reciprocal of concentration of dissolved inorganic carbon (DIC). Solid circles show the data of this study and open diamonds are cited from Ohsawa (2001). Two asterisks show saline waters found in the Oita plain, which are classified into the "Arima-type deep thermal water". Solid straight line is the regression line calculated using data obtained by NEDO (1989) and Ohsawa (2001) and represents the mixing relation between deep-originated CO_2 (magmatic or mantle origins) and soil CO_2.

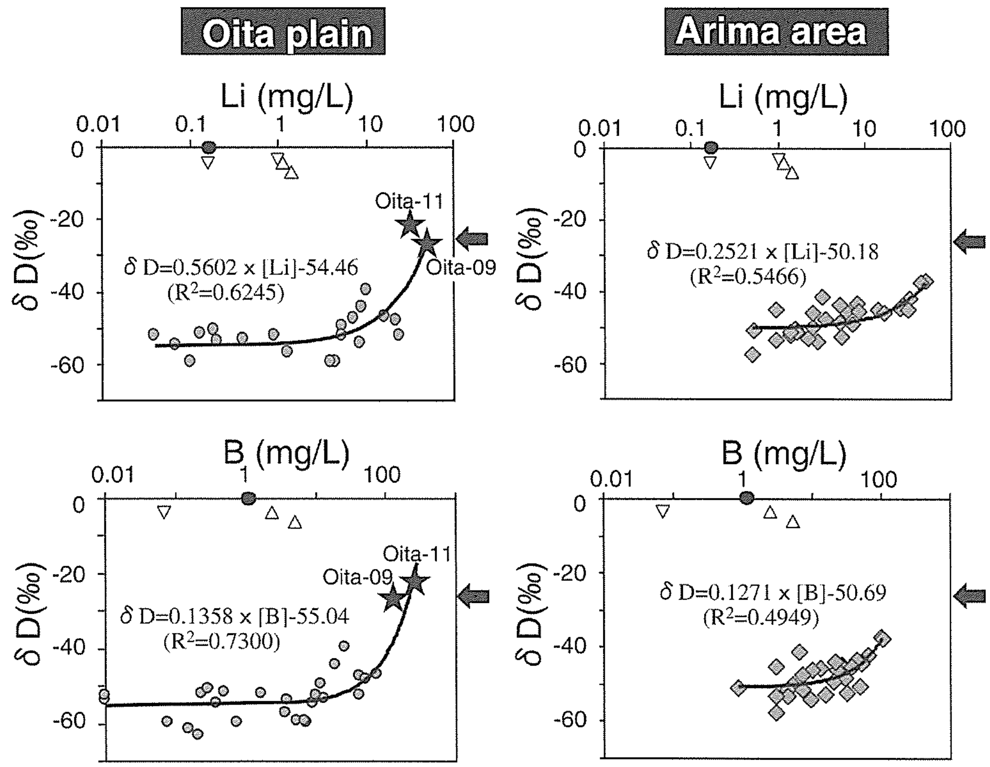

Fig.4. Plots of δD versus Li concentration and δD versus B concentration of the hot and cold spring waters collected from the Oita plain (left side) and Arima area (right side). Solid lines are regression lines. Solid circle show present sea water and open triangles show brines accompanied by natural gas from Miyazaki and Chiba areas. Asterisks are saline waters found in the Oita plain in this study. Thick allow indicates the estimated δD value of devolatilized fluid from subducting oceanic plate (Kazahaya, 1997).

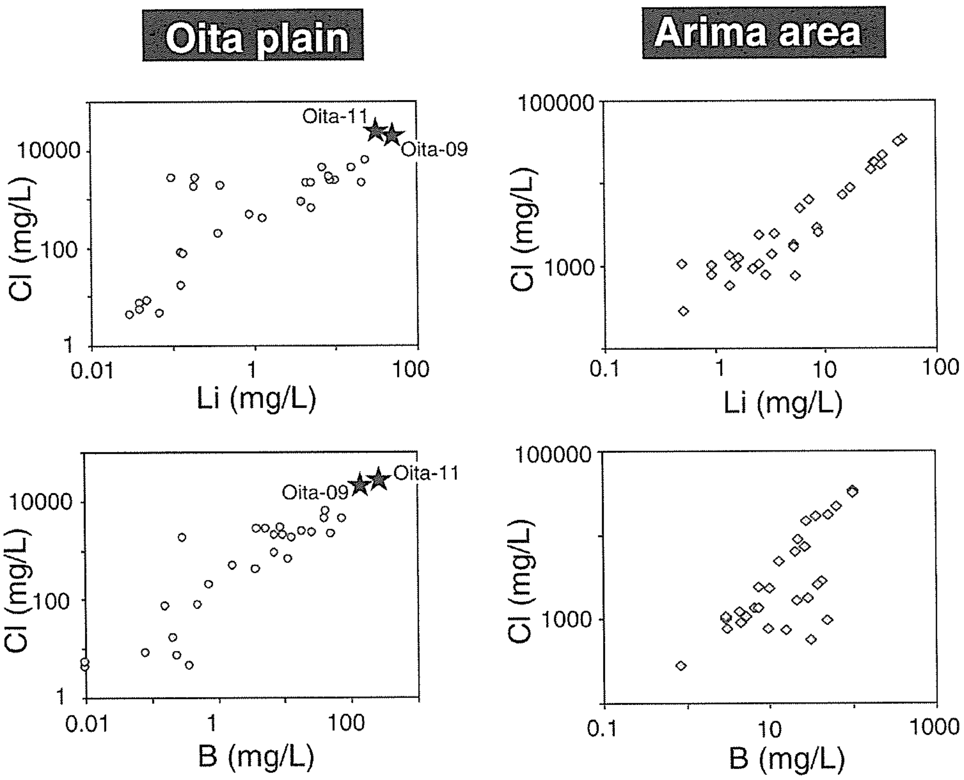

Fig.5. Plots of Li versus Cl concentrations and B versus Cl concentrations of the hot and cold spring waters collected from the Oita plain (left side) and Arima area (right side). Asterisks stand for saline waters found in the Oita plain in this study.

Table 1. Concentrations of major constituents and trace elements (Li and B) of water samples collected from wells (hot springs), cold springs and rivers in the Oita plain.

No.	Sampling date	Type	Depth of well	Temp.	pH	Na	NH_4	K	Mg	Ca	Cl	NO_3	SO_4	Li	B
			(m)	(℃)		(mg/L)									
Oita-01	Nov. 26, 2003	spring	-	16.5	5.9	1534	62.0	76.7	153	91.5	2286	n.d.	n.d.	10.4	26.8
Oita-02	Nov. 26, 2003	spring	-	15.3	6.1	1878	56.8	82.2	195	175.4	2360	n.d.	n.d.	9.0	18.6
Oita-03	Nov. 28, 2003	well	800	46.9	8.2	1711	38.5	133	14.1	37.0	2634	n.d.	2.0	0.2	3.9
Oita-04	Nov. 28, 2003	well		47.3	8.3	1509	32.8	116	8.4	9.8	1807	n.d.	n.d.	0.4	13.2
Oita-05	Nov. 28, 2003	well	800	32.7	8.0	897	38.4	69.6	528	88.9	392	n.d.	n.d.	1.3	3.8
Oita-06	Nov. 28, 2003	well	710	34.0	8.1	1649	41.2	125	84.9	44.0	2018	n.d.	n.d.	4.5	7.2
Oita-07	Dec. 2, 2003	spring	-	16.4	6.3	3255	55.8	72.3	742	125.3	4243	n.d.	n.d.	7.2	41.2
Oita-08	Dec. 2, 2003	spring	-	14.8	6.5	3721	86.0	215	195	138.4	4356	n.d.	n.d.	16.5	75.1
Oita-09	Dec. 2, 2003	well	575	34.8	6.7	12213	287	678	784	347.5	18649	n.d.	n.d.	51.8	145
Oita-10	Dec. 2, 2003	well	800	48.1	6.6	3702	90.3	244	125	77.6	2135	n.d.	n.d.	21.7	50.9
Oita-11	Dec. 3, 2003	well	900	36.1	6.7	15813	383	231	1042	282.0	23878	n.d.	n.d.	33.5	278
Oita-12	Dec. 3, 2003	well	800	48.4	8.0	1575	49.1	15.0	35.2	52.8	2675	n.d.	n.d.	0.1	5.4
OitaR-01	Nov. 26, 2003	river	-	13.7	7.5	19.0	n.d.	1.3	11.3	5.0	20.4	2.7	8.0	0.1	n.d.
OitaR-02	Dec. 2, 2003	river	-	12.4	7.4	6.4	n.d.	0.5	5.5	4.6	3.9	3.6	6.7	n.d	n.d
OitaR-03	Dec. 2, 2003	river	-	11.6	7.4	8.5	0.1	1.7	7.4	2.9	6.0	3.3	5.5	n.d.	n.d.
OitaR-04	Dec. 2, 2003	river	-	11.6	7.6	12.1	n.d.	2.4	9.8	4.9	5.6	2.5	11.9	n.d.	n.d.
OitaR-05	Dec. 3, 2003	river	-	12.6	7.9	6.2	n.d.	0.7	11.6	8.4	4.9	3.7	14.6	n.d.	n.d.
OitaR-06	Dec. 3, 2003	river	-	12.4	7.4	6.7	n.d.	0.5	9.2	4.3	5.7	2.9	9.8	n.d.	9.8

[Rem] n.d. : not detected

Table 2. δD, $\delta^{18}O$ and $\delta^{13}C$ values and DIC concentration of the water samples in the Oita plain.

No.	Type	δD_{H2O}	$\delta^{18}O_{H2O}$	$\delta^{13}C_{DIC}$	DIC
			(‰)		(mg/l)
Oita-01	spring	-39.8	-6.2	-4.6	1670
Oita-02	spring	-44.3	-6.7	-2.9	1040
Oita-03	well	-53.9	-7.5	-14.5	118
Oita-04	well	-53.3	-7.3	-13.5	320
Oita-05	well	-57.0	-8.5	-3.7	2340
Oita-06	well	-59.7	-9.0	-6.5	882
Oita-07	spring	-47.5	-5.8	-7.5	3020
Oita-08	spring	-47.1	-4.2	-5.0	2880
Oita-09	well	-27.1	+1.9	-3.2	3780
Oita-10	well	-48.3	-5.3	-6.4	1310
Oita-11	well	-22.2	+2.7	-3.8	4320
Oita-12	well	-59.4	-8.3	-7.1	200
Oita R-01	river	-48.8	-7.4	n.a.	n.a.
Oita R-02	river	-50.6	-7.8	n.a.	n.a.
Oita R-03	river	-51.8	-7.8	n.a.	n.a.
Oita R-04	river	-53.0	-8.2	n.a.	n.a.
Oita R-05	river	-50.4	-7.7	n.a.	n.a.
Oita R-06	river	-43.5	-7.3	n.a.	n.a.

[Rem] n.a. : not analyzed

Evaluation of Laser Ablation system of LA-ICP-MS in IGS

Y. Lai, **J. Yamamoto**, **T. Shibata**, and **M. Yoshikawa**

Laser ablation coupled with an inductively coupled plasma mass spectrometer is a powerful tool for the rapid and precise *in situ* of trace elemental analysis. It has been applied to determination of trace element zonation in silicate and carbonate minerals. Natural and experimental crystal-melt partition coefficients, whole rock analyses using pressed pellets and fussed glasses, determination of Pb isotopic ages of zircons, and analysis of fluid inclusions(Jackson et al. 1992, Fedorowich et al. 1993, Feng, 1994, Hirata & Nesbitt, 1995, Norman et al. 1996).

Operation conditions of LSX200 Laser ablation system (UV 266nm Nd-YAG-Laser with Q-switch mode) were studied for coinciding with ICP-MS in BGRL (Beppu Geothermal Research Laboratory). The laser is capable of operating continuously as pulse rates of 1-20 Hz with beam energy in the range of 0.1-4 mJ per pulse. The effects of pulse rate, energy level and ablation time have been evaluated by comparing time resolved signal intensities. XRF glass bead and obsidianite glass chip were used as the test samples. Because the signal produced by laser ablation is transient, raster method was used for tuning.

Both Ar and He were compared their effects as a carry gases. It is similar to results of published (Cabri et al., 2003, Ishida et al., 2004), there is few powdery material deposited around the crater under the He gas circumstance. He gas is a better carrier than Ar gas.

Crater depths were measured for understanding the effect of laser energy level and pulses. Different laser shots were selected for versus 10, 15 and 20 energy levels. Crater shapes were observed under a microscopy after cutting vertically through the crater center. The results show that depths of the crater mainly depend on the laser energy level. There is a good liner relationship between laser pulse and depth under 100 shots above 15 energy level (Fig 1). The laser can't dig a hole over 100 μm at a low energy level (e.g. lower than 10 levels) no matter how many shots (Fig 2). The craters are cone-shaped, and the deeper, the sharper. That means that only a few materials can fly out after 500 shots at any energy levels. So, for general solid geological sample (crater depth is between 100-200μm), laser energy level should be over 10 and shot be lower than 500. On the other hand, for melting inclusion sample, it is better to choose a condition of over 10 energy level and lower than 100 shots. The best spot size is between 50-200μm.

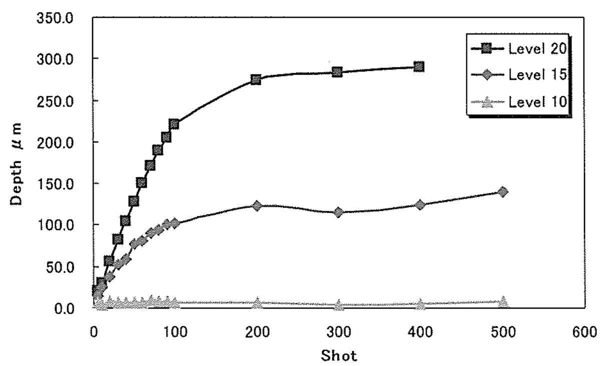

Fig 1 Shot vs. crater depth in different energy levels

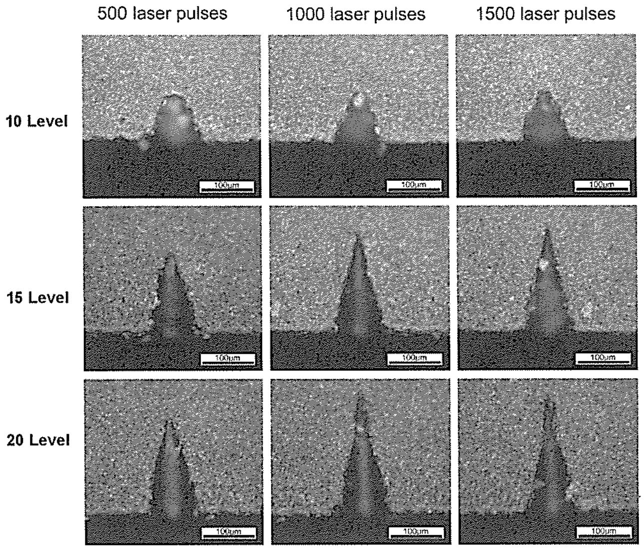

Fig 2 Cross sections of the craters made by the different laser shots

Conclusions

- He gas is a better carrier gas than argon gas during the process of laser ablation;
- The depth of hole mainly depend on the laser energy level;
- There is a good liner relationship between laser pulse and depth under 100 shots above 15 energy level;
- The best conditions for solid material analysis are 50-200μm diameter, 15-20 energy level and 5-500 shots (melting inclusion 5-100).

References

Cabri, L. J., Sylvester, P. J., Tubrett, M. N., Peregoedova, A. and Laflamme, J. H. G. (2003), Comparison of LAM-ICP-MS and micro-pixe results for palladium and rhodium in selected samples of Noril'sk and Talnakh sulfides, The Canadian Mineralogist, 41:321-329

Fedorowich, J.S., Richards, J. P., Jain, J. C. Kerrich, R. and Fan, J. (1993), A rapid method for REE and trace element analysis using laser sampling ICP-MS on direct fudsion whole-rock glasses, Chemical Geology, 106: 229-249

Feng, R. (1994), In situ trace element determination of carbonates by Laser Probe inductively coupled plasama mass spectrometry using nonmatrix matched standardization, Geochimica et Cosmochimica Acta, 58: 1615-1623

Hirata, T. and Nesbitt, R. W. (1995), U-Pb isotope geochronology of zircon: evaluation of the laser probe-inductively coupled plasma mass specyrometry technique, Geochimica et Cosmochimica Acta, 59: 2491-2500

Ishida, Y., Morishita, T., Arai, S. and Shirasaka, M. (2004), Simultaneous in-situ multi-element analysis of minerals on thin section using LA-ICP-MS, Sci. Rep. Kanazawa Univ., 48: 31-42

Jackson, S. E., Longerich, H. P., Duning, G, R. and Fryer, B. J. (1992), The application of laser-ablation microprobe-inductively coupled plasma-mass spectrometry (LAM-ICP-MS) to in situ trace element determination in minerals, Canadian Mineralogist, 30: 1049-1064

Norman, M. D. Pearson, N. J., Sharma, A. and Griffin, W. L. (1996), Quantitative analysis of trace elements in geological materials by laser ablation ICPMS: instrumental operating conditions and calibration values of NIST glasses, Geostandards Newsletter, 20: 247-261

Seismic activity in the northeastern part of Kyushu, Japan

T. Ohkura, K. Takemura, H. Mawatari and Y. Furukawa

In the northern part of Kyushu, there is a regional graben-like structure called the Beppu-Shimabara rift zone. In this zone, active volcanoes such as Tsurumi, Yufu, Kuju, Aso and Unzen are distributed almost perpendicular to the strike of the volcanic front. We have been investigating seismic activity in the eastern part of the rift zone.

In Fig.1, epicenter distribution from Jan. 2001 through Mar. 2005 is shown with E-W and N-S cross-sections. We can recognize that many small and shallow events are located in the Beppu graben where E-W striking normal faults are dominated. Another area with a high seismicity is located to the northwest of Mt. Kuju, which corresponds to high geothermal activity in this area.

Earthquakes deeper than 30km in this area are considered to be caused by subduction of the Philippine Sea plate and to have implications for the magma genesis of the area. Although we can delineate the Wadati-Benioff zone beneath Mt. Tsurumi located on the volcanic front, no deep event occurs beneath Mt. Kuju that is located to the west of the volcanic front. Also some tomography studies showed that the slab could not be imaged beneath active volcanoes in the back arc region such as Mt. Unzen and Mt. Aso. Any simple subduction volcanism cannot account for this feature. We should consider not only vertical but also lateral movement of magmatic fluid to explain the existence of such volcanoes. Therefore, in order to reveal magma system of this area, other studies such as precise seismic tomography or waveform analysis are necessary to obtain velocity and attenuation structure in the mantle wedge.

Acknowledgments

Hypocenter data was provided by Japan Meteorological Agency.

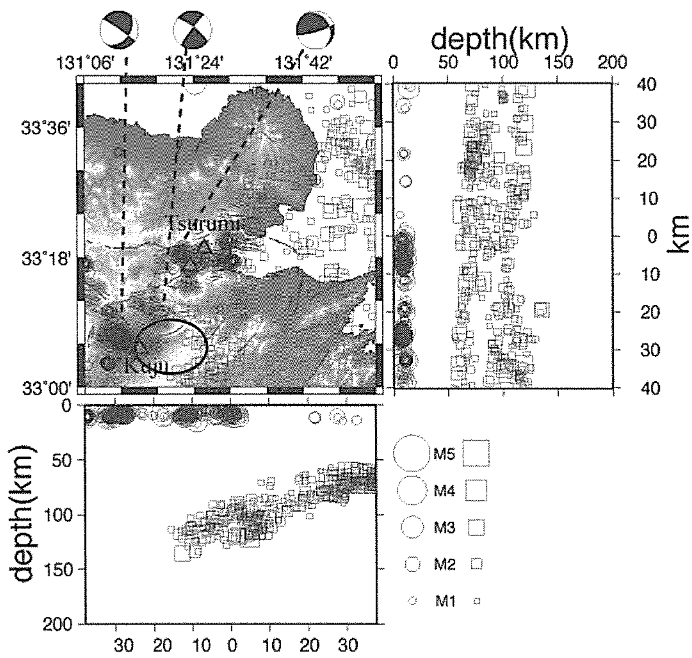

Fig.1 Epicenter distribution in the northeastern part of Kyushu from Jan. 2001 to Mar. 2005 with E-W and N-S cross-sections based on JMA hypocenters. Hypocenters with a depth of less than or equal to 30km are plotted with circles, and squares show the hypocenters with a depth of more than 30km. The oval represents the location of the Beppu graben. The solid lines and the triangles indicate the active faults and the active volcanoes, respectively. Focal mechanism solutions, projected onto the lower hemisphere, of the major events are also shown.

Trace element and Sr, Nd and Pb Isotopic compositions of Quaternary volcanics from Hime-Shima volcanic group

Tomoyuki Shibata, Jun'ichi Itho, **Keiji Takemura**

Hime-Shima is located in about 4 km north offshore of Kunisaki peninsula, Kyushu, Japan. Northeastern extend of Hime-Shima, adakite derived from slab melt heave been found from some volcanoes (e.g. Daisen; Morris, 1986). On the other hand, the obvious along arc variations of chemical compositions (e.g. Zr/Nd ratios; Shibata, 2004) are observed in the southern extend. In these areas, the Philippine Sea plate is subducting and the boundary of seismic (southern part) and aseismic zone (northeastern part) exist below Hime-Shima (Shibutani, 2002). Thus, the magma genesis of Hime-Shima volcanic group is important to understanding the relationship between the mechanisms of material transfer form subducting slab and geophysical characteristics of the slab. Therefore, we analyzed trace elements and Sr, Nd and Pb isotopic compositions of Hime-Shima volcanic rocks

It is observed that Nb/;Zr ratios (0.06 – 0.6) are high compared to general island arc magma (≈0.03). The similar results were reported by Itho (1990). In the Y – Sr/Y diagram, the Hime-Shima volcanic rocks are plotted in the field of adakite, which are considered to be generated by partial melt of subducting oceanic crust. The Pb isotope systematics show liner trends, which indicate mixing relations. Sr, Pb and Nd isotope ratios of the rocks with high Sr/Y ratios are enriched character compared to those with relatively low Sr/Y ratios. These chemical characteristics cannot be explained by the general model that the origin of island arc magma is MORB-type mantle wedge and fluid derived from subducting slab. On the other hand, contribution of the mantle plume is emphasized on the bases of the temporal and regional chemical variations of volcanics from middle Kyushu (Nakada and Kamata, 1991). However, the trends of Pb isotope systematics indicate that the enriched mantle source cannot be a source material of Hime-Shima volcanic rocks. The relationship between isotopic compositions and St/Y ratios is consistent that partial melt of subducting Philippine Sea plate is one of the source material of Hime-Shima volcanic rocks. This observation may suggest the aseismic subduction is one of the important factors to generate the slab melt in subduction zone.

Late Quaternary tephrochronology in eastern part of central Kyushu recorded in the soil-loam sequence

Takemura, K., Yamamoto, J. and **Mawatari, H.**

Tephrochronology is a valuable tool in many areas in earth sciences. In particular, distinctive and widespread tephra layers have much stratigraphic value, for they represent time-parallel markers that permit reliable correlations over long distances. In subaerial and marine sequences it is difficult to verify the original stratigraphic position of thin superimposed or disseminated tephra because of syn- and post-depositional reworking and mixing processes. To establish tephrochronology in the area, it is the first step to summarize the stratigraphical relationship among the tephra layers observed at different outcrops.

Around the Beppu region, thick soil and loam sequences were found including the tephra layers. We summarize the tephrostratigraphy of the soil and loam sequences since Late Pleistocene time. Most clear outcrop indicating the tephrostratigraphy of this area is located at the south of Mt.Yufudake (Photo 1).

Tephra layers found mainly in this region is as follows in descending order.

1. Yufu dake volcanic ash layer (Yf-1) erupted from Yufu dake volcano at 2.2ka.
2. Kikai-Akahoya volcanic ash layer (K-Ah) is found at about 30cm within the black soil (called "Kuroboku") . This ash is the product from Kikai Caldera located to south of Kyushu Island at about 7.3 ka eruption (.Photo 2), and is composed of bubble wall type glasses with brown colored glasses.
3. AT volcanic ash layer is intercalated with yellowish loam sediments just above the second dark grey soil horizon. This ash is composed of bubble wall glassed, and eruption age is about 26-29 ka. Source caldera is Aira Caldera including the present Sakurajima Volcano in south Kyushu.
4. Kuju Daiichi tephra layer (Kj-P1) is found in the yellowish brown loam sequences, and is composed of light grey volcanic sand (lower) and pumiceous volcanic ash (upper). This ash erupted from Kuju volcano at about 50 ka.
5. Aso-4 pyroclastic flow deposit is found at the basal horizon of soil sequence and erupted from Aso Caldera region at about 85-90 ka. This tephra has reddish brown color, and is composed coarse pumiceous ashes.

For constructing more precise tephrochronology with small eruptions, it is useful to analyze using microtephra analysis of continuous measurement of sequences.

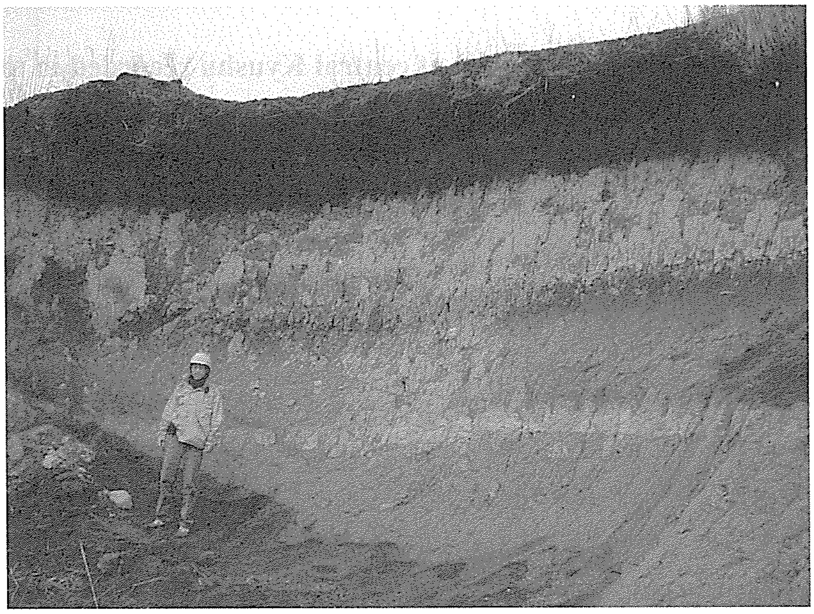

Photo 1 Soil-loam sequences at the south of Yufu-dake

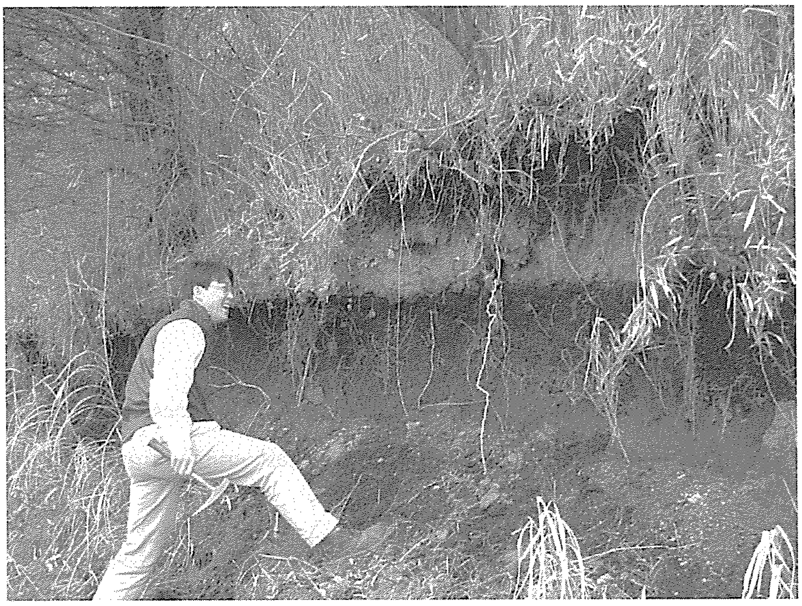

Photo 2 Kikai-Akahoya volcanic ash layer at Amama, Beppu City

Noble gas isotope constraints on the origin of Oninomi basalt: implications for subduction-related components in arc magma

Yamamoto J. and **Takemura K.**

Abstract

We have determined the elemental and isotopic compositions of noble gases in phenocrystic olivine from the Oninomi basalt, Yufuin, Japan. The $^{3}He/^{4}He$ of gas extracted by crushing olivine from the Oninomi basalt (6.7 +/- 0.9 R_A: R_A is $^{3}He/^{4}He$ of air) is slightly lower than that of MORB (8 +/- 1 R_A). It indicates that the magma was derived from the MORB-like source with slight influence of radiogenic ^{4}He such as crustal materials.

Argon isotopic ratio ($^{40}Ar/^{36}Ar$) is high (538) compared to that of air (295.5) but far lower than the values of MORB(up to 40000). It requires that the mantle source of the Oninomi basalt mixed with materials with lower $^{40}Ar/^{36}Ar$, such as materials containing atmospheric argon. Given that the helium in the sample is a mixture of two nonatmospheric components derived from MORB-like and crustal materials. It is therefore reasonable to argue that the nonatmospheric Ar in the sample is a mixture of mantle and crustal materials rich in radiogenic ^{40}Ar. Thus, the Ar in the Oninomi basalt can be accounted for by mixing of a dominant atmosphere-like component with MORB-like and crustal materials.

The crustal materials have two possible sources for the island arc basaltic magma: arc crust above the mantle wedge and subducted slab. If the arc crust has a significant influence on the magma source, the Oninomi basalt should have the production ratios of $^{4}He/^{40}Ar^{*}$ and $^{4}He/^{21}Ne^{*}$. The Oninomi basalt shows $^{4}He/^{40}Ar^{*}$ of 0.1 which is one or two orders of magnitude lower than the $^{4}He/^{40}Ar$ production ratio. The $^{4}He/^{21}Ne^{*}$ of the Oninomi basalt is also two orders of magnitude lower than the $^{4}He/^{21}Ne$ production ratio. The arc crust is not likely for the source of the crustal argon contribution to the Oninomi basalt. The low $^{4}He/^{40}Ar^{*}$ and $^{4}He/^{21}Ne^{*}$ are typical of the samples from island arc and active continental margin. These data may result from the kinetic fractionation between He and heavier noble gases in the subduction processes.

The Oninomi basalt would therefore be derived from MORB-like source that has been infiltrated by slab-derived fluids fractionated via subduction processes.

Introduction

In recent decades, the isotopic compositions of samples from the Earth's interior have been used as important tracers in the Earth's evolution. In particular, noble gas isotopic compositions of Ocean Island Basalts (OIB) and Mid-Oceanic Ridge Basalts (MORB) have provided important constraints on the evolution of the Earth and the atmosphere. The source of MORB has generally been regarded to be derived from the suboceanic mantle, and to be located in the upper-mantle. The $^{3}He/^{4}He$ in MORB shows quite uniform values of (8 +/- 1) R_A. MORB-like $^{3}He/^{4}He$ have often been observed in mantle-derived rocks from island arcs and subcontinental mantle (e.g., Yamamoto et al., 2004). There is a widespread consensus that the source of MORB is a ubiquitous component of the upper-mantle. Recently, however, occurrences of $^{3}He/^{4}He$ lower than that of MORB have been reported for some mantle wedge-derived magma (e.g., Patterson et al., 1994). The fundamental question is whether these variations in magmatic $^{3}He/^{4}He$ trace involvement of subducted slab in the generation of arc magmas, or alternatively, provide a record of interaction of ascending magma with arc crust. Helium has been the focus on noble gas studies of arc-related samples in part because contamination by atmospheric helium generally is insignificant, owing to very low abundance of helium in the atmosphere. In contrast, the heavier noble gases (Ne, Ar, Kr and Xe) in mantle wedge-derived magma and mantle xenoliths appear to be almost entirely atmospheric in origin. It should be, however, emphasized that most previous studies of subduction-related volcanic arcs have been almost restricted to the analysis of arc-related fluid samples such as water, steam and gas collected from volcanic fumaroles, hot springs and geothermal wells. In an attempt to circumvent the problem of addition of atmosphere-derived heavier noble gases to fluid samples, we have measured the elemental and isotopic composition of all five noble gases trapped in olivine phenocrysts sampled from a basalt erupted just on the current volcanic front. On the basis of these data and the present understanding of the origin and evolution of arc-magmas, we present a generalized qualitative model for the movement of noble gases through subduction zone.

We have another unsolved problem whether the magma originated from a hotspot or not. To reveal this problem, noble gas isotopes would work effectively.

Samples

Samples analyzed in this study are collected from a lava cliff in the Oninomi basalt, which is a well-preserved monogenetic volcano erupted at the Yufu-Tsurumi Graben in central Kyushu. The Oninomi volcano has very young eruption age of around 10 ka, which is found between the volcanic ashes, Kikai-Akahoya ash and Aira Tn ash, with the age of 6.5 ka and 25 ka, respectively. Though the Oninomi volcano is previously reported to be a non-arc type volcanism (Ohta et al., 1992), it should be intimately related to subduction. This is because it locates just on present volcanic front. Further, typical arc type volcanoes (Mt. Yufu and Tsurumi) contemporaneously erupted in the same area.

The Oninomi basalt contains abundant phenocrysts of olivine, clinopyroxene and plagioclase. Rarely, orthopyroxene is present as microphenocrysts. Plagioclase has large grain size of more than 1 mm in diameter and characteristically shows sector and oscillatory zoning, indicating several stages of crystallization. Olivine and pyroxene are euhedral and not zoned. Average size of olivine and clinopyroxene is about 0.5 mm in diameter. The olivine includes abundant melt inclusions.

Experimental method

Noble gases were extracted from fresh olivine by vacuum crushing. Olivine is relatively retentive for helium (Kurz, 1986; Trull et al., 1991), and *in-situ* addition of radiogenic ^{4}He is quite small due to very low contents of U and Th in olivine. Further, the crushing method is thought to be effective in extracting noble gases trapped in fluid inclusion, which contains little *in-situ* generated nuclides. Recently there have been, however, reports of cosmogenic nuclides release by this method (e.g., Yokochi et al., 2005). We consider that such an effect would have a negligible influence on results reported here because the present sample was collected from a cliff, where cliff failure occurred within 100 years inferred from a growth of surrounding trees.

Before vacuum crushing of olivine grains, a crushing vessel was preheated at 150°C overnight. During crushing, the crushed sample together with the vessel was heated at 120°C. Gases extracted were exposed to a cold trap at liquid N_2 temperature in order to remove gases adsorbed on newly created powder surfaces. Noble gas analyses were performed on a sector-type mass spectrometer (VG-5400) installed at the Earthquake Research Institute (ERI), University of Tokyo. Procedural crushing blanks for ^{3}He, ^{4}He, ^{20}Ne, ^{36}Ar, ^{84}Kr and ^{132}Xe were less than 3.0×10^{-15}, 2.0×10^{-11}, 2×10^{-12}, 1×10^{-12}, 2×10^{-14} and 4×10^{-15} cm^3STP, respectively. Analytical conditions for noble gases at the ERI have been reported by Hanyu et al. (1999).

Results

Noble gas isotope results are summarized in Table 1. The present sample shows relatively high helium isotopic ratio of 6.74 +/- 0.85 R_A, which is slightly lower than MORB value (8 +/- 1 R_A).

The present sample shows a slightly high $^{21}Ne/^{22}Ne$ (0.034 +/- 0.004) in comparison with that of atmosphere (0.029). It may be due to nucleogenic ^{21}Ne generated from (α, n) reaction on ^{18}O and (n, α) reaction on ^{24}Mg. Since the crushing minimizes contributions from noble gases in the mineral, excess ^{21}Ne would exist in fluid inclusions as nucleogenic ^{21}Ne.

Argon isotopic ratio ($^{40}Ar/^{36}Ar$) is high (538) compared to that of air (295.5) but far lower than the values of MORB (often up to 10000 and sometimes as high as 40000: Burnard et al., 1997). The $^{4}He/^{40}Ar^{*}$ is much lower (~0.1) than that of MORB (2 - 3), where $^{40}Ar^{*}$ indicates ^{40}Ar corrected for air-addition.

Krypton and xenon isotopic ratios are indistinguishable from the atmospheric values within the experimental uncertainty of 1 sigma level.

Table 1. Noble gas isotopic compositions of olivine phenocrysts in the Oninomi Basalt

weight (g)	^{3}He (10^{-14})	^{4}He (10^{-9})	^{20}Ne (10^{-11})	^{36}Ar (10^{-11})	^{40}Ar (10^{-8})	^{84}Kr (10^{-12})	^{132}Xe (10^{-14})
1.088	1.72 ± 0.25	1.74 ± 0.16	2.16 ± 0.22	7.37 ± 0.44	3.97 ± 0.23	1.94 ± 0.19	6.34 ± 0.43
	$^{3}He/^{4}He$ (R/R_A)	$^{20}Ne/^{22}Ne$	$^{21}Ne/^{22}Ne$	$^{40}Ar/^{36}Ar$	$^{38}Ar/^{36}Ar$	$^{4}He/^{40}Ar^{*}$	$^{4}He/^{21}Ne^{*}$ (10^{5})
	6.74 ± 0.85	9.96 ± 0.35	0.0340 ± 0.0037	538.0 ± 2.1	0.1883 ± 0.0010	0.097 ± 0.010	1.6 ± 1.2

N.B., Unit for abundance is cm^3STP/g. All tabulated data were corrected for blanks.

Discussion

This study shows that gas extracted by crushing olivine in the Oninomi basalt displays $^{3}He/^{4}He$ (6.7 +/- 0.9) lower than that of MORB (8 R_A). Post-eruptive addition of radiogenic ^{4}He appears unlikely given the low $^{3}He/^{4}He$ in the olivine of modern lava. The lower $^{3}He/^{4}He$ compared to that of MORB does not result from pre-eruptive accumulation of radiogenic ^{4}He in the olivine in magma chamber. This is because the accumulation time appears too long (> 1 myr) compared to the refilling interval of the magma chamber (~100 kyr). The influence of cosmogenic ^{3}He is negligible for the olivine, since the sample was collected from a lava cliff. Further, the crushing method is thought to be effective in extracting noble gases trapped in liquid inclusions or shrinkage bubbles in melt inclusions, which contain little *in-situ* generated nuclides (e.g. Kurz et al., 1983). Thus, the low $^{3}He/^{4}He$ does not result from addition of secondary generated nuclides in the olivine.

One of the most important points regarding the origin of the Oninomi basalt is whether the magma originated from an OIB-like hotspot or not. Basalts of mid-ocean ridge (MORB) and ocean island (OIB) are generally regarded to be derived from the depleted and primordial mantle, respectively. Secondary generated nuclides are expected to give more influence on the MORB-source mantle than the OIB-source. Hence, $^{3}He/^{4}He$ of the MORB (8 R_A) is generally lower than that of the OIB (up to 50 R_A: Stuart et al., 2003), because addition of radiogenic ^{4}He generated in their mantle sources works more effectively to the MORB source due to the lower abundance of He in the MORB source than the OIB source. Helium isotopic ratio of the present sample indicates that the magma was derived from the similar source to that of MORB rather than that of OIB.

The $^{3}He/^{4}He$ in MORB shows quite uniform values of around 8 R_A. MORB-like $^{3}He/^{4}He$ have also been observed in the samples from island arc and subcontinental lithospheric mantle (SCLM) xenoliths. The $^{3}He/^{4}He$ of the mantle wedge and subduction-related SCLM are, however, more variable compared to those of MORB (Fig. 1). A recent study of He isotopes in a proterozoic subcontinental lithospheric mantle xenoliths from western Europe (Gautheron et al., 2005) has shown a low and uniform $^{3}He/^{4}He$ (6.32 +/- 0.39 R_A) obtained by crushing of olivine. Gautheron et al. (2005) discusses two models to explain the low and uniform $^{3}He/^{4}He$, where the lithospheric mantle beneath western Europe was invaded by recent and local metasomatic fluid having $^{3}He/^{4}He$ of around 6 R_A; metasomatism occurs globally through the entire SCLM. It is noted that relatively low $^{3}He/^{4}He$ (4.2 R_A) have been reported for olivine separates from mantle-wedge derived spinel peridotites by crushing (Dodson and Brandon, 1999). Furthermore, extremely low $^{3}He/^{4}He$ (< 1 R_A) were reported for mantle xenoliths from Far Eastern Russia (Yamamoto et al., 2004) where the Far Eastern Russia area was located at a subduction zone in the Mesozoic Era. On the other hand, high $^{3}He/^{4}He$ like those of MORBs are reported from some subcontinental ultramafic xenoliths (Matsumoto et al., 1998; 2000). The mantle wedge may therefore be a MORB-like source that has been partly infiltrated by exotic fluids having a radiogenic ^{4}He-rich component derived from subduction-related crustal material. The Oninomi basalt may be one such example.

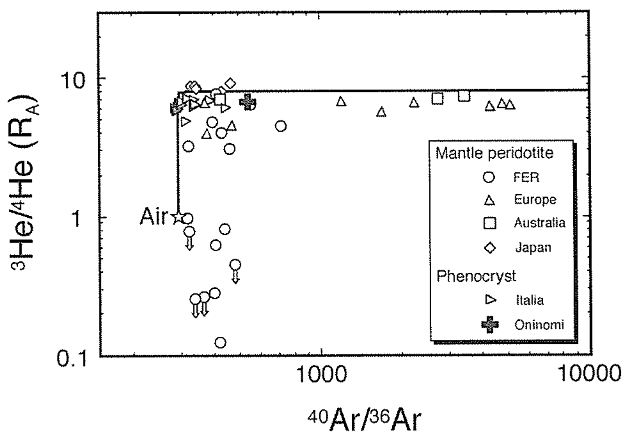

Fig. 1. $^{3}He/^{4}He$ versus $^{40}Ar/^{36}Ar$ diagram of gases extracted by the crushing method for the phenocrystic olivine of the Oninomi basalt with data obtained by crushing olivine in mantle peridotites and basaltic rocks. Data sources for the continental mantle xenoliths are as follows: FER (Far Eastern Russia) (Yamamoto et al., 2004), Europe (Gautheron et al., 2005, Australia (Matsumoto et al., 1998; 2001) and Japan (Matsumoto et al., 2001) . Data source for the basaltic magma in Italia is Marty et al. (1994). Data with uncertainties in $^{3}He/^{4}He$ of more than 5 R_A are removed.

Argon isotopic ratio ($^{40}Ar/^{36}Ar$) of the Oninomi basalt is low compared to those of MORB. Low $^{40}Ar/^{36}Ar$ have also been observed in samples from the SCLM (e.g., Yamamoto et al., 2004) and the mantle wedge (e.g., Matsumoto et al., 2001). If these low $^{40}Ar/^{36}Ar$ directly reflect the isotopic compositions in the mantle source, it requires that the mantle source mixed with materials with low $^{40}Ar/^{36}Ar$, such as materials derived from subduction-related components containing atmospheric argon (Sarda et al., 1999; 2000; Matsumoto et al., 2001). Ballentine and Barford (2000) have argued that most atmospheric contamination might occur in the laboratory especially for heavier noble gases. However, for noble gas analysis, samples and analytical lines are always preheated in order to reduce adhered atmospheric gases. If air addition has a significant effect on the gases released by crushing minerals, it makes elemental ratio of heavier noble gases of present sample air alike. Elemental ratios of heavier noble gases in the olivine of the Oninomi basalt, for example $^{84}Kr/^{36}Ar$ (0.026 +/- 0.003) or $^{132}Xe/^{36}Ar$ (0.00086 +/- 0.00008), in which errors are expressed as 1 sigma, are not similar to the modern air value (0.021 and 0.00074, respectively). Therefore low $^{40}Ar/^{36}Ar$ observed in the present olivine is considered to represent the value of sample.

As discussed above, the $^{40}Ar/^{36}Ar$ of the present sample ranges from atmospheric to the value higher than atmospheric value. This variability must reflect mixing of atmospheric and nonatmospheric noble gas components. Given that the helium in the sample is a mixture of two nonatmospheric components derived from mantle and crustal materials, it is reasonable to argue that the nonatmospheric Ar in the sample results from mixing of mantle or crustal materials rich in radiogenic ^{40}Ar. Thus, the Ar in the sample is interpreted to be a mixture of three components derived from the MORB-source, crustal materials and the atmosphere. We calculated the contribution of each component (mantle (MORB), atmoshphere and crust) to total ^{40}Ar in gas extracted from the present sample as calculated following the procedure and assumptions of Patterson et al. (1994) (Table2 and Fig. 2). The dominance of the atmospheric component is clearly apparent, accounting for 51.0% of the total ^{40}Ar. Of the nonatmospheric components, ^{40}Ar derived from the assumed MORB-source dominates, accounting for 41.3% of the total ^{40}Ar. Such data is fairly common in the previous study for both the xenolithic and phenocrystic olivine in New Zealand (Patterson et al., 1994).

Table 2. Calculated argon contribution

	Argon fraction (%)	
MORB	Crust	Atmosphere
41.3	7.7	51

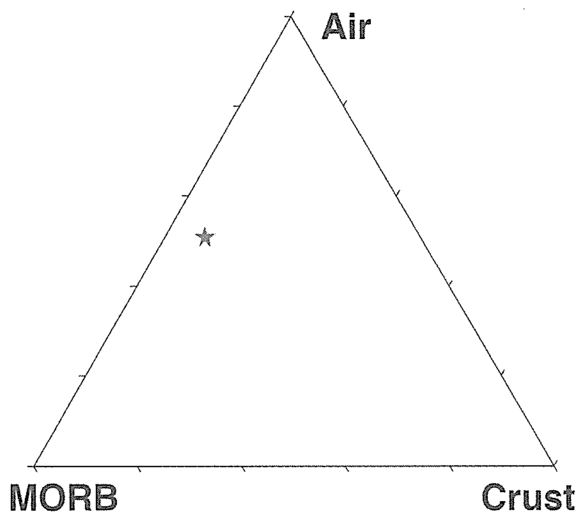

Fig. 2. Estimated argon contributions from mantle (MORB), atmoshphere and crust in gas extracted from olivine as calculated following the procedure and assumptions of Patterson et al. (1994).

The crustal materials have two possible sources for the island arc basaltic magma: arc crust above the mantle wedge and subducted slab. The $^{4}He/^{40}Ar^{*}$ and $^{4}He/^{21}Ne^{*}$ can be a useful indicator for examining the magma's source or subsequent transport processes, where $^{40}Ar^{*}$ and $^{21}Ne^{*}$ indicate nonatmospheric ^{40}Ar (^{36}Arobserved[($^{40}Ar/^{36}Ar$)observed – ($^{40}Ar/^{36}Ar$)air]) and ^{21}Ne (^{22}Neobserved[($^{21}Ne/^{22}Ne$)observed – ($^{21}Ne/^{22}Ne$)air]), respectively. For time scales of 10^{8} years or less, the instantaneous $^{4}He/^{40}Ar^{*}$ production ratio in the mantle is 5 - 20, depending on the K/U assumed (13000 - 3000) (Fig. 3). On the other hand, ^{21}Ne can be nucleogenically generated from (α, n) reaction on ^{18}O and (n, α) reaction on ^{24}Mg (Wetherill, 1954). $^4He/^{21}Ne^*$ production ratio in the mantle is estimated to be 2.2 x 10^7 (Yatsevich and Honda, 1997; Leya and Wieler, 1999). $^4He/^{40}Ar^*$ and $^4He/^{21}Ne^*$ of the lithosphere are primarily determined by its chemical composition which is are unlikely to change dramatically between reservoirs, therefore the $^4He/^{40}Ar^*$ and $^4He/^{21}Ne^*$ of the mantle is likely to be relatively constant (minor dependence of the $^4He/^{40}Ar^*$ and $^4He/^{21}Ne^*$ on accumulation time can largely be ignored for long lived reservoirs: Jambon et al., 1985; Allègre et al., 1986; Burnard et al., 1998; Honda and Patterson, 1999). ^4He – ^{21}Ne - ^{40}Ar systematics are therefore especially suited for deconvolving noble gas fractionation in mantle derived magmas. Figure 4 presents a diagram of $^4He/^{40}Ar^*$ and $^4He/^{21}Ne^*$ for the Oninomi basalt along with the data of the olivine in mantle peridotites and phenocrysts from subduction-related region. The Oninomi basalt shows minimum $^4He/^{40}Ar^*$ of 0.1 which is one or two orders of magnitude lower than the $^4He/^{40}Ar$ production ratio. The $^4He/^{21}Ne^*$ of the Oninomi basalt is also two orders of magnitude lower than the $^4He/^{21}Ne$ production ratio. Though both the $^4He/^{40}Ar^*$ and $^4He/^{21}Ne^*$ of the olivine samples are highly variable, $^4He/^{21}Ne^*$ are correlated with $^4He/^{40}Ar^*$. This result is indicative of a significant and systematic elemental fractionation of ^4He from nonatmospheric ^{21}Ne and ^{40}Ar (Patterson et al., 1994). The degree of He-Ne-Ar fractionation depending on the degassing mechanism in addition to the extent of volatile loss can be calculated using He, Ne and Ar solubilities (Fig. 4). The overall correlation between $^4He/^{40}Ar^*$ and $^4He/^{21}Ne^*$ in Fig. 4 is inconsistent with degassing as the dominant control on noble gas relative abundances. Gautheron et al. (2005) explained

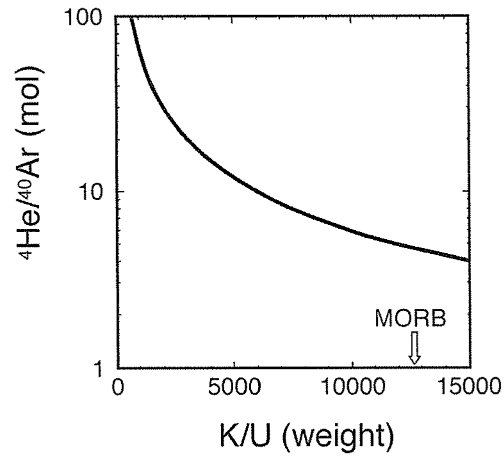

Fig. 3. Instantaneous production ratio of radiogenic He and Ar in the original mantle source having various K/U ratios in weight and uniform Th/U ratio of 3.1. The production ratio of ^4He and ^{40}Ar is strongly dependent on the K/U ratio in the source region. K/U=12700 of MORB is from Jochum et al. (1983). Th/U=3.1 is from Staudacher et al. (1989).

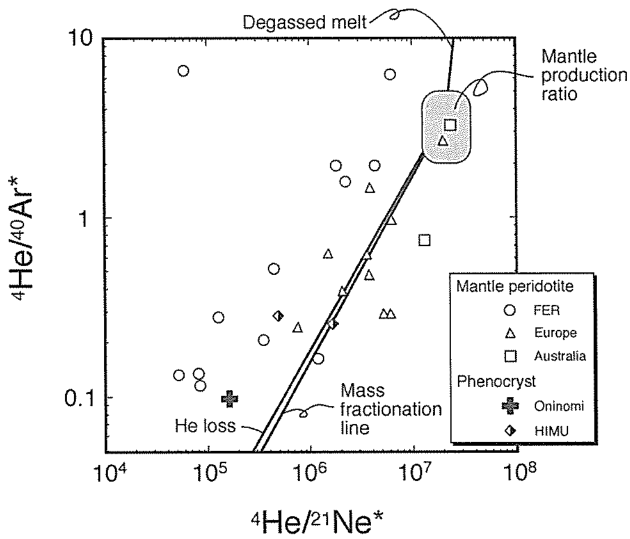

Fig. 4. $^4He/^{40}Ar^*$ versus $^4He/^{21}Ne^*$ diagram of the phenocrystic olivine of the Oninomi basalt with data obtained by crushing olivine in mantle peridotites and basaltic rocks, where $^{40}Ar^*$ indicates ^{40}Ar corrected for air-addition. Symbols as for Fig. 1. The production ratio of $^4He/^{21}Ne$ is constant in the mantle at 2.2 x 10^7 (Yatsevich and Honda, 1997; Leya and Wieler, 1999). The production ratio of $^4He/^{40}Ar$ in the mantle is around 4 (Fig. 3). The solid lines show elemental fractionation caused by He loss, mass-dependent fractionation and solubility-controlled mass fractionation from the original mantle source having mantle production ratio of $^4He/^{40}Ar$ and $^4He/^{21}Ne$.

the low He/Ar in mantle xenoliths by preferential loss of helium from fluid inclusions in the mantle xenoliths to the matrix of mineral grains. This process is not, however, supported by experimental evidence. The low $^{4}He/^{40}Ar^*$ and $^{4}He/^{21}Ne^*$ are typical of the mantle wedge and phenocrysts from subduction-related region. It suggests that the low $^{4}He/40^*$ and $^{4}He/^{21}Ne^*$ have a close relationship with subduction processes.

Before turning to elemental fractionation during subduction processes, the influence of crustal assimilation must be clarified. As mentioned above, $^{4}He/^{40}Ar^*$ and $^{4}He/^{21}Ne^*$ of the mantle-related component are unlikely to change dramatically. If arc crust has a significant influence on the magma source, the phenocrystic olivine and mantle peridotites should be plotted near the both production ratios of $^{4}He/^{40}Ar^*$ and $^{4}He/^{21}Ne^*$. Thus, the arc crust is not likely for the cause of low $^{4}He/^{40}Ar^*$ and $^{4}He/^{21}Ne^*$.

There are some possibilities of the kinetic fractionation between He and heavier noble gases in the subduction processes. Beneath the continental active margin or island arc, aqueous fluid derived from the subducted slab ascends into the mantle wedge. Hydrated peridotite is formed by the invasion of slab-derived aqueous fluid. Hydrous minerals such as amphibole, chlorite and phlogopite in the hydrated peridotite break down in downward flow of the mantle wedge and release H_2O. Interconnection of the aqueous fluid in the hydrated peridotite is controlled by dihedral angles. Such downdragged hydrous peridotite reaches a region where the dihedral angle is less than 60°, aqueous fluid is supplied continuously from the downdragged hydrous peridotite (Mibe *et al.*, 1998; 1999). When the aqueous fluid reaches the region with the solidus temperature of hydrous peridotite, partial melting in the mantle wedge takes place to produce initial magma. The melt will be extracted upwards, ascending through the mantle wedge, engendering subduction-related volcanism if melt segregation occurs. The subduction processes provide endless opportunities for noble gas fractionation during degassing or segregation of volatiles from the waterbearing silicate melt. As mentioned above, solubility of He relative to Ne and Ar in silicate melt is negatively correlated with volatile contents. Thus, during degassing or segregation, He/Ar and He/Ne of the residual volatiles may reduce due to the greater solubility of heavier noble gases in the waterbearing silicate melt. Though the mechanism explains the low $^{4}He/^{40}Ar^*$ and $^{4}He/^{21}Ne^*$ in the samples from subduction-related region briefly, the evidence regarding the mechanism by which the segregation occurs at high temperature and pressure remains equivocal.

Though the subduction-related samples cover a wide range of $^{4}He/^{40}Ar^*$ (Fig. 4), the samples with high $^{4}He/^{40}Ar^*$ like MORB

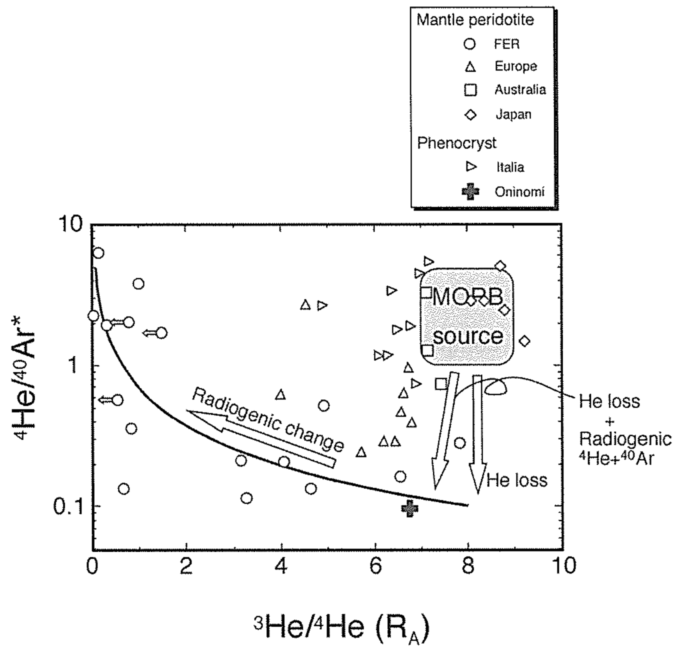

Fig. 5. $^{3}He/^{4}He$ versus $^{4}He/^{40}Ar^*$ diagram of the Oninomi basalt. $^{4}He/^{40}Ar^*$ of MORB is from Staudacher et al. (1989) and Moreira et al. (1998). Symbols as for Fig. 1. The solid line shows radiogenic change of the original mantle source with $^{3}He/^{4}He$ like MORB (8 R_A), low $^{4}He/^{40}Ar$ (0.1) and K/U of 12700 in weight.

source are separated into two groups by $^3He/^4He$ (Fig. 5). Both the $^3He/^4He$ and $^4He/^{40}Ar^*$ measured in the samples from current subduction zone (e.g., Italia and Japan) are relatively high. Also the Far Eastern Russian samples with low $^3He/^4He$ show high $^4He/^{40}Ar^*$ like MORB source. On the other hand, some samples from Far Eastern Russia show low $^4He/^{40}Ar^*$ and $^3He/^4He$. Yamamoto et al. (2004) explained that the $^3He/^4He$-$^4He/^{40}Ar^*$ trend indicates mixing of coexisting two kind of fluid inclusions in the samples: CO_2 inclusions having $^3He/^4He$ like MORB and low $^4He/^{40}Ar^*$ of ~0.5, and melt inclusions having low $^3He/^4He$ but relatively high $^4He/^{40}Ar^*$. The low $^3He/^4He$ measured in the melt inclusions may result from invasion of an exotic fluid with a high U/He and a subsequent addition of radiogenic nuclides (Yamamoto et al., 2004). In the Far Eastern Russia area, before the opening of the Japan Sea, slabs were subducted into the subcontinental mantle. If fluids derived from such subducted slab have infiltrated and remained in the mantle wedge as melt inclusions for a sufficiently long time, they would accumulate enough radiogenic nuclides to lower $^3He/^4He$ or raise $^4He/^{40}Ar$ up to the possible production ratio. Thus, the $^3He/^4He$ and $^4He/^{40}Ar^*$ in Fig. 5 can be explained by the kinetic fractionation between He and heavier noble gases in the subduction processes and a subsequent addition of radiogenic nuclides. In the case of Oninomi basalt, the extremely low $^4He/^{40}Ar^*$ may result only from the kinetic fractionation process because the sample was collected just from the active volcanic front area.

Conclusions

The Oninomi basalt is a well-preserved monogenetic volcano erupted at the Yufu-Tsurumi Graben in central Kyushu and has the potential to be OIB-like hotspot origin. We have measured the elemental and isotopic composition of all five noble gases trapped in the olivine phenocrysts from the Oninomi basalt and obtained MORB-like $^3He/^4He$. It indicates that the magma was derived from the similar source to that of MORB.

Argon isotopic ratio ($^{40}Ar/^{36}Ar$) of the olivine phenocrysyts is far lower than the values of MORB. The atmospheric $^{40}Ar/^{36}Ar$ must reflect mixing of atmospheric and nonatmospheric noble gas components. The existence of crust-derived noble gases in the Oninomi basalt is inferred from slight low $^3He/^4He$ compared to the MORB value. The Ar in the Oninomi basalt is therefore interpreted to be a mixture of three possible components derived from the MORB-source, crustal materials and the atmosphere.

The crustal components have two possible sources for the Oninomi basalt: arc crust above the mantle wedge and subducted slab. If arc crust has a significant influence on the magma source, the sample should have similar $^4He/^{40}Ar^*$ and $^4He/^{21}Ne^*$ to their production ratios. The Oninomi basalt shows extremely low ratios of $^4He/^{40}Ar^*$ and $^4He/^{21}Ne^*$ compared to the production ratio. Thus, the arc crust is not likely for the source of the crustal argon contribution.

Selective He loss can readily explain the low $^4He/^{40}Ar^*$ and $^4He/^{21}Ne^*$ of the Oninomi basalt. The low $^4He/^{40}Ar^*$ and $^4He/^{21}Ne^*$ are typical of the samples derived from mantle wedge and subduction-related SCLM. It suggests that the low $^4He/40^*$ and $^4He/^{21}Ne^*$ should have a close relationship with subduction processes.

The Oninomi basalt would therefore be derived from MORB-like source that has been infiltrated by slab-derived fluids fractionated via subduction processes.

Acknowledgements

We appreciate Y.N. Miura, T. Hanyu, Y. Lai and N. Hirano for their help in analyzing noble gases. This study has been financially supported in part by the Research Fellowship of the Institute for Geothermal Sciences, Kyoto University.

References

Allègre C.J., Dupré B. and Lewin E.(1986) *Chem. Geol.* **56,**219-227.

Ballentine C. J. and Barfod D. N. (2000) *Earth Planet. Sci. Lett.* **180**, 39-48.

Burnard P. G., Graham D. and Turner G. (1997) *Science* **276**, 568-571.

Burnard P. G., Farley K. A. and Turner G. (1998) *Chem. Geol.* **147**, 99-114.

Dodson A. and Brandon A. D. (1999) *Chem. Geol.* **160**, 371-385.

Gautheron C., Moreira M. and Allègre C. (2005) *Chem. Geol.* **217**, 97-112.

Hanyu T., Kaneoka I. and Nagao K. (1999) *Geochim. Cosmochim. Acta* **63**, 1181-1201.

Honda M. and Patterson D. B. (1999) *Geochim. Cosmochim. Acta* **63,** 2863-2874.

Jambon A., Weber H. W. and Begemann F. (1985) *Earth Planet. Sci. Lett.* **73,** 255-268.

Jochum K.P., Hofmann A.W., Ito E., Seufert H.M. and White W.M. (1983) *Nature* **306**, 431-436.

Kurz M. D. (1986) *Nature* **320**, 435-439.

Kurz M. D., Jenkins W. J., Hart S. R. and Clague D. (1983) *Earth Planet. Sci. Lett.* **66**, 388-406.

Leya I. and Wieler R. (1999) *J. Geophys. Res* **104**, 15439-15450.

Marty B., Trull T., Lussiez P. and Tanguy J.C. (1994) *Earth Planet. Sci. Lett.* **126**, 23-39.

Matsumoto T., Honda M., McDougall I. and O'Reilly S. Y. (1998) *Geochim. Cosmochim. Acta* **62**, 2521-2533.

Matsumoto T., Honda M., McDougall I., O'Reilly S. Y., Norman M. and Yaxley G. (2000) *Chem. Geol.* **168**, 49-73.

Matsumoto T., Chen Y. and Matsuda J. (2001) *Earth Planet. Sci. Lett.* **185**, 35-47.

Moreira M., Kunz J. and Allègre C. J. (1998) *Science* **279**, 1178-1181.

Ohta T., Hasenaka T., Ban M. and Sasaki M. (1992) *Bull. Volcanol. Soc. Japan* **37**, 119-131.

Patterson D.B., Honda M. and McDougall I. (1994) *Geochim. Cosmochim. Acta* **58**, 4411-4427.

Sarda P., Moreira M. and Staudacher T. (1999) *Science* **283**, 666-668.

Sarda P., Moreira M., Staudacher T., Schilling J.-G. and Allègre C. J. (2000) *J. Geophys. Res.* **105**, 5973-5996.

Stuart F.M., Lass-Evans S., Fitton J.G. and Ellam R.M. (2003) *Nature* **424**, 57-59.

Staudacher T., Sarda P., Richardson S. H., Allègre C. J., Sagna I., and Dimitriev L. V. (1989) *Earth Planet. Sci. Lett.* **96**, 119-133.

Trull T. W., Kurz M. D. and Jenkins W. J. (1991) *Earth Planet. Sci. Lett.* **103**, 241-256.

Wetherill G. W. (1954) *Phys. Rev.* **96**, 679-683.

Yamamoto J., Kaneoka I., Nakai S., Kagi H., Prikhod'ko V.S. and Arai S. (2004) *Chem. Geol.* **207**, 237-259.

Yatsevich I. and Honda M. (1997) *J. Geophys. Res.* **102**, B5, 10291-10298.

Yokochi R., Marty B., Pik R. and Burnard P. (2005) *Geochem. Geophys. Geosys.* **6**, doi:10.1029/2004GC000836.

研究報告　Scientific Reports

Concealed active faults in the eastern part of Oita Plain, east central Kyushu, southwest Japan

Chida, N., **Takemura, K**. et al.

In the eastern part of Oita Plain, there are concealed active faults with ENE-WSW direction, and they have been active in Holocene epoch. To presume the position and the activity of the faults which lay beneath the plain, the reflection method, the drilling survey and Geo-slicer investigation were done.

The northern fault named Misa Fault passes the vicinity of a former coast line and the fault in the south named Shimura Fault can be confirmed even in the vicinity of Otozu river. The Oita group and equivalent layers are covered directly with Holocene deposit in the south of the Shimura Fault. The deposit of Late Glacial-Late Interglacial Stage is thick covered with Holocene deposit on the north side. In addition, marine deposit of Late Interglacial Stage exists in the subordinate position and the Late Glacial deposit is considerably thicker than that of the south from the Misa Fault.

On the other hand, the fault confirmed in the Hioka district, thick deposit of Late Interglacial Stage distributes at the south of the fault, and is different from the Shimura Fault. Judging from the geological features, the fault confirmed in the Hioka district has a similar character as the Funai Fault.

Thus, the Misa and Shimura Faults which are concealed by Late Quaternary deposit in this region, greatly restrict the distribution of the stratum sine Late Pleistocene. The base of Holocene marine deposits (ca 10,000 years ago) is about 48m, in amount of displacement and the K-Ah volcanic ash layer is 26.5-30m by the Misa Fault, and the vertical slip rates are about 4.8 m and 4.2-4.8m/1000 years each other. The activity of the Misa Faults since Holocene is judged to be A class.

(Active Faults Research, vol.24)

Thermal response of sediment with vertical fluid flow to periodic temperature variation at the surface

Shusaku Goto (Aso Volcanological Laboratory, Kyoto University), Makoto Yamano (Earthquake Research Institute, University of Tokyo), Masataka Kinoshita (Japan Agency for Marine-Earth Science and Technology)

Characteristics of thermal responses of sediment with vertical fluid flow to periodic temperature variation at the surface are examined by the one-dimensional analytical solution of Stallman [1965]:

$$T(z,t)=\sum_i A_i \exp\left(\frac{vz}{2\kappa_m}-\frac{z}{2\kappa_m}\sqrt{\frac{\alpha_i+v^2}{2}}\right)\cos\left(\frac{2\pi t}{P_i}-\theta_i-\frac{z}{2\kappa_m}\sqrt{\frac{\alpha_i-v^2}{2}}\right) \quad (1)$$

where $T(z,\ t)$ is the sediment temperature at depth z and time t. A_i and θ_i are the amplitude and phase, respectively, of the sediment surface temperature variation of period P_i. κ_m is the thermal diffusivity of fluid-saturated sediment and v is the specific fluid flow velocity, which is a product of the fluid flow velocity v_f and the ratio of the heat capacity of the fluid $(\rho c_p)_f$ and fluid-saturated sediment $(\rho c_p)_m$:

$$v=\frac{(\rho c_p)_f}{(\rho c_p)_m}v_f \quad (2)$$

α_i is a function of P_i, κ_m and v:

$$\alpha_i=\sqrt{v^4\left[1+\left(\frac{8\pi\kappa_m}{P_i v^2}\right)^2\right]} \quad (3)$$

Equations (1) to (3) indicate that the amplitude of the thermal response decays exponentially and the phase is delayed linearly with increasing depth, but these depend on direction and velocity of vertical fluid flow, thermal diffusivity of fluid-saturated sediment, and period of surface temperature variation. Downward fluid flow propagates the effects of surface temperature variation efficiently. On the other hand, upward fluid flow enhances decay of amplitude of the thermal response. In both fluid flow directions, the effect of surface temperature variation propagates faster than that in conductive heat transport.

To examine the general characteristics of the subsurface thermal response, we defined two dimensionless parameters, ξ (related to thermal diffusivity of sediment (κ_m), specific fluid flow velocity (v) and period of surface temperature variation (P)) and Pe (thermal *Peclet number*), which is a measure of relative importance of heat transport by advection and conduction, as [Goto et al., 2005]:

$$\xi=\frac{8\pi\kappa_m}{Pv^2} \qquad (v_f\neq 0) \quad (4)$$

$$Pe=\frac{z_s|v|}{\kappa_m} \qquad (v_f\neq 0) \quad (5)$$

where z_s is the specific penetration depth at which the amplitude of the thermal response decays to e^{-1} of that at the surface. Examinations using these two dimensionless parameters show that there are three heat transport regimes for downward fluid flow as (i) heat transport strongly governed by advection (ξ < ca. 0.2 and Pe > ca. 400), (ii) heat transport strongly governed by conduction (ξ > ca. 40000 and Pe < ca. 0.01) and (iii) transition between these two regimes (ca. 0.2 < ξ < ca. 40000 and ca. 0.01 < Pe < ca. 400) (Fig. 1a) [Goto et al., 2005]. When $\xi = 17$, $Pe = 1$, indicating that heat transport by advection and conduction have the same contribution to the downward propagation of surface temperature variation. For upward flow (Fig. 1b), there is also three heat transport regimes as (i) balance of heat transports by advection and conduction (ξ < ca. 0.2 and $Pe \approx 1$), (ii) heat transport strongly governed by conduction (ξ > ca. 40000 and Pe < ca. 0.01) and (iii) transition between these two regimes (ca. 0.2 < ξ < ca. 40000 and ca. 0.01 < Pe < ca. 1) [Goto et al., 2005]. Equations (1) to (3) could be applied to studies of subsurface thermal and hydrological regimes in geothermally active areas.

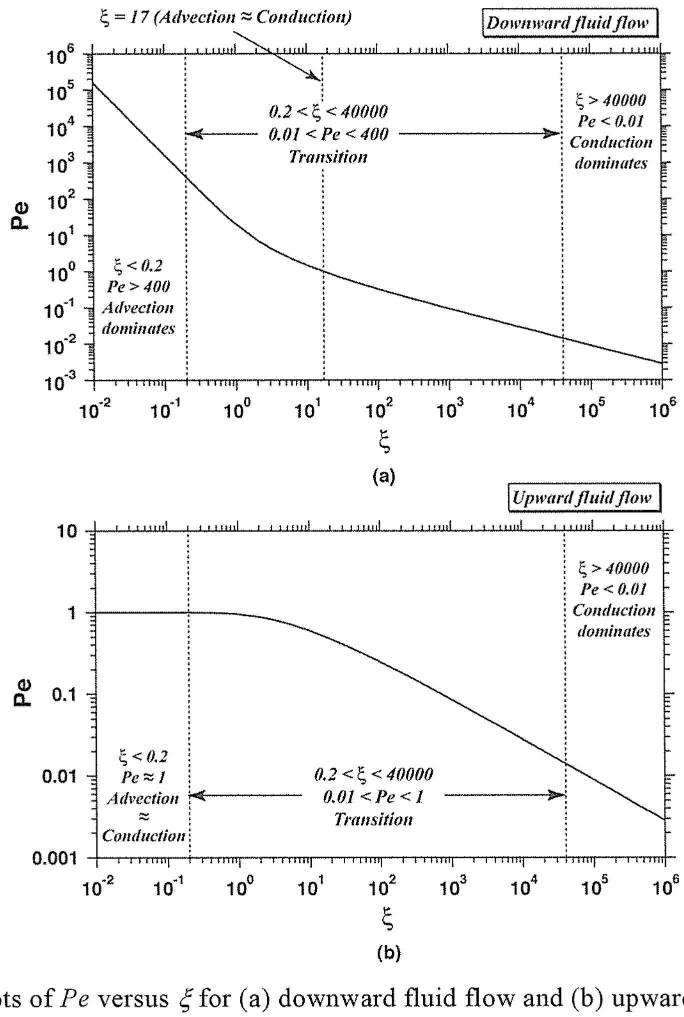

Fig. 1 Plots of Pe versus ξ for (a) downward fluid flow and (b) upward fluid flow.

References

Goto, S., M. Yamano, and M. Kinoshita (2005), Thermal response of sediment with vertical fluid flow to periodic temperature variation at the surface, *J. Geophys. Res.*, *110* (B1), B01106, doi:10.1029/2004JB003419.

Stallman, R.W. (1965), Steady one-dimensional fluid flow in a semi-infinite porous medium with sinusoidal surface temperature, *J. Geophys. Res.*, *70*, 2821-2827.

ζ-potential measurements for rock samples from Takano-obane lava

H. Hase, T. Ishido, K. Furukawa and T. Hashimoto

Ground water within a volcanic edifice plays an important role not only in controlling the manner of a volcanic eruption but in effective transfer of thermal energy through hydrothermal circulation. Electrical self-potential (SP), stationary component of the earth currents, has been recently utilized to assess subsurface hydrothermal system in active volcanic fields. The electrokinetic effect, or the streaming potential associated with fluid flow in a porous media, is a dominant cause of the SP generation in volcanic fields.

Quantitative assessment of subsurface fluid flow from the field SP data requires the streaming potential coefficient, a conversion factor between electric current and fluid flow. The ζ-potential of a rock-water interface is essentially important to evaluate the streaming potential coefficient. Recent laboratory study (Hase et al., 2003) has reported a significant variability of the ζ-potential, including its polarity, for volcanic rock samples from Aso caldera.

The present study focuses on the variability of the ζ-potential due to the difference of mineral species on the solid side. For this purpose we have done a systematic measurement of the ζ-potential for rock samples from a well core. The core was taken from a drill hole at Takano-obane lava dome, a rhyolitic unit of 100m thick, in the western part of Aso caldera (courtesy of Aso volcanological laboratory, Kyoto University). It has been reported in the petrological study by Furukawa et al. (2004) that a gradual change in mineral species such as from hematite to magnetite can be seen from top to bottom, though the major elemental component is almost stable through the core. We took 16 core samples from the surface to about 100m deep. The samples were grained into 0.5mm for ζ-potential measurement by using the streaming potential method.

Temperature, concentration, pH conditions of the liquid side are 30 °C, 10^{-3} mol/l (KCl), 2.5~11.5 (by 1.0 step), respectively. We made a surface conduction correction by using 0.1 mol/l (KCl).

The isoelectric point (IEP, the pH condition at which the ζ-potential becomes apparently null) was almost the same for all the samples. In contrast, the ζ-potential itself showed an increasing trend in magnitude from top to bottom. One of the implications of this result is that the ζ-potential is affected by the valence number of Fe.

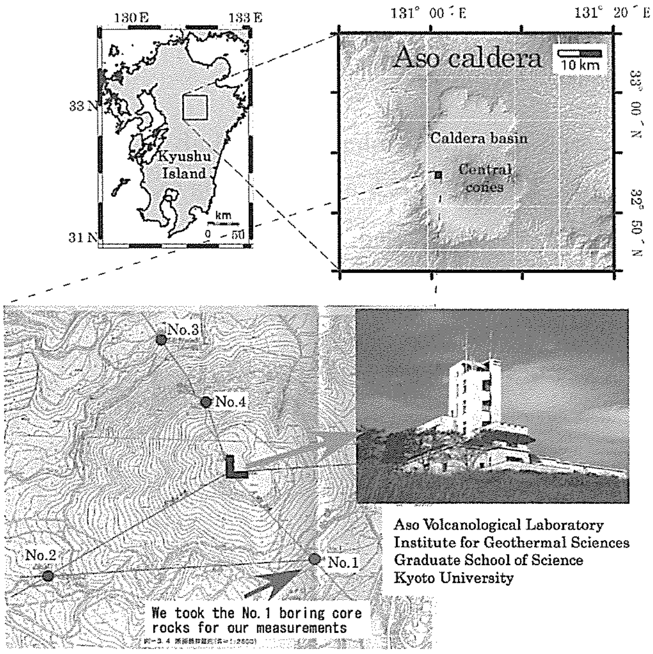

Fig.1 Location of drilling hole

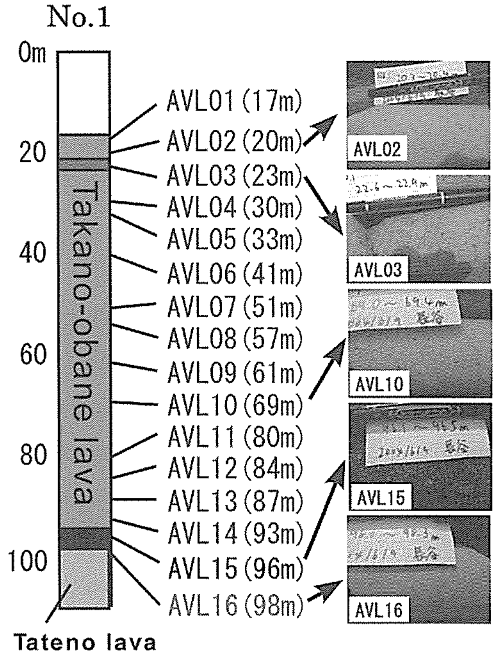

Fig.2 Sampling depth of the core

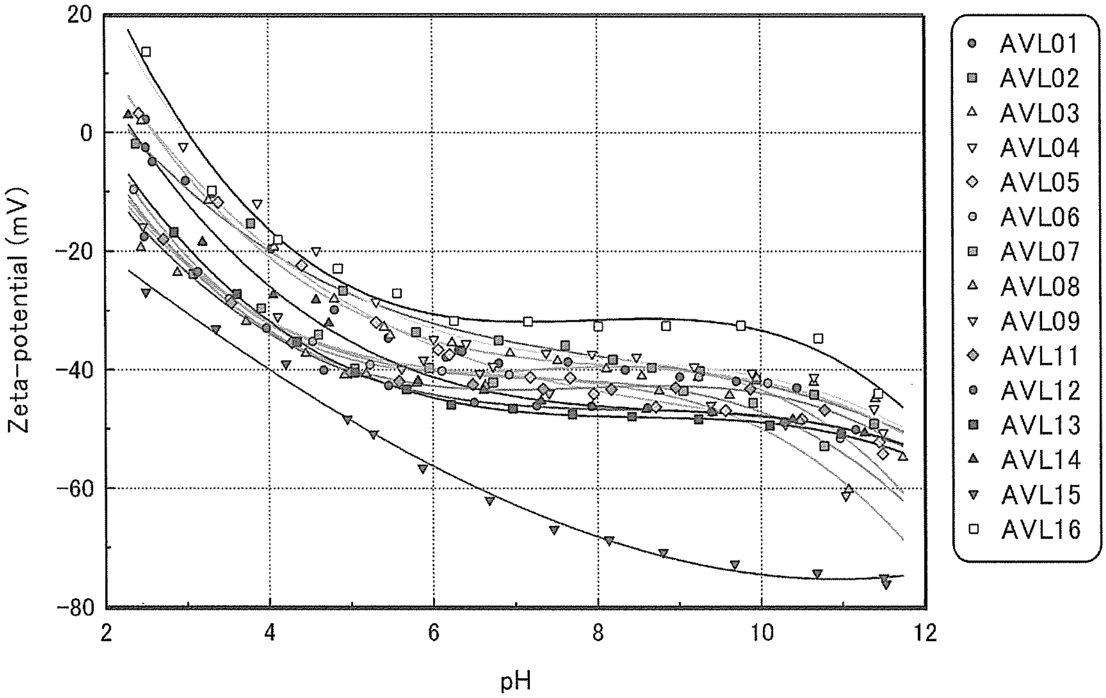

Fig.3 Results of ζ potential measurements

Relationship between subjacent source faults and surface faults
- 3D visualization of integrated information -

N. INOUE (KITADA), N. Kitada. (Geo-Research Inst.), M. Kohara (Muse Lab.), T. Kagawa (Geo-Research Inst.), **K. TAKEMURA** and A. Okada (Kyoto Univ.)

1. Introduction

We have studied relationship between subjacent source fault and surface fault (the concept of both faults are shown in Fig. 1). The purpose of the study is to infer the geometry of subjacent source fault from that of surface rupture or active fault on the surface. We selected 15 earthquakes which were investigated from geological and seismological viewpoint (Fig.3) by the published papers. There are many available papers for 15 earthquakes. We attempted to reveal the relationship between both faults based on collected information. We made table of both faults (strike, dip, length, location of focus, geology and so on) based on the compiled information. We visualized collected data to comprehend relation among various information. We carried out correlation analysis of geometric parameters of the faults. We show the result of visualization of various data and indicate results of the principal component and cluster analysis of relation among various information.

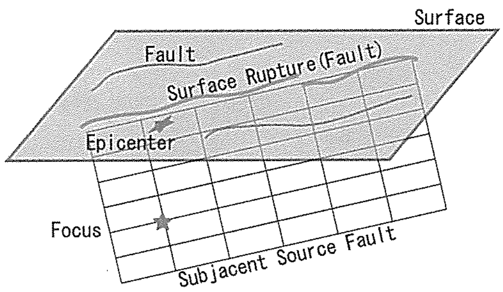

Fig.1 Concept of faults in this study

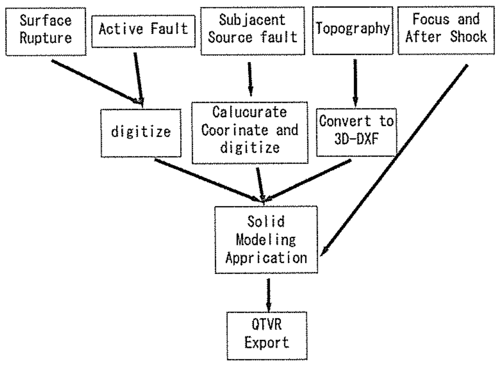

Fig.2 Flow of visualization

2. Visualization of various data

The topographic data and focus were also collected to visualize. The visualization procedure is indicated in Fig.2. Constructed visualization models were exported QTVR format, which could be viewed by Quick Time player at any view angle and scale. Fig. 3 shows examples the data set and the result of visualization.

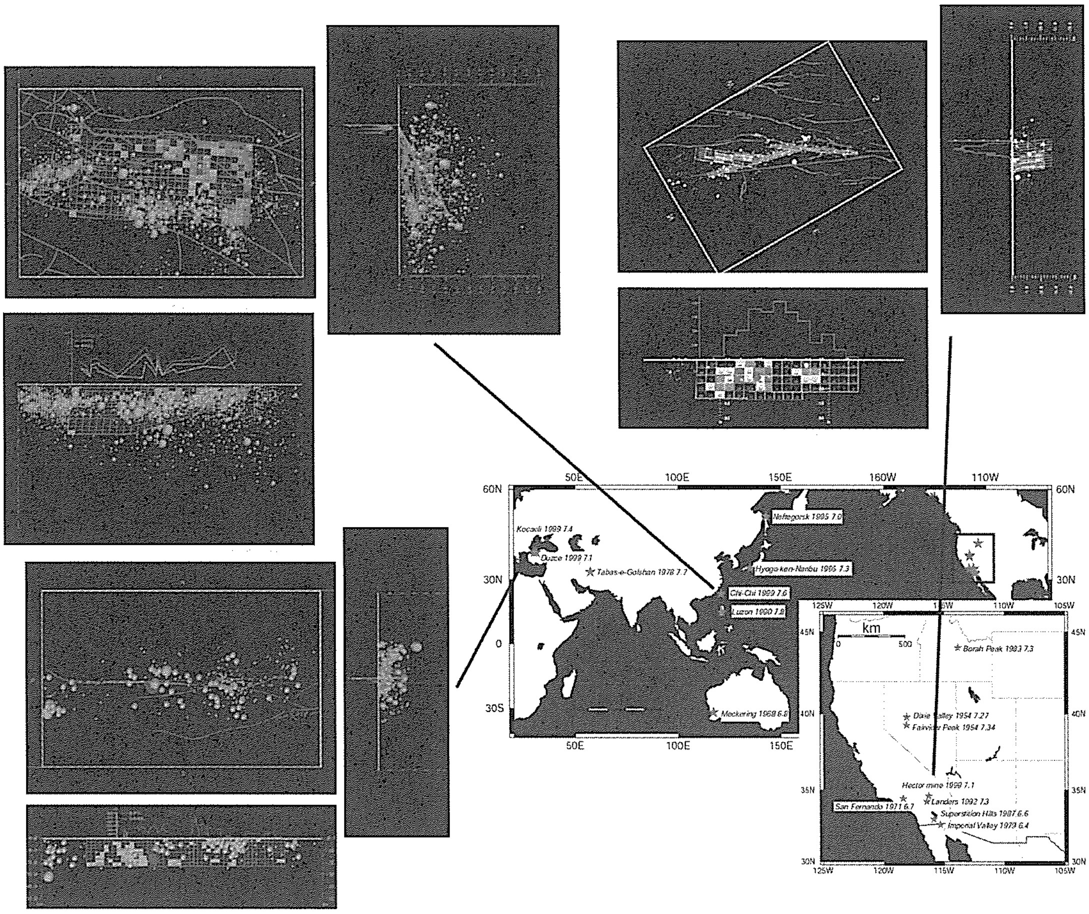

Fig.3 Index map of 15 earthquakes in this study and few result of visualized model
Solid lines indicate surface rupture and active faults. Solid circles show focus and aftershock.

3. Principal Component and Cluster Analysis

We carried out principal component analysis of geometric parameters of surface rupture and source fault. Fig.4 indicates the concept of defined parameter for analysis.

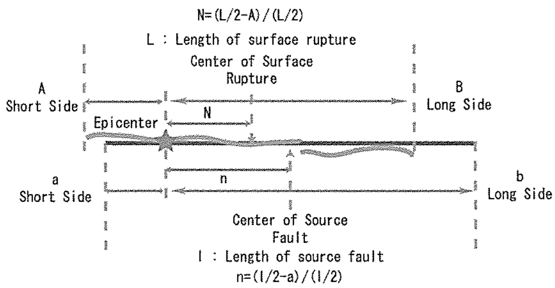

Fig.4 Concept of parameter for correlation analysis
Solid lines indicate surface rupture and active faults.

4. Discussion and Conclusion

The relation among magnitude, L, l A, a, B and b indicates higher correlation coefficients over 0.7. The relation among N and n are correlation coefficient 0.5-0.7. Fig.5 shows relationship between 1st. and 2nd principle components and clustered earthquakes derived from the result in cluster analysis.

Based on the factor (principle) loading, 1st. principle component corresponds to the scale of the earthquake and rupture area (magnitude, L, l). On the contrary, 2nd. principle component corresponds to location of focus and gap of surface and source faults (N, n). As shown in Fig.5, these earthquakes were classified into three groups (A-group, B-group and C-group).

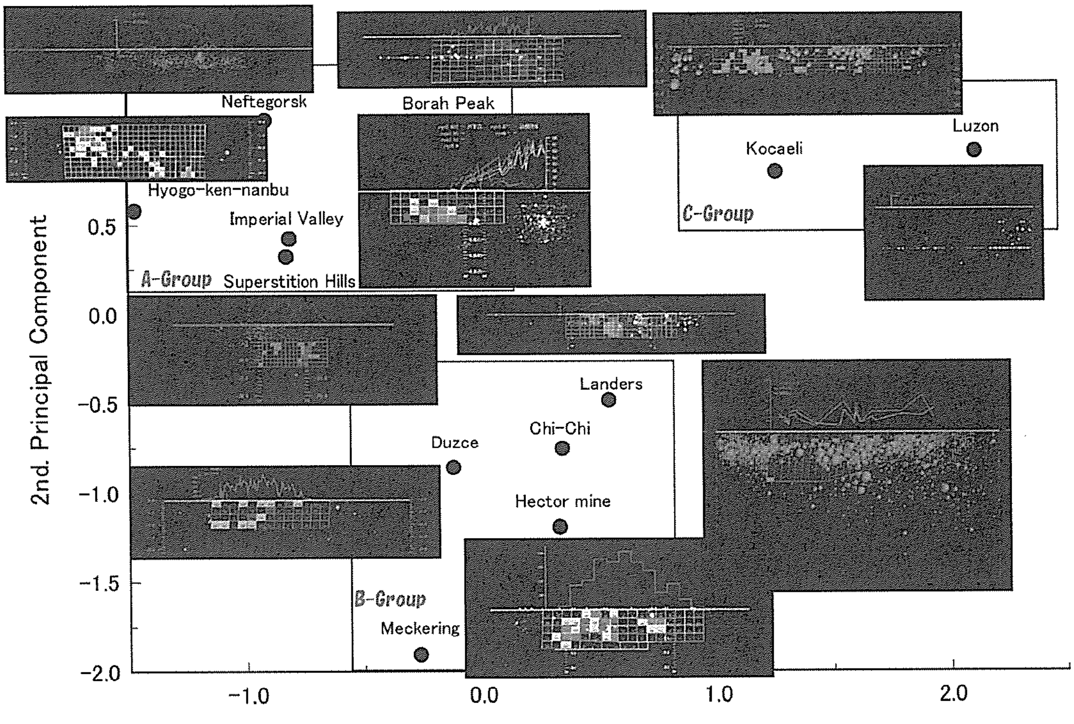

Fig.5 Relationship between 1st. principle component and 2nd principle component
Solid lines indicate surface rupture and active fault, respectively. Solid circles show focus and aftershock.

Characteristics of three groups were described in brief.

A-group

Focus was located at edge of the fault and scale of earthquake was small. Focus does not correspond to location of maximum displace or high asperity in A-group.

B-group

Focus was located at center of the fault and scale of earthquake was intermediate. Focus located at center of maximum displacement and high asperity in B-type.

C-group

Focus was located between edge and center of the fault and scale of earthquake was large.

However, relation between displacement and asperity depend on the depth of the high asperity region. We will compare subjacent source fault with distribution of aftershock region as next problem.

Report of Absolute Geomagnetic Measurement in Aso Volcanological Laboratory

N. Inoue (Kitada), M. Utsugi and **Y. Tanaka**

The Aso volcanological laboratory has constructed the geomagnetic observatory near Aso volcano to record the geomagnetic variation and disturbance. The new digital recording observation system was installed in 2002. Our institute has been carried out continuous observation of total force and three components of geomagnetic field in the new observation system from 2002. We reported the result of the absolute measurement and determined the base value of the fluxgate magnetometer.

Absolute measurement and determination of base value

We carried out several absolute geomagnetic measurements to determine base value of the fluxgate magnetometer. Declination and inclination were observed referring to the mark near absolute observatory. The azimuth of the mark was estimated by several observations of the Pole star. The observed declination and inclination are shown in Fig.1. The F, H, D and Z are also indicated. In Fig.1, after 2002/11/28, the sensitivity of the fluxgate magnetometer was changed. The F in 2003/5/15 and 2003/6/19 were not available and not used in this study. We separated data to period 1 (before 2002/11/28) and period 2 (after 2002/11/28).

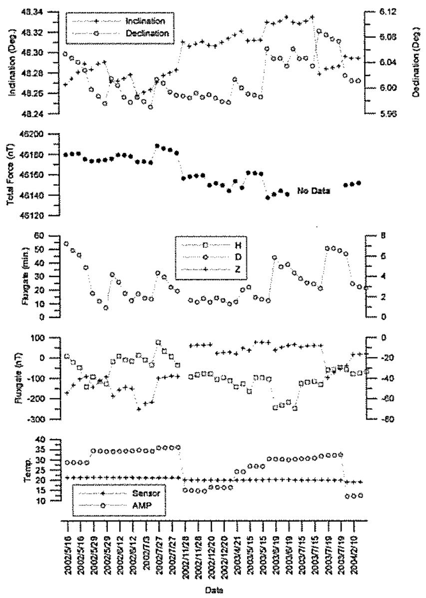

Fig.1 Result of Absolute measurement and F, H, D and Z.

Table.1 List of constant.

Period 1

Component	Sensitivity	Temperature correction
H	0.100	−0.380
D	0.101	−0.057
Z	0.100	0.060

Period 2

Component	Sensitivity	Temperature correction
H	0.999	0.234
D	1.005	−0.010
Z	1.000	0.146

To determine the base value, the coefficients of sensitivity and temperature correction of each component were required. The sensitivity was derived from calibration system of fluxgate magnetometer. We attempted to estimate temporary temperature coefficient by regression analysis between absolute and fluxgate data. The constant are shown in Table.1. The coefficient of the sensitivity during period 1 was not available. The temporary value of (sensitivity of period 2) /10 was applied. The base values were obtained based on the constant in Table 1. Table.2 is the estimated base value of 1-day absolute data set. Fig.2 indicates the fluxgate data corrected by base value and residual (total force – synthetic total force by H and Z). The temperature dependency was seen in the residual. We were attempted to remove the temperature dependency by the linear regression.

Talbe.2 List of base value.

No	Date	Tempureture Corrected			No Temperature Correction		
		H	D	Z	H	D	Z
1	2002/5/16	31268.02	359.5052	35060.30	31302.66	315.8401	35174
2	2002/5/29	31267.08	359.9430	35060.43	31355.23	347.0193	35166
3	2002/6/12	31267.08	359.9430	35060.43	31355.23	347.0193	35166
4	2002/7/3	31272.30	359.1555	35056.30	31268.26	343.7501	35266
5	2002/7/27	31267.84	359.4982	35061.03	31236.15	334.0504	35147
6	2002/11/28	31252.43	357.7705	35056.05	31255.91	357.6217	35058
7	2002/12/20	31251.66	357.5257	35056.58	31255.51	357.3612	35058
8	2003/4/21	31251.30	357.8241	35058.56	31256.95	357.5826	35062
9	2003/5/15	31252.80	357.6702	35056.27	31258.91	357.4092	35060
10	2003/6/19	31254.24	358.0442	35054.31	31261.31	357.7419	35058
11	2004/2/10	31254.46	357.9262	35052.07	31257.31	357.8042	35053

Fig.2 Recorded data corrected by base value and constants.
Residual of gray line is obtained by F - synthetic F by H and Z (F'). Residual of dotted line is obtained by removing temperature dependency from the residual F - F' based on linear regression. Residual of black line is obtained by removing dependency of temperature and D component from the residual F - F' based on linear regression.

Configuration of Paleogene rocks around Unzen volcano, Shimabara Peninsula, Kyushu, Japan, inferred from gravity analysis

N. Inoue (Kitada) and **K. Takemura**

1. Introduction

The Unzen volcanic scientific Drilling Project (USDP) has been performed flank- and conduit drillings around the Unzen volcano in the Shimabara Peninsula, Kyushu, Japan. The results of the flank-drillings revealed the subsurface structure, geological history and physical property around the Unzen volcano in the eastern part of the Shimabara Peninsula. On the contrary, the New Energy Development Organization (NEDO) has conducted various surveys on the geothermal field research project in the western part of the Shimabara Peninsula.

The purpose of this study is to reveal the basement structure in the Shimabara Peninsula by integration of previous gravity study and recent surveys.

2. Gravity Data

The gravity data published from (AIST) was used for analysis. The reduction density was estimated by correlation between gravity anomaly and topography. The density, 2.30 g/cm^3 indicated the minimum correlation with the topographic variation.

3. Density for gravity analysis

The stratigraphy of the Shimabara Peninsula is as follows in descending order.
Unzen product, Pre-Unzen, Paleogene sediment

The density of Unzen product and Pre-Unzen depend on the lithofacies rather than the stratigraphy. The density of volcanic rock is higher than that of pyroclastic flow deposit or sediment. Thus, it is difficult to construct the density model of the Unzen based on the stratigraphy. In the western part of the Shimabara peninsula, high density body was considered for constructing of the subsurface model (NEDO, 1984). The basement corresponds to the Paleogene deposits. The outcrop or borehole information about distribution of the Paleogene deposits is sparse in the study area. The overlaying layer of the model consisted of the Unzen volcano products and the Neogene - Quaternary deposits. Based on the previous study, the density of the basement and overlaying layer were decided 2.50 and 2.30 g/cm^3, respectively.

4. Trend surface analysis

The previous gravity analysis carried out by NEDO (1984) indicated density variation due to complex stratigraphy resulted from Unzen volcanic activity. In this section, simple trend surface analysis was performed to find out the outline of the basement. This method supposes local gravity anomaly is the linear relationship with the depth of the basement. The regional trend is fitted by polynomial surface. The assumption of linear relation between the local gravity and the depth of the basement corresponds to the 2 layer assumption. The collected basement information is located outside of the graben.

The basement configuration obtained outside data set indicated shallower depth in the graben than the base of the Unzen Products. This was contrary to the graven structure of the basement of the Pre-Unzen (Hoshizumi et al, 2002). This suggests that difficulty of determining graben depth from gravity analysis.

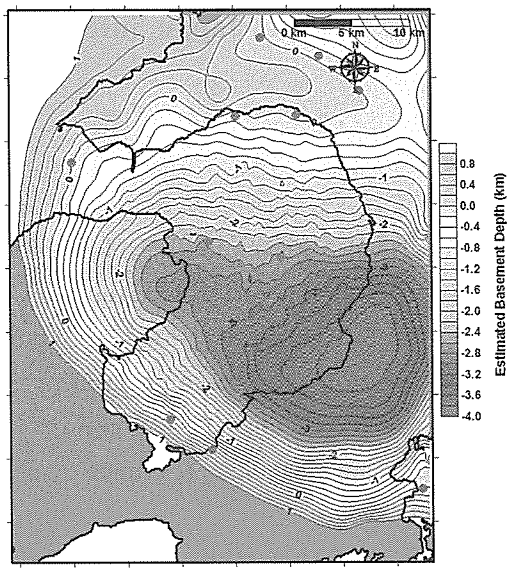

Fig.1 Basement configuration derived from trend surface analysis. Contour interval is 0.2 km. Solid circle indicates data point which was used for analysis. 3rd Order of polynomial surface was applied for removing the regional trend.

We assumed the depth of the basement in the graben corresponded to the base of the Pre-Unzen. The basement configuration (Fig.1) obtained with temporary data set indicates the graben structure.

5. 2-D Gravity Analysis

The basement structure obtained by the trend surface was not considered structure and density variation. Thus, we performed 2-D gravity analysis. The basement corresponds to the Paleogene deposits. The overlaying layer of the model consisted of the Unzen volcano products and the Neogene - Quaternary deposits. Based on the previous study, the density of the basement and overlaying layer were decided 2.50 and 2.30 g/cm^3, respectively. The top surface of the basement was iteratively adjusted to improve the difference between the observed and calculated gravity anomalies. The control points were referred to the result of the trend surface analysis (Fig.1). Fig.2 indicates the location of 2-D gravity analysis profiles. Figs.3 and 4 indicated the result of the two-layer models. Figs. 5 and 6 indicated the multi-layered models considering the high density volcanic rocks (gray lattice pattern and the density is 2.50 g/cm^3).

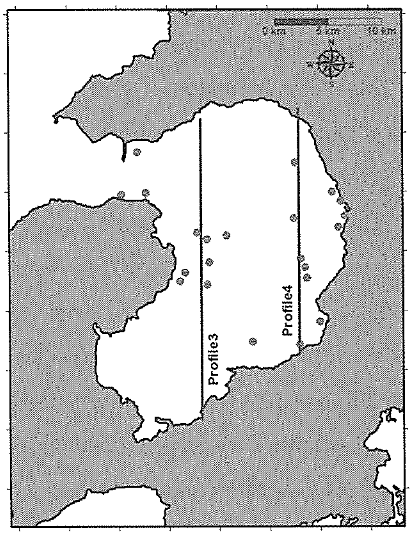

Fig.2 Location of 2D analysis profiles. Solid circle indicate the location of borehole.

6. Discussion and Conclusion

The basement configuration inferred from trend surface indicated the graben shape. The center of the graben moved southwards compared with that of Unzen Products base.

The result of 2D two-layer analysis indicated uneven surface of the basement. If the basement show smooth graben surface as inferred by trend surface, there is the possibility of existence high-density material between basement and Pre-Unzen.

To reveal basement structure from quantitative gravity analysis requires the basement information in the graben from surface to the basement. The regional geophysical data modeling was also need to solve gravity problem.

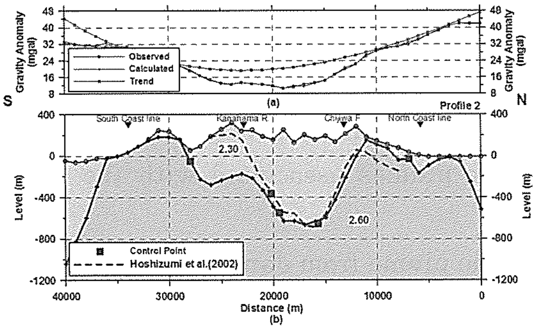

Fig.3 Profile 3
(a) Gravity Anomaly. (b) Density structure. Red and black broken lines indicate the basement derived from trend surface and Unzen Products base (Hoshizumi et al, 2002). Numerical value is density in g/cm³.

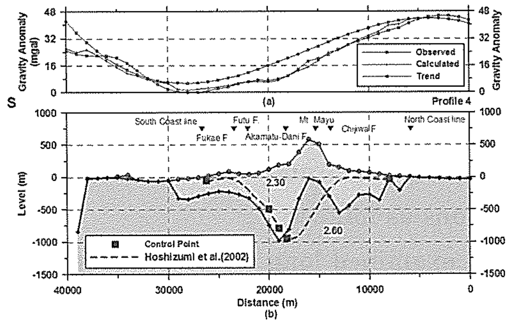

Fig.4 Profile 4
(a) Gravity Anomaly. (b) Density structure. Red and black broken lines indicate the basement derived from trend surface and Unzen Products base (Hoshizumi et al, 2002). Numerical value is density in g/cm³.

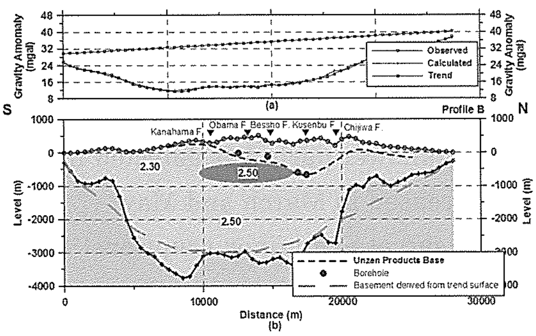

Fig.5 Profile 3 (Multi-layer)
(a) Gravity Anomaly. (b) Density structure. Gray and black broken lines indicate the basement derived from trend surface and Unzen Products base (Hoshizumi et al, 2002). Numerical value is density in g/cm³. The gray lattice pattern in figure shows the high density volcanic rocks.

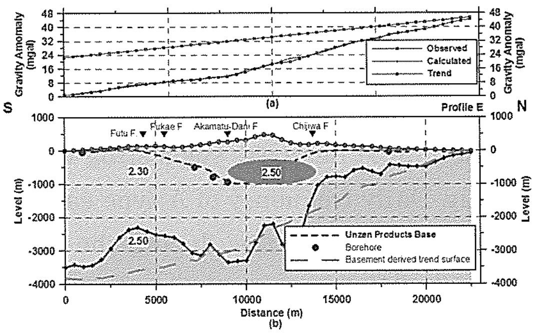

Fig.6 Profile 4 (Multi-layer)
(a) Gravity Anomaly. (b) Density structure. Gray and black broken lines indicate the basement derived from trend surface and Unzen Products base (Hoshizumi et al, 2002). Numerical value is density in g/cm³. The gray lattice pattern in figure shows the high density volcanic rocks.

Time variation of volcanic plume related with the eruptions of Asama Volcano in 2004

Tsuneomi Kagiyama

Volcanic plumes have been recognized to have a certain kind of periodic variation according to the volcanic activity. In recent years, acquisition and processing techniques for continuous infrared or visible images have been developed to examine a time variation of volcanic plume easily. Kagiyama et al. (2003) examined time variations of volcanic plumes of the 2000 Eruption in Usu Volcano, and found a periodic variation of 12 seconds. It is very interesting to examine if such a rhythm commonly exists or not in other volcanoes. It is also interesting if such a rhythm depends on the state of volcanic activity or not. In Asama Volcano, we have carried out infrared observation since August 2002, and have succeeded in capturing successive imageries before and after the eruptions in 2004 (Figure 1). We can detect long term and short term variations in volcanic plumes associated with the 2004 Eruptions as follows.

We examined long term variations of the height of the plume from January to November 2004 as shown in Figure 2. The height of the plume was low until February 2004, but tended to increase gradually in March and May, respectively, and anomalously increased from July 25. The height of the plume continued to be high by the middle of August, and decreased in the end of August, just before the eruption on September 1. The height of the volcanic plume was low just after the eruption, and increased again from September 12. Eruptions occurred again from September 14, and changed successively from September 16 to 17. After the successive minor eruption stage, large explosions occurred intermittently and the height of the plume decreased. This variation reflects the change of the volcanic activity. According to the GPS observation by the Geographical Survey Institute, gradual inflation suggesting a supply of magma was detected 2 or 3km beneath the western part of Asama Volcano from April, and a rapid increase, suggesting moving magma to shallower part, was detected in the end of July. Daily frequency of A-type earthquakes also increased in March and May.

We examined imageries during the early stage of the successive minor eruptions; from 00:57 a.m. to 08:00 a.m. on September 16, and detected short term variation of the volcanic plume as follows. We obtained time series data of the average temperature on the certain vertical line segment, which was crossed by the moving volcanic plume, and examined a spectrum. As a result of the analysis, some power peaks were confirmed at the multiples of 0.0025Hz until 4 a.m. And this peak was found to move to high frequency according to the eruptive activity; 0.013Hz at 7 a.m. (Figure 3). This result suggests two possible interpretations; (1)Asama Volcano has some resonance beneath the crater (conduit), and the characteristic length of the conduit changed to be shorter during the successive minor eruptions. (2) The confining pressure decreased to activate bubbling within the conduit. Japan Meteorological Agency reported the number of eruptions increased from 4 a.m., and Geographical Institute found lava cake within the crater about 11 a.m. These evidences suggest rising of magma around 4 or 7 a.m., and are consistent with our estimates.

References
Kagiyama, T., Hiyama, Y., Kaneko, T. and Hirabayashi, J., Short period variation of volcanic plume Usu Volcano detected by IR imagery, IUGG 2003, V11/03P/D-022 Poster 1400-298

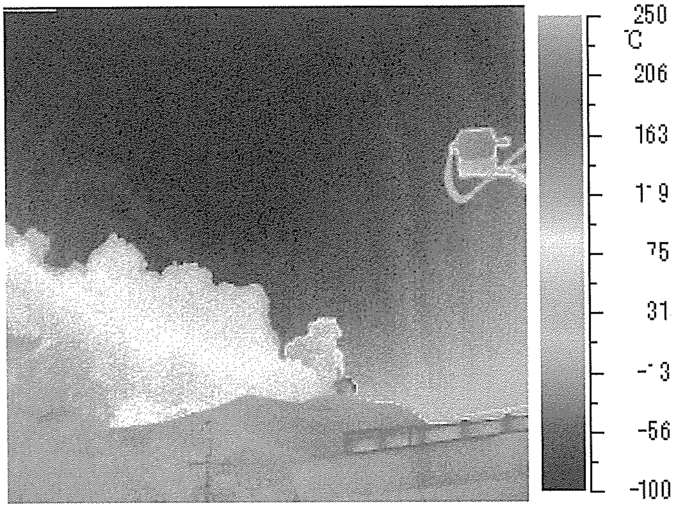

Figure 1. Infrared imagery of a volcanic plume in Asama Volcano on September, 16, 2004.

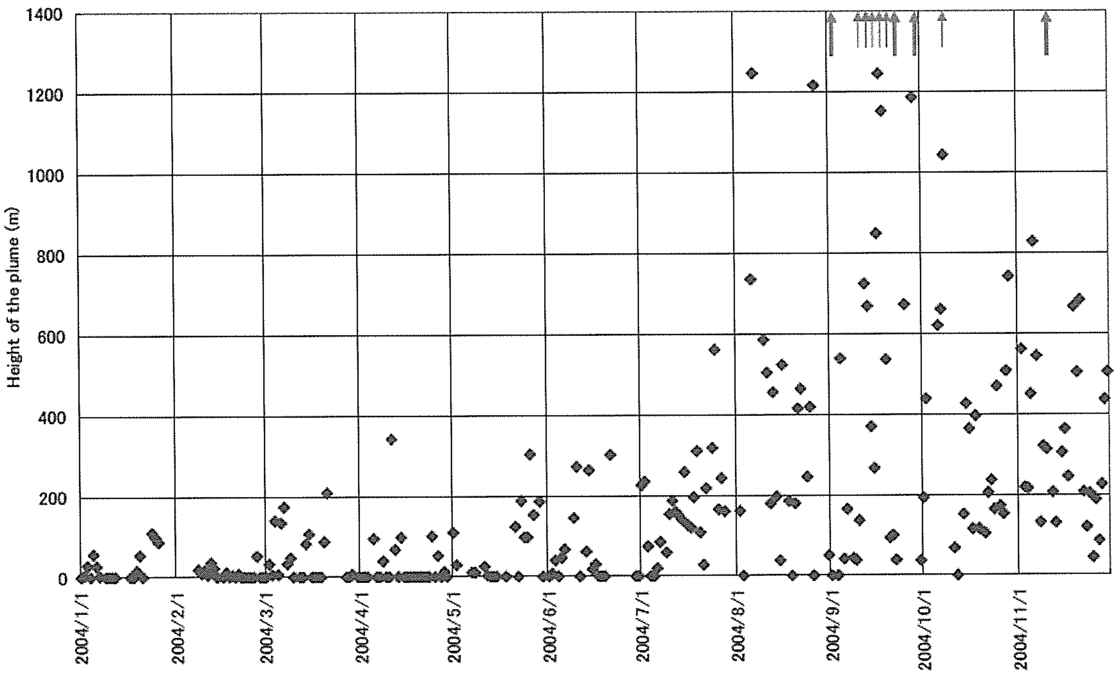

Figure 2. Daily mean of the plume height of Asama Volcano from January to October, 2004. Large arrows indicate middle size explosions, small arrows indicate minor eruptions

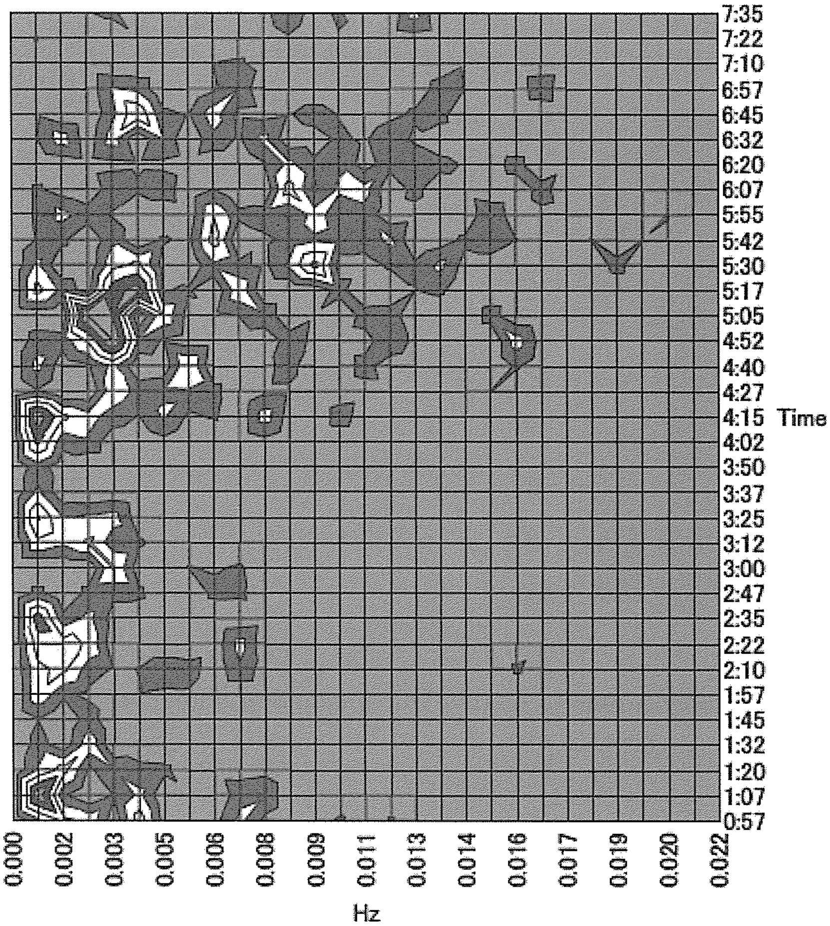

Figure 3. Change of power spectrum during the evolution stage of the successive minor eruptions from 00:57 to 07:35 on September 16, 2004.

Late Quaternary movement of active faults in the Unzen Graben, western Kyushu, based on trenching study at Chijiwa Town and observation of a fault outcrop at the north slope of the Mt. Fugendake

Matsuoka, A., Tsutsumi, H. and **Takemura, K.**

The Unzen Graben is located on the western end of the Beppu-Shimabara Graben and is bounded by normal faults on the north and south sides. The faults in the Unzen Graben have developed in association with the growth of the Unzen volcanoes and offset volcanic materials such as lavas and pyroclastic deposits. The detailed location and amount of offsets of these active faults have been reported by previous studies, but timing of faulting was poorly constrained.

The Ogura fault is located on the northern margin of the Unzen Graben and offsets the alluvial fan surfaces formed by the Chijiwa River. We excavated a trench across the Ogura fault at Chijiwa Town in order to reveal the timing of recent faulting events. The faults exposed on the trench walls strike N70° W-EW and dip 70° -90° S, and offset the terrace gravels of the Chijiwa River. These faults may have moved after the deposition of the AT Volcanic ash (26-29 ka), which was found in fine sands filling coseismic open cracks.

We also found an outcrop across the Kusenbu fault inside the Unzen Graben, A layer containing K-Ah volcanic ash (7.3 ka) is offset by the Kusenbu fault, suggesting that the fault has moved during the Holocene.

(Matsuoka et al., Active Faults Research, 2004)

A quantitative model for trace element behavior during crystal settling and reequilibration in silicic magma chambers

Koshi Nishimura

In a magma chamber, heat loss, and thus crystallization, occurs primarily along the margin. In the interior of the chamber, the melt is hotter and chemically less evolved, and crystals that settle from the upper part are likely to react with the melt. High-silica ash-flow tuffs erupted instantaneously from the zoned magma chambers provide ample evidence that crystals have sunk and reacted with the surrounding melts. In order to quantify the trace element behavior in such magma chambers, I developed a heat and mass transfer model for crystal settling and reequilibration with the following equations:

$$\phi = 1 - \frac{C_{\mathrm{b}}^{\mathrm{w}}(T_{\mathrm{h}} - T_{\mathrm{s}})}{C_{\mathrm{s}}^{\mathrm{w}}(T_{\mathrm{h}} - T)} \quad (1)$$

$$\frac{\partial T}{\partial t} = \kappa \frac{\partial^2 T}{\partial z^2} - (\phi v_s + \phi_d v_d)\frac{\partial T}{\partial z} + \frac{L}{c}\frac{\partial \phi}{\partial t} \quad (2)$$

$$\frac{\partial C_b^{\alpha}}{\partial t} = \left\{ \frac{\partial (C_m^{\alpha}\phi)}{\partial z} - \frac{\partial (C_x^{\alpha}\phi)}{\partial z} \right\} v_s \quad (3)$$

where ϕ is the crystal fration, C^{w}_{b} is the bulk H_2O content of the magma, T_h is the y-intercept of the linear liquidus curve, T_s is the H_2O-saturated solidus temperature and C^{w}_{s} is the melt H_2O content at the saturated solidus, κ is the thermal diffusivity, v_s is the crystal settling velocity, ϕ_d is the fraction of upward migrating melt, v_d is the migration velocity of the melt, L is the latent heat, c is the specific heat, C^{α}_{b}, C^{α}_{x} and C^{α}_{m}, are the concentration of element α in the bulk magma, that in the crystals, and that in the melt, respectively. Equations (1), (2) and (3) represent equilibrium state, energy balance, and mass balance, respectively.

A unique and important feature of this model is the temporal variation of liquid lines of descent (Fig. 1). Previous crystallization models such as fractional and equilibrium crystallization have assumed that a melt with a single composition evolves along a single liquid line of descent with increasing degree of solidification. In the present model, however, melts of various compositions exist within the chamber at a given time, and the liquid line of descent itself changes with time. The chemical evolution expected from crystal settling and reequilibration is consistent with the data from the Bishop Tuff high-silica magma chamber and may account for some of the characteristic patterns of chemical zonation observed in high-silica magma chambers.

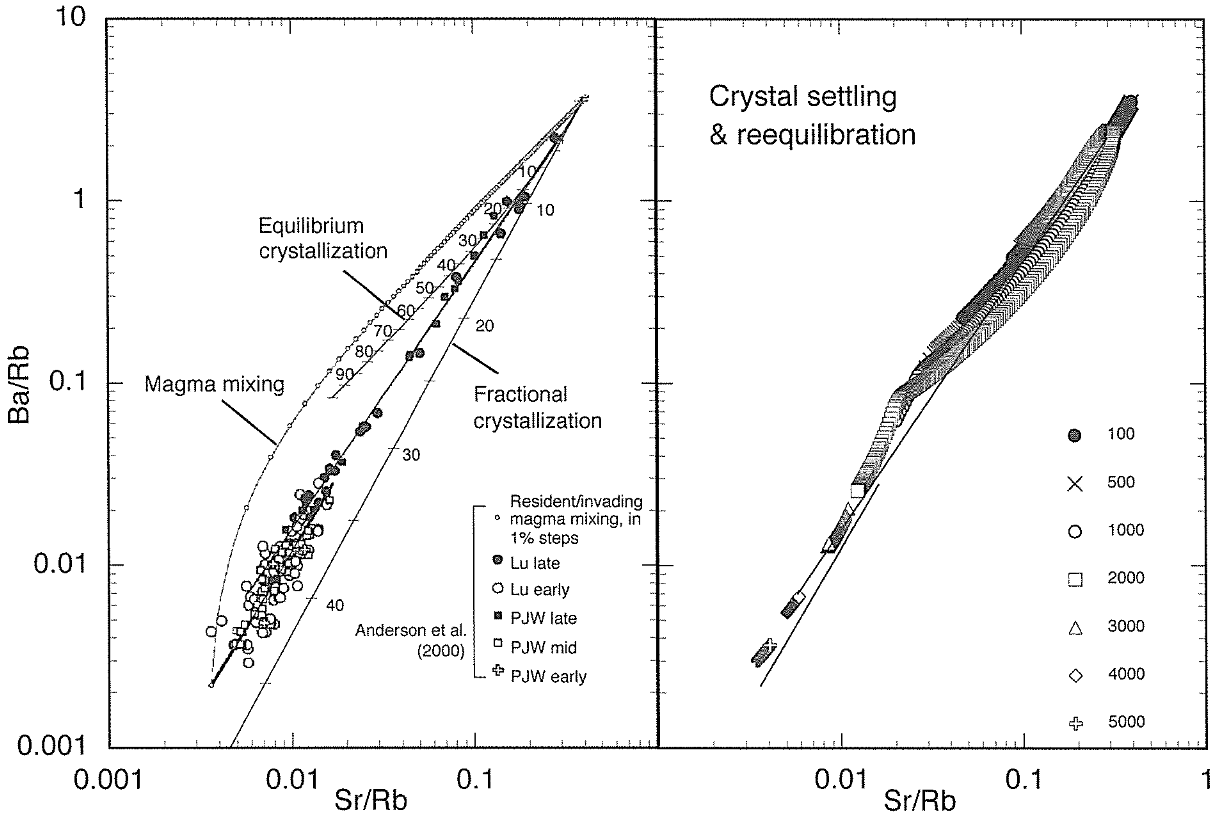

Fig. 1 Comparison of liquid lines of descent for crystal settling followed by reequilibration, equilibrium and fractional crystallization, and a magma mixing path [*Anderson et al.*, 2000] with the liquid evolution of the Bishop Tuff. Melt inclusion data are from *Anderson et al.* [2000] ('Lu' in legend) and *Wallace et al.* [1999] ('PJW' in legend). Weighted regression lines through the data (late-erupted inclusions, 1.460 ± 0.008; early- and mid-erupted inclusions, 1.673 ± 0.063 [*Anderson et al.*, 2000]) are also shown in the figure for the crystal settling and reequilibration paths (right-hand figure).

Pressure response of Raman spectra of water and its implication to the change in hydrogen bond interaction

Okada, T. (Osaka Univ.), Komatsu, K. (Tohoku Univ.), **Kawamoto, T.,** Yamanaka (Osaka Univ.), T., Kagi, H. (Univ. Tokyo)

In situ Raman spectroscopic measurements of water in the region of OH vibration were conducted up to 0.4 GPa at 23 and 52 degree C. The frequencies of the decomposed OH stretching bands initially decreased with increasing pressure, reached a minimum at 0.15 GPa and increased up to 0.3 GPa and then decreased, which corresponds to the variations of the strength of hydrogen bonding. This variation was observed at 23 degree C, but not at 52 degree C, which suggests a change in pressure dependence on the hydrogen bond interaction between these two temperatures. Based on the equilibration model between hydrogen-bonded and non hydrogen-bonded molecules, the present experimental results indicate that the pressure variation of the viscosity depends on the ratio of hydrogen-bonded molecules, rather than the strength of hydrogen bonding between molecules.

Geochemical Investigation of Rivers Running through the Beppu Geothermal Field

S. Ohsawa, H. Yamasaki, N. Takamatsu, **K. Amita**, **M. Yamada**, N. Kato

In the urban area of Beppu City, whose population is more than ten million, five rivers (the Shin, Hirata, Haruki, Sakai and Asami Rivers) are running from west to east and flowing into Beppu Bay (Fig.1). In this area, warm and boiling waters of about 20000 ton/day are discharged from as many as 3000 hot spring wells. Hot water of more than 45℃ is prohibited to flush down the sewer by a municipal bylaw of Beppu City. So, there is a possibility that the rivers in the urban area of Beppu City are affected by drain of hot spring water. The purpose of our investigation is to grasp the present state of water qualities of these rivers and to determine whether the waste water of hot spring has an influence on the rivers and also on the coast of Beppu Bay or not.

We collected water samples from the rivers along the river current for chemical analysis of major components and trace elements in Aug. 31 and Sep. 1, 2003 (Fig. 1) and also sampled waters from cold springs, domestic wastes and the Hiya River (there is no hot spring around the basin) for reference. Major components: Cl, SO_4, HCO_3, Na, K, Ca, Mg were analyzed by ion-chromatography and titration, and trace elements: Li, B, Al, Sc, V, Cr, Mn, Fe, Co, Ni, Cu, Zn, Ga, Ge, As, Rb, Sr, Mo, Cd, Cs, Ba, W, Pb were determined by ICP-MS from preservative sample by HNO_3. Variations in Total dissolved salt (TDS) of the river waters from upstream to downstream are shown in Fig. 2. At every river, TDS concentration increases as river water is going downstream. This variation is not uncommon, but we must make special mention of high TDS concentration of the river waters and this strongly suggest that the waste water of hot spring has a harmful influence on the rivers. At the Sakai and Asami Rivers, TDS concentrations slightly decrease at the lower reaches of the rivers by inflow of the tributaries: the Itachi and Ayukaeri Rivers, respectively, however TDS concentrations are still high.

Lithium will be a good tracer to determine whether the waste water of hot spring has an influence on the rivers or not, because Li content of hot spring waters in Beppu: 50-8000 μ g/L (NEDO, 1990) is lager than that of waters from cold spring and domestic waste: 0.4-0.6 μ g/L and 7.6-8.5 μ g/L ,respectively. Li/Cl ratios of the waters from the hot spring, cold springs and the domestic wastes are 0.0031-0.029, 0.00007-0.00025 and 0.0007-0.00077, respectively, consequently Li/Cl ratio is a good tool for recognition of contamination of the hot spring waste waters to the rivers. Figure 3 shows relationships between Li/Cl ratio and TDS of waters from the rivers, hot springs, cold springs and domestic wastes. The river waters having high TDS more than about 300mg/L show almost constant Li/Cl ratio regardless of TDS concentrations and the Li/Cl ratios are within the range of that of the hot spring waters. Therefore, it is unmistakable that all rivers except for the Hiya River are contaminated with the waste waters from the hot springs.

Examination of relations between TDS and the 23 trace elements including Li was carried out and the summary is shown in Table 1 and Fig. 4. Correlation factors (R^2) of regressions for TDS versus B, Li, Ge, Rb, Cs, As are more than 0.9, therefore these trace elements should be derived from the waste waters of hot springs. Concentrations of B and As in the river waters are extremely higher than the environmental standard values for public water area in Japan. This result warns that Beppu Bay would be polluted with B, As and etc. through the rivers from the hot springs in the Beppu geothermal field.

Fig.1 Map showing rivers in the Beppu geothermal field and sampling points of river waters. Sampling points of each river are numbered in Arabic numerals order from upstream.

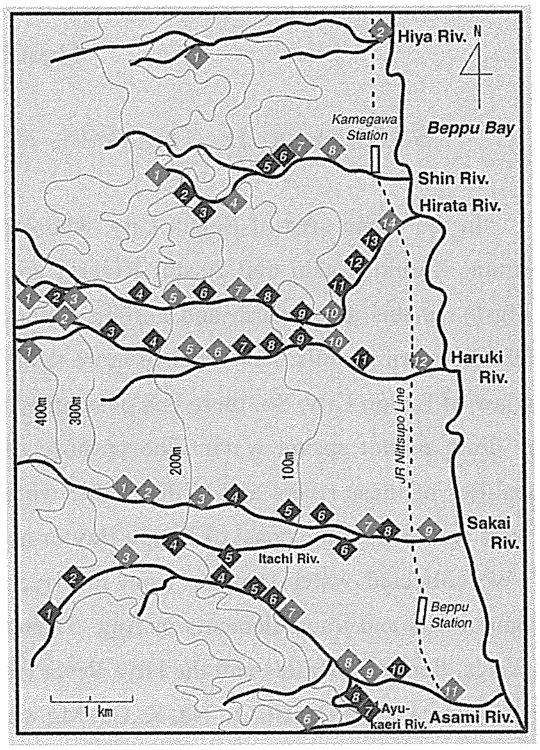

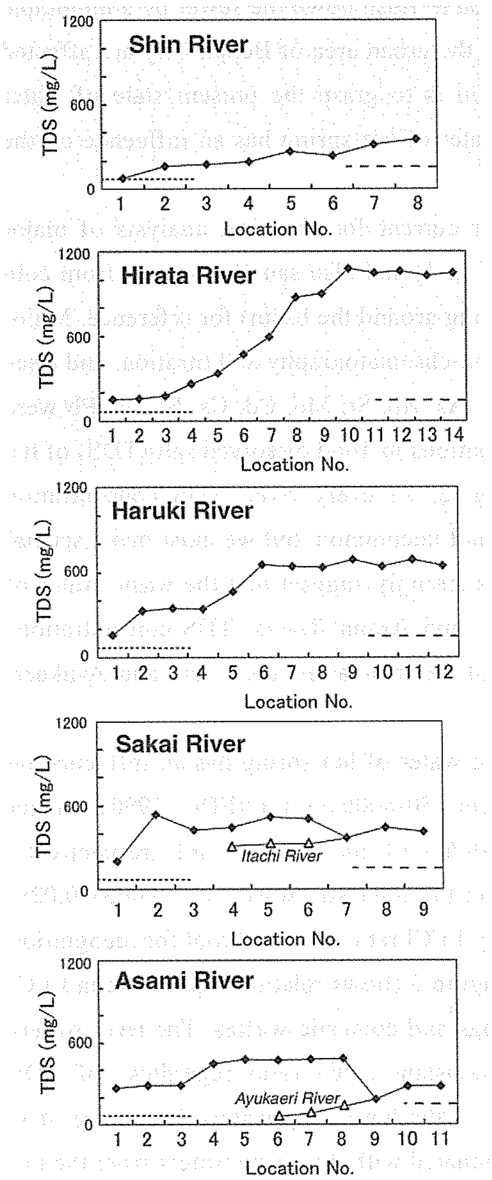

Fig.2 Variations in TDS concentrations of each river from upstream to downstream. Dot and broken lines show concentration levels of waters in upstream and downstream of the Hiya Rivers, respectively.

Fig.3 Relationship between TDS concentration and Li/Cl ratio of waters from each river, hot springs, cold springs and domestic wastes in the Beppu geothermal field.

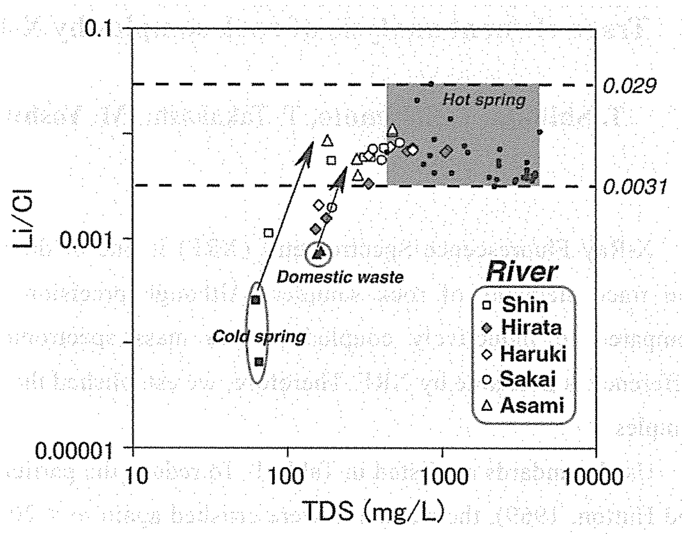

Table 1 Maximum, minimum and average values of trace elements of river waters in the Beppu geothermal field and correlation factors (R2) of regression lines for relations between trace element and TDS concentrations. Environmental standard values are for public water area in Japan.

Trace element	Concentration (μ g/L) Max.	Min.	Average	Environmental standard value (μ g/L)	R^2 of regression line＊
B	6130	7.9	1530	1000	0.9607
Li	2620	0.6	679		0.9501
Ge	14	0.1	4.0		0.9395
Rb	318	9.1	87		0.9387
Cs	168	0.3	41		0.9363
As	340	0.2	79	10	0.9265
Sr	323	56	163		0.7950
Ga	1.4	0.03	0.5		0.7521
W	6.9	0.01	2.1		0.7367
Sc	22	6.9	13		0.7011
Ba	54	1.0	17		0.7006
Ni	2.2	0.6	1.4		0.5498
Mo	5.6	0.1	2.3		0.5014
V	36	1.4	18		0.1198
Fe	1090	42	324		0.0281
Al	1650	2.2	200		0.0264
Mn	449	0.1	48		0.0113
Cd	0.6	0.002	0.06	10	0.0081
Pb	0.9	0.02	0.2	10	0.0076
Cu	4.0	0.1	1.5		0.0074
Co	1.5	0.02	0.2		0.0072
Cr	2.2	0.03	0.4	50 as Cr(VI)	0.0024
Zn	144	0.6	15		0.0023

＊ for relation to between TDS concentration

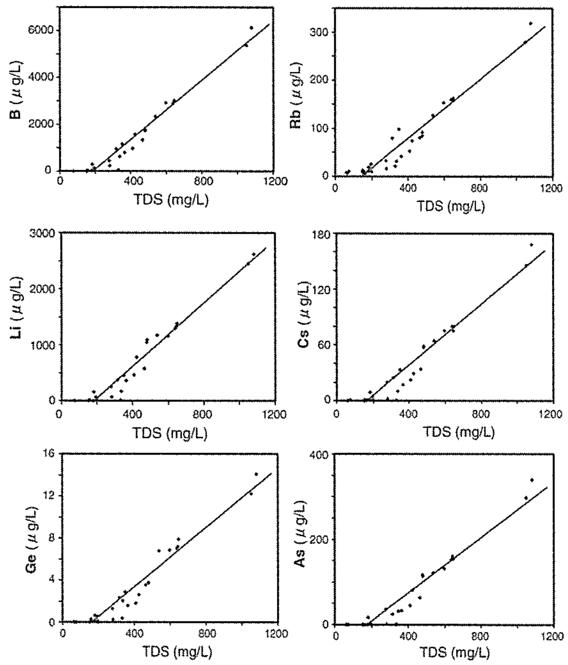

Fig.4 Six trace elements in the Beppu river waters whose concentrations have good correlations to TDS concentrations. For correlation factors, see Table 1.

Trace element analysis of rock samples by X-Ray Fluorescence Spectrometry

T. Shibata, T. Sugimoto, T. Takahashi, **M. Yoshikawa,** T. Miyazaki and **K. Nishimura,K. Takemura**

X-Ray Fluorescence Spectrometry (XRF) is one of the most versatile methods for analyzing major and trace elements of rock samples. Although precision and detection limit of analysis is inferior compared to inductively coupled plasma mass spectrometer, rapid analysis with small individual difference is available by XRF. Therefore, we established the method for analyzing trace elements of rock samples.

Used standards are listed in Table 1. To reduce the particle-size and mineralogical effect (e.g. Norrish and Hutton, 1969), the standards were crushed again to < 200 mesh with vibration mill made of alumina ceramic. The powdered standard, to which 0.4 ml of 3% polyvinyl alcohol has been added, is filled into the ring made of polyvinyl chloride and pressed. After overnight evaporation, standards were measured by XRF. The used anode tube and detector are rhodium (50kV, 50mA) and scintillation counter, respectively.

Detailed parameters for those calibration curves are described in Table 2. The calibration curves show the good linearity, and the dispersion is small. The results of quantitative analyses for standards are also shown in Table 1. The obtained concentrations show good agreements with recommended values except for yttrium. Therefore, it can be concluded that the method for trace element analysis by XRF established in this study is able to apply for the analyses of natural rock samples.

Table 1 The results of regression analysis

Sample	Ba (ppm)			Rb (ppm)			Nb (ppm)			Pb (ppm)			Sr (ppm)			Zr (ppm)			Y (ppm)		
	r.v.	XRF	diff.	r.v.	XRF	diff.	r.v.	XRF	diff.	r.v.	XRF	diff.	r.v.	XRF	diff.	r.v.	XRF	diff.	r.v.	XRF	diff.
AGV-2	1140	1082	0.95	69	68	0.99	15	15	0.98	13	15	1.17	658	657	1.00	230	230	1.00	20	23	1.17
BCR-2	683	600	0.88	48	45	0.93		13		11	12	1.05	346	326	0.94	188	182	0.97	37	37	1.01
BHVO-2	130	177	1.36	10	10	1.00	18	18	0.98		3		389	375	0.96	172	166	0.96	26	27	1.03
BIR-1	7	20	2.87		0		1	1	2.00	3	3	0.93	110	108	0.98	18	18	0.99	16	16	1.00
DNC-1	118	106	0.90	5	4	0.87	3	2	0.77	6	5	0.86	144	144	1.00	38	40	1.05	18	18	1.02
GSP-2	1340	1342	1.00	245	245	1.00	27	26	0.98	42	37	0.87	240	244	1.02	550	539	0.98	28	13	0.45
JA-2	321	322	1.00	73	71	0.97	9	10	1.08	19	19	0.98	248	250	1.01	116	114	0.99	18	18	1.01
JA-3	323	316	0.98	37	36	0.99	3	4	1.20	8	8	0.97	287	292	1.02	118	118	1.00	21	23	1.06
JB-1b	493	492	1.00	41	35	0.84	33	27	0.80	10	7	0.69	444	432	0.97	141	129	0.91	24	26	1.06
JB-2	222	234	1.06	7	7	0.88	2	1	0.82	5	4	0.75	178	173	0.97	51	49	0.95	25	25	1.02
JB-3	245	241	0.98	15	14	0.94	2	3	1.13	6	5	0.91	403	400	0.99	98	93	0.95	27	30	1.12
JF-1	1750	1938	1.11	266	273	1.03	1	1	1.49	33	34	1.01	172	172	1.00	39	33	0.85	3	4	1.30
JF-2	298	340	1.14	218	222	1.02	1	1	1.43	49	50	1.02	200	205	1.02	7	4	0.58	3	1	0.41
JG-1a	470	485	1.03	178	182	1.02	11	12	1.07	26	27	1.03	187	194	1.04	118	119	1.01	32	36	1.13
JG-2	81	75	0.93	301	301	1.00	15	16	1.10	32	29	0.93	18	20	1.09	98	105	1.08	87	102	1.18
JG-3	466	460	0.99	67	67	1.00	6	7	1.16	12	12	1.03	379	384	1.01	144	150	1.04	17	18	1.06
JGb-1	64	88	1.37	7	6	0.90	3	3	0.93	2	1	0.36	327	311	0.95	33	32	0.98	10	11	1.06
JGb-2	37	33	0.90	3	2	0.69	2	2	0.89	2	1	0.47	438	441	1.01	12	14	1.22	5	7	1.64
JH-1	106	114	1.07	14	15	1.02	4	4	0.98	3	2	0.58	153	150	0.98	48	49	1.02	14	12	0.91
JR-1	50	62	1.23	257	260	1.01	15	16	1.08	19	18	0.92	29	33	1.12	100	100	1.00	45	53	1.18
JR-2	40	38	0.95	303	308	1.01	19	20	1.07	22	20	0.92	8	11	1.34	96	96	1.00	51	60	1.16
JR-3	66	86	1.30	453	442	0.98	510	515	1.01	33	35	1.08	10	11	1.09	1494	1488	1.00	166	129	0.77
Jsy-1	16	-8	-0.50	66	72	1.09	1	1	1.96	5	4	0.86	19	23	1.18	70	73	1.04	3	-2	-0.81
RGM-1	810	926	1.14	150	155	1.03	9	10	1.12	24	24	0.99	110	113	1.02	220	238	1.08	25	20	0.81
STM-1	560	631	1.13	118	122	1.04	270	262	0.97	18	24	1.36	700	710	1.01	1210	1215	1.00	46	18	0.39
W-2	170	181	1.07	21	20	0.97	8	8	0.99	9	7	0.75	190	194	1.02	100	93	0.93	23	22	0.95

r.v., recommended values; XRF, measured values; diff,. Values of XRF/r.v..

Table 2 Regression functions of the calibrations lines for each element

Element	Calibration Constant*				Matrix Correction
	A	B	C	accuracy**	
Ba	0.0000	260.6860	−21.9957	43.4598	$45.3999 \cdot C_{Ti}$
Rb	0.0000	57.6303	0.2737	4.2910	$-0.0018 \cdot C_{Sr} + 0.0434 \cdot C_{Nb}$
Nb	0.0000	67.5046	0.9224	2.4824	0
Pb	0.0000	237.2580	−1.1957	2.2445	$0.0035 \cdot C_{Sr} + 0.0061 \cdot C_{Zr}$
Sr	0.0000	58.9483	2.3152	6.9751	0
Zr	0.0000	63.7892	4.2073	6.3908	$-0.0734 \cdot C_{Sr} - 0.0257 \cdot C_{Rb} + 0.0829 \cdot C_{Nb} - 0.0290 \cdot C_{Y}$
Y	0.0000	82.2626	−4.1427	10.2438	$0.0159 \cdot C_{Sr} - 0.0395 \cdot C_{Zr} - 0.2333 \cdot C_{Rb} + 0.0175 \cdot C_{Nb}$

*$W = AI^2 + BI + C$

W, standard value; I, measured intensity

**$\text{accuracy} = \sqrt{(Ci - Wi)^2/(n-2)}$

Ci, analysis value; Wi, standard value; n, number of samples

Tectonic movements in the central Kyushu, Japan

Takemura K.

The central part of Kyushu, Japan is a locus of active arc-volcanism associated with northwest subduction of the Philippine Sea plate, and there the regional graben-like structure ("Beppu-Shimabara graben") from Beppu Bay to the Shimabara peninsula extends. Subduction of the Philippine Sea plate has played an important role in volcanic, geothermal and tectonic activity in central Kyushu.

There are two main graben–like areas in central Kyushu such as Hohi-volcanic zone in the eastern part and Unzen graben in the west. The tectonic movements in the Hohi-volcanic zone are affected by the activity of Median Tectonic Line and Kokura-Tagawa Line related with the movement of Philippine Sea Plate subduction. Initial northward subduction in late Miocene was formed the half graben structure of initial Hohi-volcanic zone. Relative convergence direction of the Philippine Sea plate shifted counterclockwise at about 1.5 Ma, and the same time west-northwestward subduction enhanced right slip on the Median Tectonic Line. Geologic, gravimetric and seismic data indicate that the Median Tectonic Line has shifted its active trace northward in central Kyushu. As a result, the depocenter adjacent to the transcurrent fault migrated northeastward in the Hohi volcanic zone, from Shonai basin (early Quaternary) to Beppu Bay basin (late Quaternary). The latest depocenter of the Beppu Bay is surrounded by active faults that delineate a rhomboidal basin on the Median Tectonic Line. Eastern Central Kyushu (Hohi-volcanic zone) shows the basin forming history and tectonic evolution at the termination of a large transcurrent fault system of Median Tectonic Line.

Combining fault motions, which were modeled as dislocation planes embedded in an elastic isotropic half space, restored the subsurface structure in Hohi-volcanic zone.

The tectonic movements in Unzen graben must be related to the activity of back arc spreading of Okinawa Trough or volcanic activity around Northwest Kyushu hot region.

(Balneological Society of Japan, Vol.53, no.4)

Lake deposits: Record of volcanic activity and climate variation

Takemura K.

Lake deposits have advantages to get the high-resolution information of environmental change rather than marine sequence. Sedimentation rate of tectonic lakes is ten times or more than ocean environments. Further more the annually deposited sediments in lakes are very useful for detection of environmental change in the similar time interval of observation during last 100 years if we can get good annually sediments sequence.

In convergent island arc, there are different types of lake such as tectonic lakes, volcanic lakes. Lake deposits preserve well the record of volcanic activity and climatic changes at different time solution of annual to 100 thousands years.

Lake Biwa is the largest and oldest fresh-water lake in Japan. Lake Biwa was formed as tectonic depressions, where lacustrine sediments have been continuously deposited at least since the Middle Pleistocene. Deep drillings were carried out in 1970's and 1980's. These studies revealed that the Lake Biwa basin bears a sedimentary sequence of about 900 m thickness, which were deposited in lacustrine or fluvial environments in the Pliocene and the Pleistocene. The uppermost unit is a continuous sequence of lacustrine clay of 250 m thick intercalating more than 50 layers of volcanic ashes. The tephrochronological and paleoclimatological data suggest that the 250 m clay unit has been deposited from the last 430 kyrs and is correlated to major glacial-interglacial cycles. The sequences in Lake Biwa can be correlated in detail by tephras and magnetic stratigraphy (paleointensity and paleosecular variation). The composite records will provide a database and conceptual framework for understanding paleoenvironmental history of Asian summer and winter monsoon.

Pioneer studies on the long (1,400 m deep) sediment core from Lake Biwa revealed that the fluctuations of climatic signals were successfully correlated to the Milancovitch cycles. However, the resolution of analyses was also not high enough to detect shorter-term climate fluctuations. In 1990's, 15 to 20 m long piston cores were taken from three sites in Lake Biwa, and analytical studies at higher-resolution have been done. These studies suggested that the Lake Biwa sediments record climatic fluctuations at millennial to century order, which can be correlated to the Heinlich events or Dansgaard-Oeschger cycles. Some newly discovered fine lamination in the cores implies high potential of the good age control. If we succeed in recovering deep multiple cores without disturbance, it will be a fine source of high-resolution paleoenvironmental proxies of the last 430 kyrs. The paleolimnological setting of Lake Biwa offers outstanding advantages for high-resolution study of the East Asian monsoon climate of the late Quaternary.

Detection on annual or decadal environmental change is very hopeful using the annual sediments from Lake Suigetsu and another maar or coastal lakes.

There are many tephra layers in the sequence of Lake Biwa and other lakes in Japanese Island. We have a catalogue on tephra distributed in Japanese island and surrounding areas during 1 Ma, and those data let us indicate the distribution pattern of wind blow system during geolgic time. Most of tephra were transported from their source volcanic regions by west wind system, and we found tephra of the west distribution from source volcano using the microtephra analysis that is very important tool for finding the trace of volcanic materials. Kawagodaira tephra erupted at about 3000years before in Izu Peninsula is one of them. In the mid-latitude area of the northern hemisphere, westerly wind prevails throughout the year. However, the Kawagodaira volcanic ash layer was found on the western side of the source volcano, indicating that an easterly wind must have prevailed at the time of the Kawagodaira eruption. Three types of pressure distribution result in a prevailing easterly wind: the Baiu frontal type in early summer, the Akisame frontal type in autumn, and the type associated with a huge typhoon.

Another possibility can be indicated that lake sediments are well preserved the record of sea level changes and loess transportation.

(KAGI International Symposium, Beppu, 2004)

Isotope-hydrological study on formation mechanism of carbonate springs at the southeastern foothills of Kuju Volcano, Central Kyushu, Japan

M.Yamada, **K.Amita** and **S.Ohsawa**

Groundwater, which discharge as hot springs, mineral springs, cold springs and well at the southeastern foothills of Kuju Volcano, Central Kyushu, Japan, were collected for δD, $\delta^{18}O$, $\delta^{13}C$ and concentration of dissolved inorganic carbon (DIC) analyses. δD and $\delta^{18}O$ values of the samples definitely show that all of the waters are derived from the local meteoric water. Recharge elevation of the waters is estimated to be about 870−1230m by δD values. The groundwater recharged at such elevations of the southeastern flank of the volcanic edifice discharges as mineral springs at relatively high elevations of the southeastern foothills of Kuju Volcano and partly discharges as hot springs at relatively low elevations there (Nagayu area). The characteristics of $\delta^{13}C$ values and PCO_2 show that magmatic CO_2 is mixed into groundwater discharged from hot springs, the mineral springs and some cold springs. Topographical distribution of concentrations of DIC and the result of groundwater flow analysis by δD values suggest that highly carbonated groundwater is produced by the mixing of magmatic CO_2 into the recharged groundwater at the southeastern flank of the volcanic edifice and the mixed groundwater flow from west to east and form the carbonate water zone at the southeastern foothills of Kuju volcano. These highly carbonated groundwater discharges as the mineral and hot springs, which are mixed with shallow groundwaters dissolved soil CO_2 nearby the discharge areas.

Occurrence of subduction-related fluid in mantle wedge-derived rocks.

Junji Yamamoto, Ichiro Kaneoka, Shun'ichi Nakai, Hiroyuki Kagi, Keiko Sato, Vladimir S. Prikhod'ko and Shoji Arai

To reveal the occurrence of subduction-related fluid in mantle wedge we have investigated the mantle wedge-derived xenoliths based on both trace element and noble gas chemistry.

At least two compositionally distinct groups of fluid are observed in the rocks. One is liquid inclusions filled mostly with CO_2. The other is melt inclusions. Such a melt may have introduced into intergranular region. The grain-boundary component of rocks can be separated by chemical treatment using hot nitric acid. The leachates of the constituent minerals shows an apparent negative Ce anomaly and large depletion in Hf and Zr with W-type tetrad effect. The tetrad effect and negative anomaly in Ce and HFSE in mantle rocks indicate mantle metasomatism related to the specific subduction environments. Further, the melt inclusions show low $^{3}He/^{4}He$ and $^{40}Ar/^{36}Ar$ indicating a component related to the subducted slab. Therefore, these results indicate the contribution of melt derived from a partial melting zone. On the other hand, 3He/4He observed in the CO_2 inclusions, which similar to the MORB-like value, reflect the general character of the upper mantle.

These figures illustrate schematic cross-section beneath the paleo-Far Eastern Russia. We explain history of infiltration of some kinds of fluid into the mantle wedge in the order of events.

1. In the Jurassic-early Cretaceous Period, a subduction zone was formed in Far Eastern Russia. Hydrated peridotite is formed by the addition of slab-derived H_2O beneath convergent margin with subduction zone.

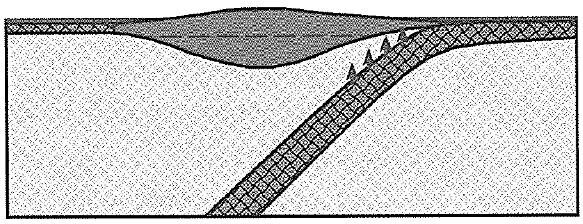

2. Hydrous minerals such as amphibole, chlorite and phlogopite in the hydrated peridotite break down in downward flow of the mantle wedge and release H_2O. Interconnection of the aqueous fluid in the hydrated peridotite is controlled by dihedral angles. At low pressure and temperature, most of the aqueous fluid generated by the successive decomposition of the hydrous minerals in downdragged hydrous peridotite cannot segregate from solids and will be transported to greater depths as free fluid in isolated pores among crystals.

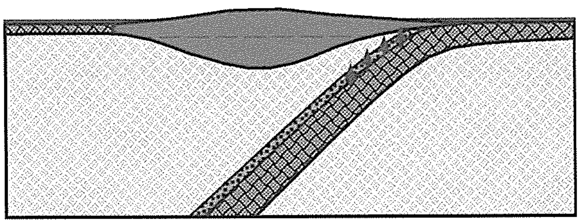

3. The downdragged hydrous peridotite reachs at a region (shaded area) where the dihedral angle is less than 60° aqueous fluid is supplied continuously from the

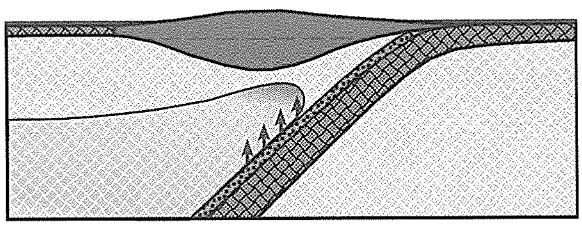

downdragged hydrous peridotite.

4. When the aqueous fluid reaches the region with the solidus temperature of hydrous peridotite (inner shaded area), partial melting in the mantle wedge takes place to produce initial magma.

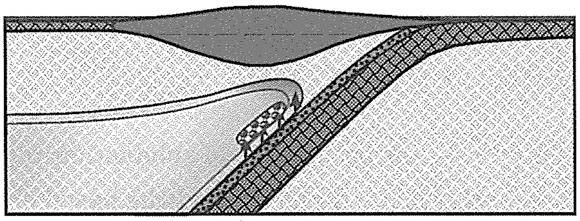

5. If melt segregation occurs, melt will be extracted upwards and ascend through the mantle wedge, leading to subduction-related volcanism.

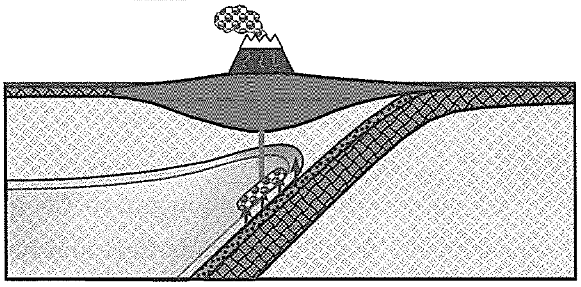

6. Part of the melt should remain in the mantle wedge as a grain-boundary component or as melt inclusions. This melt should also contain an atmospheric component inherited from the water from the subducted slab. Also, the fluids derived from the subducted slab are likely to have inherited high U/^{3}He. This is because U is mobile in water, so that it is likely to partition into aqueous fluids when the slab dehydrates. The high U/^{3}He in the fluids will lead to a rapid decrease in the ^{3}He/^{4}He. Further, depletion in HFSE and Ce with tetrad effect in the grain-boundary component indicates a relationship with the melt.

On the other hand, ^{3}He/^{4}He observed in the CO_2 inclusions, which are similar to the MORB-like value, might reflect the general character of the upper mantle. The Far Eastern Russian mantle was therefore a MORB-like source that has been partly infiltrated by subduction-related fluids.

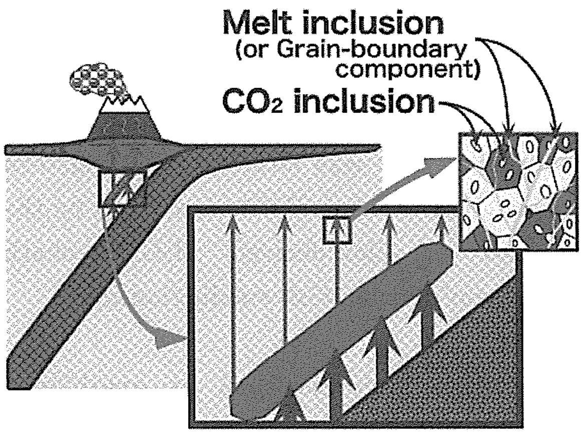

Sr and Nd isotopic composition of dunite channels in the Horoman peridotite complex, Hokkaido, Japan: inference of the origin of passed melt

Masako Yoshikawa[1)] and Kiyoaki Niida[2)]

[1)] Beppu Geothermal Research Laboratory, Institute for Geothermal Sciences Graduate School of Science

Kyoto University, Beppu, 874-0903, Japan

[2)] Division of Earth and Planetary Sciences

Hokkaido University, Sapporo 060-0810, Japan

Peridotites are believed to be upper mantle material and provide direct information on the chemical and isotopic compositions of the upper mantle. Orogenic lherzolite complexes are tectonically emplaced large (kilometer size) pieces of the upper mantle compared with peridotite xenoliths which only represent centimeter to meter size pieces of the mantle. They are thus capable of furnishing structural information about the upper mantle than is provided by xenoliths. These complexes are mainly composed of a depleted peridotite with a small propotion of pyroxenites, dunite and mafic dykes. The mafic and pyroxenite dykes have been interpreted to be formed by crystallization from passed melt (e.g. Shiotani and Niida, 1997). On the bases of the traverse change of isotopic and chemical compositions from peridotite to these dykes, it has been explained that isotopic and chemical heterogeneity of the wall peridotites was caused by melt - solid interaction (e.g. Bodinier et al., 1991). Furthermore, it has been suggested that this interaction was important process to change the composition of upwelling melt through mantle (Kelemen et al., 1990; 1992).

The Horoman peridotite complex is one of the freshest orogenic peridotite complex and has been provided detail petrological and geochemical studies (e.g. Niida, 1984; Obata and Nagahara, 1987; Frey et al., 1991; Takahashi, 1991; 1992; Takazawa et al., 1992; 1995, 1996; Yoshikawa, 1993; Yoshikawa and Nakamura, 2000). In this complex, many dykes, that is spinel rich dunite and wehrlite (Takahashi, 1991, 1992), gabbro (Niida, 1984; Shiotani and Niida, 1997; Takazawa et al., 1999), websterite (Niida and Shiotani, 1997) and dunite (e.g. Niida, 2000), was reported. Isotopic analyses of Sr and Nd of rocks and constituent minerals are powerful tool to constrain the origin of the rocks and minerals. However, isotopic systematics of Sr and Nd for most of dykes in the Horoman complex has not published ,although those of host peridotites (e.g. Yoshikawa and Nakamura, 2000) and gabbro dykes (Takazawa et al., 1999) were reported. Consequently, origin of the melt from which dyles were crystallized is controversial. To discuss the origin of the melt, we analyzed mineral major compositions, trace element and isotopic compositions of separated clinopyroxenes from three dunite dykes which were recent discovered, (Niida, 2000; Niida et al., 2002) and wall rock (harzburgite to lherzolite).

Niida (2001) and Niida et al., (2002) reported following structural and textual characteristics of dunite dykes. They vary from 1cm to more than 3 meters in width, cutting the pre-existing layering and metamorphic fabric of the host rock. Boundaries between the dunite and the wall rock are sharp. A peculiar characteristic of them is the grain size of olivine, which is major constitute mineral (> 90 vol. %) of dunite, various from <100 m to .1.6 m length. Small segregations consisting of clinopyroxene orthopyroxene and spinel is observed apparently in re-entrants at the outer rim of olivine megacryst. On the basis of them, (1) transport of melt through fracture of host rock, (2) crystallization of megacrystic olivine, and (3) successive melt transport resulting in the two-pyroxenes + spinel segregations, were inferred for formation process of dunite dykes (Niida, 2000; Niida et al., 2002).

The Cr# (Cr/(Cr+Al) atomic ratio) values of spinel in each segregations from the three dykes show different ranges, that is 38-42 (sample 1.6) , 48-50 (sample SPR4), 57- 61 (sample 811) and 47-51 (host rock of SPR4, SPR14). The averaged $(Ce/Yb)_N$ ratios (subscript N means chondrite-normalized value) of clinopyroxenes in the segregations are 4.22 for sample 1.6, 2.59 for sample SPR4, 1.15 for sample 811. If the three dykes were made by a simple chemical fractionation process from a single melt, it must be observed correlation between the Cr# - $(Ce/Yb)_N$ ratios. However, it is not given a such correlation from our result. Furthermore, Sr and Nd isotopic composition of them are differ with each samples and each of them is plotted in the range of different mantle component, that is MORB, HIMU and EMII (e.g. Zindler and Hart, 1986) on a Sr-Nd isotope diagram. It has been presumed that the HIMU and EM I components were originated from dehydrated ancient subducted slab and sedimentary materials (e.g. Weaver et al., 1986; Woodhead and McCulloch, 1989; Kogiso et al., 1997). These observations are suggested that each dyke was likely to formed from different melt and these melts might be involved with recycled subducted slab and sediment.

Keywords: geochemistry, upper mantle peridotite, isotopic composition of Sr and Nd, melt-wall rock interaction

(Abstract of The 2nd Kagi21 Internationl Symposium Beppu, 2004)

公表論文および著書 Publications

＜原著論文＞

Du J., Cheng W., Zhang Y., Jian C., and Guan Z. (2005) Helium and Carbon Isotopic Compositions of Thermal Springs in Earthquake Zone of Sichuan, Southwestern China. *Journal of Asia Earth Science*, (in press).

Du J., Liu C., Fu B., Zhang Y., Wang C., Wang H., and Sun Z. (2005) Variations of geothermometry and chemical-isotopic compositions of hot spring fluids in the Rehai geothermal field, Southwest China. *J. Volcano. Geotherm. Res.*, **142**(3-4), 243-261.

Fu B., Awata Y., Du J., and He W. (2005) Late Quaternary systematic stream offsets caused by repeated large seismic events along the Kunlun fault, northern Tibet. *Geomorphology*, (in press).

Fu B., Awata Y., Du J., and He W. (2004) Surface deformations associated with the 2001 Mw 7.8 Kunlun earthquake, northern Tibet: geomorphic growth features of a major strike-slip fault. *Engineering Geology*, **75**, 325-339.

Goto, S., M. Kinoshita, and K. Mitsuzawa (2004) Heat flux estimate of warm water flow in low temperature diffuse flow site, southern East Pacific Rise 17°25'S. *Mar. Geophys. Res.*, in press.

Goto, S., M. Yamano, and M. Kinoshita (2005) Thermal response of sediment with vertical fluid flow to temperature variation at the surface. *J. Geophys. Res.*, **110**, B01106, doi:10.1029/2004JB003419.

Goto, S., H. Hamamoto, and M. Yamano (2005) Climatic and environmental changes at southeastern coast of Lake Biwa over past 3000 years, inferred from borehole temperature profiles, accepted for publication in Phys. *Earth Planet. Int.*

Glasby G. P., Yamanaka T., Yamamoto, J., Sato H., and Notsu K., (2004) Kuroko and Hydrocarbon Deposits from Northern Honshu, Japan: A Possible Common Hydrothermal/Magmatic Origin? , *Resource Geology*, **54**, 413-424.

Hase, H., T. Hashimoto, S. Sakanaka, W. Kanda and Y. Tanaka, (2004) Hydrothermal system beneath Aso volcano as inferred from self-potential mapping and resistivity structure. *J. Volcano. Geotherm. Res.*, accepted December 3, in press.

Hashimoto, T., T. Mogi, Y. Nishida, Y. Ogawa, N. Ujihara, M. Oikawa, M. Saito, Nurhasan, S. Mizuhashi, T. Wakabayashi, R. Yoshimura, A. W. Hurst, M. Utsugi, Y. Tanaka, (2004) Self-potential studies in volcanic areas (5) -Rishiri, Kusatsu-Shirane, and White Island-. *北海道大学理学部紀要第７集（地球物理学）* Vol.**12**, 97-113.

Hirano N., Yamamoto J., Kagi H., and Ishii T., (2004) Young olivine xenocryst-bearing alkali-basalt from the oceanward slope of the Japan Trench. *Contributions to Mineralogy and Petrology* **148**, 47-54.

井上直人・田中靖之・伊藤陽之・岩野祥子・北田奈緒子・福田洋一・竹村恵二, (2004) ２次元重力解析より推定された京都盆地における未固結堆積層の密度－堀川-巨椋池測線および久世橋測線－. *地震*2, **57**, 45-54.

Ishiyama, T., Mueller, K., Togo, M., Okada, A. and Takemura, K., (2004) Geomorphology, kinematic history, and earthquake behavior of the active Kuwana wedge thrust anticline, central Japan. *Jour. Geophys. Res.*, **109**, B12408, doi:10.1029/2003JB002547.

鍵山恒臣, (2005) 火山噴火を決める要素. *土と基礎*, **53**, 33-31.

Kagiyama, T., (2004) Water saturated layer beneath volcano and its implications to volcanic activity. *Indonesian Journal of Physics*, **15**, 1, 6-11.

Kawamoto, T., Matsukage, K. N., Mibe, K., Isshiki, M., Nishimura, K., Ishimatsu, N., Ono, S., (2004) Mg/Si ratios of aqueous fluids coexisting with forsterite and enstatite based on the phase relations in the Mg_2SiO_4-SiO_2-H_2O system. *American Mineralogist*, **89**,1433-1437.

川本竜彦, (2004) マグマと水の間の臨界現象. *高圧力の科学と技術*, **14**, 235-241.

Kawamoto T., Matsukage, K., Nagai, T., Nishimura, K., Mataki, T., Ochiai, S., Taniguchi, T., (2004) Raman spectroscopy of cubic boron nitride under high temperature and pressure conditions: a new optical pressure marker. *Review of Scientific Instruments*, **75**, 2451-2454.

Kawamoto, T., Ochiai, S., Kagi, H., (2004) Changes in the structure of water deduced from the pressure dependence of the Raman OH frequency. *Journal of Chemical Physics (Communications section)*, **120**, 5867-5870.

Kawamoto, T., (2004) Hydrous phase stability and partial melt chemistry of H_2O-saturated KLB-1 peridotite up to the uppermost lower mantle conditions. *Physics of Earth and Planetary Interior*, **143-144**, 387-395.

京都市活断層調査委員会（尾池和夫・岡田篤正・竹村恵二・植村善博・吉岡敏和・松井和夫・古澤　明・園田玉紀・杉森辰次・梅田孝行・斎藤　勝）(2004) 京都盆地の地下構造を南北に分ける宇治川断層の第四紀断層活動. *活断層研究*, **24**, 139-156.

Matsukage, K.N., Ono, S., Kawamoto, T., Kikegawa, T., (2004) The compressibility of a natural apatite. *Physics and Chemistry of Minerals*, **31**, 580-584.

松岡　暁・堤　浩之・竹村恵二 (2004) 雲仙活断層群の第四紀後期における活動-千々石町のおけるトレンチ調査と普賢岳北斜面で確認された断層露頭の解析-. *活断層研究*, **24**, 199-208.

McCammon, C.A., Frost, D.J., Smyth, J.R., Lausten, H.M.S., Kawamoto, T., Ross, N.L., van Aken, P.A. (2004) Oxidation state of iron in hydrous mantle phases: Implications for subduction and mantle oxygen fugacity, *Physics of Earth and Planetary Interior*, **143-144**, 157-169.

Mibe, K., Kanzaki, M., Kawamoto, T., Matsukage, K. N., Fei, Y., Ono, S., (2004) Determination of the second critical endpoint in silicate-H_2O systems using high-pressure and high-temperature X-ray radiography. *Geochimica et Cosmochimica Acta*, **68**, 5189-5195.

Miyazawa, M., I. Nakanishi, Y. Sudo and T. Ohkura (2005) Dynamic response of frequent tremors at Aso volcano to teleseismic waves from the 1999 Chi-Chi, Taiwan earthquake. *J. Volcano. Geotherm. Res.*, in press.

Mizukami T., Wallis S. R. and Yamamoto J. (2004) Natural examples of olivine lattice preferred orientation with a flow-normal a-axis maximum. *Nature*, **427**, 432-436.

Moriguti, T., Shibata, T., Nakamura, T., (2004) Lithium, boron and lead isotope and trace element systematics of Quaternary basaltic volcanic rocks in northeastern Japan: mineralogical controls on slab-derived fluid composition, *Chemical Geology*, **212**, 81– 100.

Nakada, S., Matsushima, T., Yoshimoto, M., Sugimoto, T., Kato, T., Watanabe, T., Ramon, C., Juan T. C. (2005) Geological aspects of the 2003-04 eruption of Anatahan Volcano, Northern Mariana Islands. *J. Volcanol. Geotherm. Res.*, (in press)

Nakanishi, T., Takemura, K., Okada, A., Morino, M., Hayashida, A., Nakamura, M., Tazawa, Y., Ogino, Y., Matsumoto, H. and Hirose, M., (2004) Identification of multiple faulting events of the Median Tectonic Line active fault system in the Tokushima Plain, Japan, based on close-interval radiocarbon dating. *Nuclear Instruments and Methods in Physics Research* B, **223-224**, 573-578.

Nishimura, K., Kawamoto, T., Kobayashi, T., Sugimoto, T., and Yamashita, S., (2005) Melt inclusion analysis of the Unzen 1991-1995 dacite: implications for crystallization processes of dacite magma. *Bull. Volcanol.*, (in press)（doi:10.1007/s00445-004-0400-8）

Nishio Y., Nakai S., Yamamoto J., Sumino H., Matsumoto T., Prikhod'ko V. S., Arai S., and Kumagai H.,

(2004) Lithium isotopic systematics of the mantle-derived ultramafic xenoliths: implications for EM1 origin. *Earth and Planetary Science Letters,* **217**, 245-261.

Notsu K., Sugiyama K., Hosoe M., Uemura A., Shimoike Y., Tsunomori F., Sumino H., Yamamoto J., Mori T. and Hernandez P.A. (2004) Diffuse CO_2 efflux from Iwojima volcano, Izu-Ogasawara arc, Japan. *Journal of Volcanology and Geothermal Research,* **139**, 147-161.

Okada, T., Komatsu, K., Kawamoto, T., Yamanaka, T., Kagi, H., (2005) Pressure response of Raman spectra of water and its implication to the change in hydrogen bond interaction. Spectrochimica Acta A, （印刷中）（doi:10.1016/j.saa.2005.02.022）.

Okubo A., Y. Tanaka, M. Utsugi, N. Kitada, H. Shimizu, T. Matsusima, (2005) Magnetization Intensity Mapping on Unzen Volcano, Japan, Determined from High-Resolution, Low-Altitude Helicopter-Borne Aeromagnetic Surveys. *Earth, Planets and Space,* (in press)

大久保綾子・田中良和・宇津木充・北田直人・清水洋・松島健 (2004) High-Resolution, Low-Altitude Helicopter-Borne Aeromagnetic Survey over Unzen Volcano, Kyushu, Japan, CA研究会2004年論文集, 4-11.

Ren, Z-Y., Shibata, T., Yoshikawa, M., Johnson, K and Takahashi, E., (2005) Isotope compositions of the submarine Hana Ridge lavas, Haleakala volcano, Hawaii: implications for source compositions, melting process and the structure of Hawaiian plume, *J. Petrol*, in press.

Saito T., Ishikawa N. and Kamata H., (2004) Iron-titanium oxide minerals in block-and-ash-flow deposits: implications for lava dome oxidation processes. *J. Volcanol. Geotherm. Res.* **138**, 283-294.

Saito, T., Sakai S., Iizawa I., Suda E., Umetani K., Kaneko K., Furukawa Y. and Ohkura T., (2005) A new technique of radiation thermometry using a consumer digital camcorder: Observations of red glow at Aso volcano, Japan. *Earth Planets Space*, **57** (No. 2), pp. e5-e8.

坂中伸也・M.J.S. Johnston・笹井洋一・田中良和・宇津木充・西田泰典・J.F. Delarue・P.Yvetot, (2004) カリフォルニア州オーウェンズバレーにおける自然電位繰り返し測定、*CA研究会2004年論文集*, 112-119.

千田　昇・竹村恵二・松田時彦・島崎邦彦・池田安隆・岡村　眞・水野清秀・松山尚典・首藤次男 (2004) 大分平野東部に伏在する活断層. *活断層研究*, **24**, 185-198.

Shibata, T. and Yoshikawa, M., (2004) Precise isotopic determination of trace amounts of Nd in magnesium-rich samples, *J. Mass. Spectrom. Soc. Jpn*, **52**, 317-324.

Smyth, J. R., Holl, C. M., Langenhorst, F., Laustsen, H. M. S, Rossman, G. R., Kleppe, A., McCammon, C. A., Kawamoto, T., and van Aken, P. A. (2005) Crystal chemistry of wadsleyite II and water in the Earth's interior. *Physics and Chemistry of Minerals*, **31**, 691 – 705.

杉本　健・石橋秀巳・松島　健（2005）伊豆鳥島火山の岩石学的研究. *火山*, **50**, 87-101.

杉本　健・松島　健（2005）伊豆鳥島火山の噴気活動. *九州大学大学院理学研究院研究報告*, vol. **22**, no. 1, 23-27.

Sugimoto, T., Ishibashi, H., Wakamatsu, S. and Yanagi, T. Petrologic evolution of Pre-Unzen and Unzen magma chambers beneath the Shimabara Peninsula, Kyushu, Japan: Evidence from petrography and bulk rock chemistry. *Geochem. J.* (in press).

竹村恵二 (2004) 中部九州の地殻変動. *温泉科学会誌*, **53**(4), 143-150. 2004.

竹村恵二・香川敬生 (2004) 近畿地方の活断層と強震動. *基礎工*, **32**, (3), 12-15., 2004.

Tatsumi, Y., H. Shukuno, M. Yoshikawa, C. Qing, K. Sato and M.-W. Lee, (2005) The Petrology and Geochemistry of Volcanic Rocks on Jeju Island: Plume Magmatism along the Asian Continental

Margin, *J. Petrol.*, **46**, 523-553.

上原大二郎・角田地文・工藤　健・梅田浩司・小川康雄・棚瀬充史・武田祐啓・千葉昭彦・菊池晃・鍵山恒臣 (2005) 紀伊半島南部地域の重力異常と深部比抵抗構造から推定される地熱構造, *地震*, **57**, 245-255.

Wang C., Du J., Wang W., Xie H., Chen G., Duan Y., (2005) Zhou X. Experimental evidence on existence of hydrocarbon under high pressure and temperature. *Chinese Sci. Bull*, (in press).

Xue, X., Kanzaki, M., Neuville, D. R., Kawamoto, T. (2004) Structure and properties of silicate melts and fluids. *Geochimica et Cosmochimica Acta*. **68**, 5011-5011.

山田誠・網田和宏・大沢信二 (2005) 同位体水文学的手法による九重火山南東麓に湧出する炭酸泉の形成機構の解明, *温泉科学*, **54** (4) , 163-172.

Yamamoto J., Kaneoka I., Nakai S., Kagi H., Prikhod'ko V.S. & Arai S. (2004) Evidence for subduction-related components in the subcontinental mantle from low $^3He/^4He$ and $^{40}Ar/^{36}Ar$ ratio in mantle xenoliths from Far Eastern Russia. *Chemical Geology* **207**, 237-259.

Yamamoto J. and Burnard P. G. (2005) Solubility controlled noble gas fractionation during magmatic degassing: implications for noble gas compositions of primary melts of OIB and MORB. *Geochimica et Cosmochimica Acta* **69**, 727-734.

Yamano, M., S. Goto (2005) Long-term monitoring of the temperature profile in a deep borehole: temperature variations associated with water injection experiments and natural ground water discharge, accepted for publication in *Phys. Earth Planet. Int.*

Yum, J.G., Yu, K.M., Takemura, K., Naruse, T., Kitamura, A., Kitagawa, H. and Kim, J.C. (2004) Holocene evolution of the outer lake of Hwajinpo lagoon on the eastern coast of Korea: environmental changes with Holocene sea-level fluctuation of the East Sea (Sea of Japan). *Radiocarbon*, **46**, (2), 797-808.

＜総説・解説＞

川本竜彦、落合周吉、鍵裕之、(2004) ラマン分光法でみた高温高圧条件での水の構造変化、*現代化学*、９月号, 56-61.

角野浩史, 山本順司, 熊谷英憲 (2005) マントル捕獲岩の希ガス研究：希ガスで探るマントルメタソマティズム, *岩石鉱物科学*, 印刷中.

山本順司, 石橋秀巳, 川上曜子, 鍵裕之 (2005) マントル捕獲岩に適用できる地質圧力計, *岩石鉱物科学*, 印刷中.

山本順司, 鍵裕之 (2005) 二酸化炭素の分子振動をものさしにして地球内部を見る" *現代化学* **409**, 44-49.

<著書＞

火山地震データ編集グループ (2004) 日本の火山性地震・微動のデータベース, 京都大学出版会, (鶴見岳・阿蘇山編集担当)

竹村恵二 (2004) 堆積環境と考古学, 環境考古学ハンドブック（安田喜憲編集）, 朝倉書店,86-98.

竹村恵二 (2004) 分担執筆. 日本の地形６　近畿・中国・四国　（太田陽子ほか編）.

竹村恵二・太田陽子：養老山地・鈴鹿山地と伊勢平野.

増田富士雄・竹村恵二：完新統からみた六甲山南麓の浜堤列の形成過程.

竹村恵二　：鮮新世以降の地層堆積域の変遷からみたテクトニクスの転換期.

＜報告書等＞

Fu B., Awata Y., Du J., and He W., (2004) Rupture geometry and multi-segment rupture of the November 2001 earthquake in the Kunlun fault system, northern Tibet, China. *Annual Report on Active Fault and Paleoearthquake Researches*, No.4:243-264.

Goto Y., Nakada S., Yoshimoto M., Shimano T., Kurokawa M., Sakuma S., Sugimoto T., Noguchi S., Toramaru A., Hoshizumi H., Oguri K. and Uto K. (2005) Conduit drilling at Unzen Volcano, Japan: Descriptions and interpretations of drill cores. *International Workshop on Unzen Scientific Drilling Project, Extend Abstract Volume*, O-9.

長谷英彰・石戸経士・橋本武志・神田径・田中良和 (2004) 九州４火山(開聞岳・九重山・猿葉山・雲仙岳)の岩石のゼータ電位測定, *Conductivity Anomaly 研究会 2004 年論文集*, 25-32.

平林順一・小川康雄・大場武・野上健治・森健彦・鬼澤真也 (2004) 草津白根山の最近の活動状況, 第４回草津白根火山の集中総合観測報告書, 2004, 1-8.Kagiyama, T., Srigutomo, W., Kanda, W., Hashimoto, T., Tanaka, Y. Ogawa, T. and Utsugi, M., Magma supply & emission system of Unzen Volcano deduced from resistivity structure, *International Workshop on Unzen Scientific Drilling*, 41-42.

井上直人・竹村恵二・由佐悠紀, (2004) 由布院盆地の地下構造と堆積物に関する研究（２）, *大分県温泉調査研究会報告*, **54**, 1-6.

井上直人・竹村恵二・由佐悠紀 (2004) 由布院盆地の地下構造と堆積物（２）. *大分県温泉調査研究会報告*, **55** 号, 77－80.

鍵山恒臣・小山悦郎 (2005) 浅間火山 2004 年噴火における噴煙の時間変動, *特定領域研究「火山爆発のダイナミックス」報告書*, 54-56.

鍵山恒臣・小山悦郎 (2005) 浅間火山 2004 年噴火に関連した噴煙の時間変動, *特別研究促進「2004 年浅間火山の噴火に関する総合的調査」報告書*, 54-64.

鍵山恒臣 (2005) 富士山の構造と火山活動－富士山研究がめざすもの, *月刊地球*, 号外 **48**, 12-16.

鍵山恒臣・小河　勉・長田　昇・小山悦郎・小山　茂 (2005) 富士山山麓における熱・電磁気観測, *月刊地球*, 号外 **48**, 35-41.

Kurokawa M., Nakada S., Yoshimoto M., Shimano T., Sugimoto T., Oguri K. and Hoshizumi H. (2005) Magama history of Unzen Volcano, investigated using drilling slime from the conduit drilling (USDP-4). *International Workshop on Unzen Scientific Drilling Project, Extend Abstract Volume*, P-1.

Mori, T., Ishihara, K., Hirabayashi, J., Kazahaya, K. and Mori, T., (2004) SO_2 gas monitoring by DOAS at Sakurajima and Suwanosejima volcanoes. *Annuals of Disas. Prev. Res. Inst., Kyoto Univ.*, **47**, C, 157-162.

森健彦・平林順一・野上健治・鬼澤真也 (2005) 草津白根火山観測システムの構築とその運用について, *第４回草津白根火山の集中総合観測報告書*, 9-16.

Nakada S., Sakuma S., Uto K., Shimizu H., Yoshimoto M., Sugimoto T., Kurokawa M., Shimano T., Goto Y., Hoshizumi H., Oguri K., Nakai S. and Noguchi S. (2005) Real images and petrology of magmatic conduit: results of the conduit drilling at Unzen. *International Workshop on Unzen Scientific Drilling Project, Extend Abstract Volume*, O-8.

大久保綾子・田中良和・宇津木充・北田直人・清水洋・松島健 (2004) High-Resolution, Low-Altitude Helicopter-Borne Aeromagnetic Survey over Unzen Volcano, *京都大学防災研究所年報*第 **47** 号 B, 735-742.

大久保綾子・田中良和・宇津木充・北田直人・清水洋・松島健 (2005) Aeromagnetic Study of Unzen

Volcano, Kyushu, Japan. *Proceeding of 1st International Workshop on Active Monitoring in the Solid Earth Geophysics*, 印刷中).

及川　純・鍵山恒臣・田中　聡・宮町宏樹・筒井智樹・他 8 名, (2004) 人工地震を用いた富士山における構造探査, *月刊地球*, 号外 **48**, 23-26.

鬼澤真也・森健彦・筒井智樹・平林順一・野上健治・小川康雄・松島健・鈴木敦生・草津白根集中観測人工地震探査グループ (2004) 人工地震探査より推定した草津白根火山白根火砕丘表層のＰ波速度構造, 2003 年草津白根火山人工地震探査概要, *第 4 回草津白根火山の集中総合観測報告書*, 91-104.

齊藤政城・平林順一・野上健治・森健彦・水橋正英・及川光弘 (2004) 草津白根山山頂地域から放出される二酸化炭素ガス量, *第 4 回草津白根火山の集中総合観測報告書*, 175-181.

Saito T., Ishikawa N. and Kamata H., (2004) Magnetic petrology of Unzen volcano, Japan: implications for lava dome oxidation processes. *Annuals of Disas. Prev. Res. Inst., Kyoto Univ.*, No 47B, 785-802.

Sugimoto T., Hoshizumi H. and Shimizu H. (2005) Stratigraphy and Petrological Feature of the Borehole Cores from Mayuyama, Unzen Volcano, Japan. *International Workshop on Unzen Scientific Drilling Project, Extend Abstract Volume*, P-7.

杉本　健, 松島　健 (2004) 伊豆鳥島火山の噴気活動. *第 98 回火山噴火予知連絡会資料*

松島　健, 杉本　健 (2004) 伊豆鳥島火山の地震活動および地殻変動. *第 98 回火山噴火予知連絡会資料*

筒井智樹・草薙智浩・梶井達矢・鬼澤真也・森健彦・野上健治・平林順一・小川康雄・水橋正英・及川光弘・齊藤政城・若林亨・高木憲朗・鈴木敦生・田中麻貴・及川純・中道治久・山下祐一郎・吉川慎・松島健・河野裕希・掘美緒 (2004) 草津白根火山湯釜火口周辺の地震反射断面－擬似反射記録法による反射断面の推定－, *第 4 回草津白根火山の集中総合観測報告書*, 105-120.

筒井智樹・鬼澤真也・森健彦・野上健治・平林順一・小川康雄・水橋正英・及川光弘・齋藤政城・若林亨・高木憲朗・鈴木敦生・草薙智浩・梶井達矢・田中麻貴・及川純・中道治久・山下祐一郎・及川純・中道治久・山下祐一郎・吉川慎・松島健・河野裕希・堀美緒 (2004) *第 4 回草津白根火山の集中総合観測報告書*, 81-90.

山田誠・大沢信二　(2004) くじゅうタデ原地域指山湧水の水文化学的研究, *大分県温泉調査研究会報告*, **55**, 5-10.

Yamamoto J. and Burnard P. G. (2004) Solubility controlled noble gas fractionation during magmatic degassing. *Geochimica Cosmochimica Acta* **68**, A572.

吉川慎・須藤靖明 (2004) 阿蘇火山中岳第１火口の温度変化と火山活動　*京都大学防災研究所年報* Vol.**47 B**, 803-807

由佐悠紀・柴田知之・芳川雅子, (2004) 別府温泉南部域の温泉水への海水混入の検出　（１）ストロンチウム同位体による試み、*大分温泉調査研究会報告*, **55**, 1-4.

学会発表　Conference Presentations

相澤広記・吉村令慧・山崎健一・宇都智史・中尾節郎・大志万直人・小川康雄・タンク ブレント・神田 径・橋本武志・坂中伸也・上嶋 誠・小河 勉・小山 茂・鍵山恒臣・塩崎 一郎，広帯域 MT 観測から示唆される富士山周辺地域のテクトニクス，地球惑星科学関連学会 2004 年合同大会 T054-P006, 2004 年 5 月

網田和宏・大沢信二・Jianguo Du・山田誠，大分平野の深部に賦存する有馬型熱水，日本温泉科学会（2004 年 9 月　昭和女子大学）

Amita, K., Utsugi, M., Ichiki, M., Ohsawa, S., Hashimoto, T., Uyeshima, M., Mawatari, H., Kagiyama, T. and Tanaka, Y., Resistivity structure beneath the Kyushu Island inferred from the Network-MT data, The 2nd KAGI21 Symposium, Beppu, Oita, November 1-4, 2004

Aoki, Y. and Kagiyama, T., Crustal deformation of the Kyushu iland, Japan, The 2nd KAGI21 Symposium, Beppu, Oita, November 1-4, 2004.

浅森浩一・梅田浩司・小川康雄・武田祐啓・上原大二郎・鍵山恒臣，鳴子火山下における深部比抵抗構造，地球惑星科学関連学会 2004 年合同大会 V055-012, 2004 年 5 月

常 青、柴田　知之・芳川　雅子、巽　好幸、Precise determination of zirconium, niobium, hafnium and tantalum　for geological samples by inductively coupled plasma mass　spectrometry(ICP-MS)、2004 年度質量分析学会同位体比部会、山形、2004.

Fang, K.C, Chen, C.H, Takemura, K., Song, S.R. and Danhara, T. : Tephra Study in Lake Biwa. The 2nd KAGI21 International Symposium (Beppu, November, 2004).

後藤秀作，濱元栄起，藤野恵子，山野　誠，木下正高，熊野海盆泥火山における長期温度モニタリング，地球惑星科学関連学会 2004 年合同大会（千葉），May 9–13, 2004.

後藤秀作，濱元栄起，山野　誠，孔内温度から推測した琵琶湖南湖東岸の過去 3000 年の気候・環境変動，地球惑星科学関連学会 2004 年合同大会（千葉），May 9–13, 2004.

後藤芳彦，中田節也，吉本充宏，嶋野岳人，黒川　将，杉本　健，野口　聡，寅丸敦志，星住英夫，宇都浩三（2004）雲仙科学掘削によるコアの記載と解釈：火道域の内部構造．日本火山学会 2004 年度秋季大会．

Hamamoto, H., M. Yamano, S. Goto, Heat flow measurement in shallow seas through long-term temperature monitoring, International Workshop on "New and Classical Applications of Heat Flow Studies" (Aachen, Germany), Oct. 4–7, 2004.

濱元栄起，山野　誠，後藤秀作，浅海域における熱流量測定のための海底水温長期観測，地球惑星科学関連学会 2004 年合同大会（千葉），May 9–13, 2004.

Hase, H., T. Hashimoto and T. Ishido, z-potential measurements for volcanic rocks, Grants-in-Aid for Scientific Research "Dynamics of Volcanic Explosion" International workshop on volcanic explosion in KOBE, Japan, 2005.

長谷英彰・石戸経士・橋本武志・古川邦之，ボーリングコアサンプル(高野尾羽根溶岩)のゼータ電位測定，Conductivity Anomaly 研究会，2004.

長谷英彰・石戸経士，火山・地熱地域の岩石ゼータ電位測定の重要性，日本地熱学会，2004.

長谷英彰・石戸経士・橋本武志・長谷中利昭・三好雅也，自然電位と岩石ゼータ電位を利用した地質構造の推定，日本火山学会，2004.

長谷英彰・宇津木充・橋本武志・吉川慎，自然電位分布から推定される阿蘇杵島岳の構造，地球電磁気・地球惑星圏学会，2004.

長谷英彰・宇津木充・橋本武志・吉川慎・田中良和，阿蘇杵島岳の SP 測定，地球惑星科学関連学会，2004.

井口 正人・為栗 健・森 健彦・高山 鉄朗・八木原 寛・平野 舟一郎・大倉 敬宏・吉川 慎: 諏訪之瀬島火山の小規模噴火に伴う長周期地震波パルスについて., 地球惑星科学関連学会 2004年合同大会（2004 年 5 月 ：幕張メッセ）
井口正人・山本圭吾・橋本武志・筒井智樹・田中聡・鬼沢真也・青木陽介・渡俊樹・大倉敬宏・清水洋・八木原寛・宮町宏樹・平松秀行・為栗健・高山鉄朗・福嶋麻沙代・Hetty Triastuty・石原和弘・大島弘光・鈴木敦生・前川徳光・梶井達矢・渡辺義明・荻原庸平・野上健治・及川光弘・平林順一・辻浩・平田安廣・奥田隆・伊藤拓・吉川慎・井上寛之・池田さや香・堀美緒・斎藤政城・平野舟一郎・上釜友大・井口元冶・竹下孝弘: 口永良部島火山における人工地震探査の目的と概要, 防災研究所研究発表講演会 2005年2月
池田さや香・大倉敬宏: 阿蘇火山における長周期微動一発生源の時間変化一. 防災研究所研究発表講演会 2005年2月
Inoue N. and Takemura K., 2004, Regional tectonic feature of Southwest Japan based on integrated study of separated gravity anomalies and various geological and geophysical information, WPGM (Hawaii), 12 Aug.
井上直人・黄 昭姫・相場 学・林田 明・松藤和人・Kidong BAE, 2004, 韓国全谷里遺跡周辺における比抵抗調査, 第四紀学会 2004 年大会（山形）, 8 月 23-24 日.
井上直人・土志田 正二・竹村恵二, 2004, 2 次元重力解析による山科盆地の基盤構造, 地震学会秋季大会, 10 月 13 日（福岡）.
Inoue N., Kitada, N. and Takemura, K.: Integrated study of Osaka sedimentary basin with geosciences-Basement structure of northeastern part of Osaka-wan fault based on integrated study of gravity and seismic reflection data-. Hokudan 2005 International Symposium on Active Faulting, Hokudan, Japan, January 17th ~ 24th, 2005
Inoue N., Kitada, N., Kohara, M., Kagawa, T., Takemura, K. and Okada, A.:Relationship between subjacent source faults and surface faults- 3D visualization of integrated information -. Hokudan 2005 International Symposium on Active Faulting, Hokudan, Japan, January 17th ~ 24th, 2005
井上直人・小島健司・竹村恵二, 2004, 反射法地震探査および重力探査を統合した琵琶湖における地下構造, 地震学会秋季大会, 10 月 13 日（福岡）.
Inoue, N. and Takemura K.: Configuration of Paleogene rocks around Unzen volcano, Shimabara Peninsula, Kyushu, Japan, inferred from gravity analysis. Nagasaki (Japan), Unzen Workshop 2005, (2005)
Inoue N. and Takemura K., 2004, Underground structure around Unzen volcano, Shimabara Peninsula, Kyushu, Japan, inferred from gravity analysis, 13 Dec. AGU, (San Francisco).
Inoue (Kitada) N., Utsugi M. and Tanaka Y., 2004, Continuous and absolute geomagnetic field observation in Aso Volcanological Laboratory, Kyoto University, Japan, IAGA WS, 16 Nov. (Tsukuba).
Ito H., Kitada, N., Iwaki, H., Kawamura, D., Takemura, K. and Mitamura, M.: Subsurface geology around Osaka Bay area using borehole data. Hokudan 2005 International Symposium on Active Faulting, Hokudan, Japan, January 17th ~ 24th, 2005
Ito H., Kitada N., Takemura K., Mitamura M. and Suwa S.: Subsurface Geology around Osaka Bay area using Borehole Data. Western Pacific Geophysics Meeting (Hawaii, USA, August 2004)
Hiroko Ito, Kitada, N., Takemura, K., Mitamura, M. and Suwa, S.: Holocene deposit in Osaka tectonic basin, southwest Japan– Subsurface structure obtained from borehole database –. Hokudan 2005

International Symposium on Active Faulting, Hokudan, Japan, January 17th ~ 24th, 2005

Iwaki H., Kitada, N., Inoue, N., Kagawa, T., Takemura, K. and Okada, A.:Relationship between subjacent source faults and surface faults- Compiling the catalog of study earthquake -. Hokudan 2005 International Symposium on Active Faulting, Hokudan, Japan, January 17th ~ 24th, 2005

鍵山恒臣・井口正人, インドネシア・ブロモ火山における噴煙の短周期変動, 日本火山学会 2004年秋季大会 P69, 2004 年 10 月 19-21, 静岡

鍵山恒臣・小山悦郎, 赤外映像装置で捉えた浅間火山における噴煙活動の活発化, 日本火山学会 2004 年秋季大会 S16, 2004 年 10 月 19-21, 静岡

鍵山恒臣・井口正人・小山悦郎, 赤外・可視映像による火山噴煙の短周期時間変動の解析, 地球惑星科学関連学会 2004 年合同大会 V065-012, 2004 年 5 月

鍵山恒臣・小山悦郎, 浅間火山 2004 年噴火における噴煙の時間変動, 火山爆発シンポジウム, 東京, 3 月 1-3 日, 2005

Kagiyama, T., Srigutomo, W., Kanda, W., Hashimoto, T., Tanaka, Y. Ogawa, T. and Utsugi, M., Magma supply & emission system of Unzen Volcano deduced from resistivity structure, International Workshop on Unzen Scientific Drilling 2005, 2005.2.28, Shimabara.

Kagiyama, T. and Iguchi, M, Analysis of short-period variation of volcanic plume by infrared-visible image, International Workshop on Volcanic Explosion, 2005.1.11-13, Kobe.

Kagiyama, T. and Tanaka, Y., Structure of volcano and its implications to volcanic activity, The 2nd KAGI21 Symposium, Beppu, Oita, November 1-4, 2004.

金田平太郎・井上　勉・竹村恵二・金原正明：山地斜面におけるピット調査から推定された駄口断層の短い活動間隔. 地球惑星科学関連学会 2004 年合同大会（幕張メッセ, 千葉, 2004 年 5 月）

風早康平・森俊哉・首藤知昭・森健彦・平林順一・中堀康弘・宮下誠・飯野英樹・篠原宏志・斎藤元治, ポータブル SO2 放出量測定器の開発（その３）：観測方法の評価および COSPEC との比較, 地球惑星科学関連学会合同大会予稿集(CD-ROM), 2004, V055-P039.

木村　亮, 後藤秀作, 溝口智信, 木下正高, 表層コア・ODP 物性の詳細な検討による室戸沖南海トラフ付加前縁構造の推定, 地球惑星科学関連学会 2004 年合同大会(千葉), May 9–13, 2004.

北田奈緒子・井上直人・竹村恵二・香川敬生・岡田篤正：地表地震断層と深部起震断層について. 日本第四紀学会 2004 年大会（山形大学, 山形, 2004 年 8 月）

Kitada N., Ito H., Iwaki H., Suwa S., Kawamura D., Takemura K. and Mitamura M.: Holocene Deposit in Osaka tectonic basin, Southwest Japan –Subsurface Structure Obtained from Borehole Database –. Western Pacific Geophysics Meeting (Hawaii, USA, August 2004)

Kitada N., Inoe N., Takemura K., Kagawa T,, Tsutusmi H. and Okada A.: Relationship between surface ruptures and subjacent source faults. AGU Fall Meeting (San Francisco, USA, December 2004)

Kitada N., Inoue, N., Takemura, K., Kagawa, T., Tsutsumi, H. and Okada, A.:Relationship between subjacent source faults and surface faults- Correlation analysis -. Hokudan 2005 International Symposium on Active Faulting, Hokudan, Japan, January 17th ~ 24th, 2005

Kitada N., Inoue, N., Takemura, K., Hayashida, A. and Suwa, S.: Integrated study of Osaka sedimentary basin with Geosciences- Late Quaternary activity of Osaka-wan fault near the urban area along Kobe on the basis of high-resolution sedimentological analysis -. Hokudan 2005 International Symposium on Active Faulting, Hokudan, Japan, January 17th ~ 24th, 2005

小山真人・鍵山恒臣・中川和之・橋本 学・第４回地震火山こどもサマースクール実行委員会, 第

４回地震火山こどもサマースクール「活火山富士のひみつ」，地球惑星科学関連学会 2004 年合同大会 J035-P006, 2004 年 5 月

黒川 将，中田節也，杉本 健,嶋野岳人,星住英夫,吉本充宏，下司信夫,宇都浩三 : USDP-4 試料（カッティングス）より推定される雲仙火山のマグマ発達史．地球惑星科学関連学会 2004 年合同大会,幕張．

黒川 将，中田節也，吉本充宏，嶋野岳人，杉本 健，小栗和清，星住英夫（2004）火道掘削試料（カッティングス）を用いた雲仙火山の岩石発達史．日本火山学会 2004 年度秋季大会．

楠本 成寿・竹村 恵二：カルデラの規模とマグマ溜りの収縮条件の関係．地球惑星科学関連学会 2004 年合同大会（幕張メッセ，千葉，2004 年 5 月）

楠本成寿・竹村恵二: カルデラ形成に必要なマグマ溜りの収縮．日本火山学会（東海大学、清水、2004 年 10 月）

Kusumoto S. and Takemura K.：「Depth of a magma chamber deciding an initial caldera geometry」, Nagasaki (Japan), Unzen Workshop 2005, (2005)

松岡 暁・堤 浩之・竹村 恵二・服部 泰久・小宮 大伸：雲仙活断層群の第四紀後期における活動-千々石町におけるトレンチ掘削調査と普賢岳北斜面で確認された断層露頭の解析-．地球惑星科学関連学会 2004 年合同大会（幕張メッセ，千葉，2004 年 5 月）

松島 健，杉本 健（2004）伊豆鳥島火山の地震活動および地殻変動．日本火山学会 2004 年度秋期大会

松島 健，杉本 健（2004）伊豆鳥島火山の地殻変動と地震活動．日本地震学会 2004 年度秋期大会

宮崎 隆・柴田 知之・芳川 雅子・坂本 竜彦・飯島 耕一、表面電離型質量分析計による鉛同位体分析に使用するシリカゲルイオン化活性剤の粒度とイオンビーム強度との関係解明の試み（鉛同位体分析に有効なシリカゲルの物理化学条件の解明を目指して）、2004 年度質量分析学会同位体比部会、山形、2004.

宮崎 隆，柴田 知之，芳川 雅子、表面電離型質量分析計による鉛同位体分析のための新しいシリカゲル合成方法．2003 年度質量分析学会同位体比部会、伊東、2003.

宮崎 隆・柴田 知之・芳川 雅子，南インド，ダルワールクラトン周辺部における始生代大陸下リソスフェアマントルの形成と進化．2004 年度日本地球化学会第 51 回年会．9 月 静岡，2004.

宮崎 隆・柴田 知之・芳川 雅子，南インド大陸下エンリッチリソスフェアマントルの形成と進化．地球惑星科学関連学会 2004 年度合同学会，千葉（幕張）、千葉、2004.

Miyazaki, T., Shibata, T., Yoshikawa, M. and Ram Mohan, V., Source of the Yelagiri and Sevattur alkaline plutons, south India -Examination based on lead isotope ratios-. International Symposium and Field Workshop on Gondwana Evolution and Dispersal. Kochi, 2004.

森健彦・吉川慎・平林順一・野上健治・及川光弘・水橋正英・風早康平・篠原宏志・森俊哉・首藤知昭，九州の火山の SO2 放出量と火山活動について～DOAS による計測（阿蘇・諏訪之瀬島・桜島）～，地球惑星科学関連学会 2004 年合同大会，地球惑星科学関連学会合同大会予稿集(CD-ROM)，2004，V055-P027.

森健彦・吉川慎・吉川美由紀・須藤靖明・平林順一，二酸化硫黄放出量の変化と阿蘇火山の活動について，日本火山学会講演予稿集，2004，No.2，67-67.

中坊真・吉川慎・須藤靖明・筒井智樹・小野博尉・吉川美由紀・迫幹雄・井上寛之・森健彦・大倉敬宏・宇津木充: 1993 年一2004 年までの阿蘇火山の地盤変動について．防災研究所研究発

表講演会 2005 年 2 月

中田節也，吉本充宏，杉本　健，嶋野岳人，黒川　将，星住英夫，後藤芳彦，野口　聡，小栗和清，宇都浩三（2004）火道の実態：雲仙火山火道掘削の成果（２）．日本火山学会 2004 年度秋期大会

中村 洋介・岡田 篤正・竹村 恵二：北陸地方東部の活断層とその上下変位速度．地球惑星科学関連学会2004年合同大会（幕張メッセ，千葉，2004年5月）

中村洋介・岡田篤正・竹村恵二：火山灰稀産地域における，ほぼ同一時代に形成された河成段丘面の分布形態に関する研究～北陸地方東部の河成段丘群を事例として～．日本第四紀学会2004年大会（山形大学，山形，2004年8月）

Nakamura Y., Okada, A. and Takemura, K.: Late Quaternary activity of active faults in the eastern Hokuriku region, northern part of central Japan, on the basis of precise microtephra analysis of fluvial terraces. Hokudan 2005 International Symposium on Active Faulting, Hokudan, Japan, January 17th ~ 24th, 2005

Nakanishi T., Takemura K., Okada A., Sugai T., Naruhashi R., Hayashida A., Nakamura M., Tazawa Y., Ogino K., Matsumoto H. and Hirose M.: Recurrence interval of the Kuwana fault Reconstructed from Holocene synfaulting shallow marine Sediments on the western margin of the Nobi Plain, central Japan. Hokudan 2005 International Symposium on Active Faulting, Hokudan, Japan, January 17th ~ 24th, 2005

Nishimura, K. The role of water in the evolution of silicic magma chambers: A numerical approach to crystal settling followed by partial resorption and renewed growth, The 2nd KAGI21 Symposium, Beppu, Oita, November 1-4, 2004

西村光史、珪長質マグマ溜まりにおける分別結晶作用と再平衡化の熱物質輸送モデル、日本地質学会大111年学術大会、2004年9月、千葉

大倉敬宏・及川純: 阿蘇火山におけるGPS観測(序). 火山学会　秋季大会　2004年10月

大沢信二：前弧地殻内流体の生成機構解明のための Probe としての深層熱水：温泉科学からのアプローチ．2004 年地球惑星科学関連学会合同大会，セッション J078 断層帯のレオロジーと地震の発生過程，幕張メッセ，2004 年 5 月 10 日

Ohsawa, S. : Geochemical characteristics of carbonated brines along Median Tectonic Line, South-West Japan: Implication for upward migration of dehydrated fluids from subducting Philippine Sea Plate. The 2nd KAGI21 International Symposium Beppu, 2004. B-con Plaza, Beppu, 1-4 November 2004

大沢信二：中央構造線に沿って分布する塩水の地球化学的特徴：プレート脱水流体との関連性の解明．東京大学海洋研究所共同利用シンポジウム「南海トラフ地震発生帯の深海掘削」，東京中野，2005年1月20日

及川光弘・平林順一・井口正人・森健彦・八木原寛，諏訪之瀬島の爆発的噴火とSO2放出量，日本火山学会講演予稿集，2004，No.2，66-66.

及川 純・鍵山恒臣・田中 聡・宮町宏樹・筒井智樹・池田 靖・渦山弘明・松尾のり道・西村裕一・山本圭吾・渡辺俊樹・大島弘光・山崎文人・富士山人工地震構造探査グループ，富士山における 2003 年人工地震探査：初動読み取りと解析，地球惑星科学関連学会 2004 年合同大会 V055-019, 2004 年 5 月

及川 純・鍵山恒臣・田中 聡・宮町宏樹・筒井智樹・池田 靖・渦山弘明・松尾のり道・大島弘光・西村裕一・山本圭吾・渡辺俊樹・山崎文人・富士山人工地震構造探査グループ，人工地

震を用いた富士山における地下構造探査，日本火山学会 2004 年秋季大会 A09, 2004 年 10 月 19-21，静岡

岡田篤正・植村善博・東郷正美・竹村恵二・吉岡敏和・堤　浩之・梅田康弘・尾池和夫・松井和夫・杉森辰次・園田玉紀・杉山直起・梅田孝行：亀岡断層帯（京都府）の第四紀断層運動と地下構造．日本第四紀学会 2004 年大会（山形大学，山形，2004 年 8 月）

Okada A., Suzuki Y., Watanabe M., Takemura K., Kyung J. and Kitagawa H.: Trench excavation surveys across the Ulsan fault system in the southeastern part of Korean Peninsula : Additional data at Kalgok-ri trench and recent informations. Hokudan 2005 International Symposium on Active Faulting, Hokudan, Japan, January 17th ~ 24th, 2005

Okubo, Y., H.-C. Kim, Y. Uchida, S. Goto, J. Safanda, Borehole data and climate reconstruction in Korea, International Workshop on "New and Classical Applications of Heat Flow Studies" (Aachen, Germany), Oct. 4–7, 2004.

鬼澤真也・森健彦・筒井智樹・平林順一・野上健治・松島健，草津白根火山における人工地震探査－P 波速度構造－，地球惑星科学関連学会 2004 年合同大会，地球惑星科学関連学会合同大会予稿集(CD-ROM)，2004，V055-P014.

齋藤政城・平林順一・野上健治・森健彦・水橋正英・及川光弘，草津白根山山頂域から放出される二酸化炭素ガス量，日本火山学会講演予稿集，2004，No.2，150-150.

Saito T., Ishikawa N. and Kamata H., Magnetic petrology through Fe-Ti oxide minerals in various modes of eruption: case studies of Unzen and other volcanoes. 2004 AGU fall meeting, San Francisco, USA, 2004年12月.

Saito T., Ishikawa N. and Kamata H., Deuteric oxidation process through magnetic petrology of Fe-Ti oxide minerals - case study of dome growth at Unzen volcano. International Workshop on Unzen Scientific Drilling Project, Shimabara, Japan, 2005年2月.

齋藤武士・石川尚人・鎌田浩毅，雲仙火山の平成噴火溶岩のmagnetic petrology：溶岩ドーム内部の高温酸化現象．地球惑星科学関連学会，千葉，2004年5月.

齋藤武士，マグネティックペトロロジーで何がわかるのか？．三朝ジオダイナミクスワークショップ2004，三朝，2004年10月.

齋藤武士・鎌田浩毅・石川尚人・小林哲夫・井口正人，鉄チタン酸化物からみた噴火様式の多様性–雲仙・由布・諏訪之瀬島火山の事例–．火山学会，静岡，2004年10月.

Shibata, T., Contribution of Crustal Materials to Island Arc Magmas: Implication for Detailed Investigation of Material Recycling in Subduction Zone Inferred from Trace and Isotopic Compositions of Arc Magmas, The KAGI21 Intern. Symp. Beppu, Beppu, Japan, 2004.

柴田　知之、九州弧第四紀マグマの微量元素・同位体組成の島弧縦断方向の変化、2004 年度質量分析学会同位体比部会、山形、2004.

柴田　知之、同位体・液相濃集元素組成を用いた沈み込み帯における物質循環の研究、地球惑星科学関連学会合同学会 2004、幕張、千葉、2004.

柴田知之・酒寄　淳史・常　青・巽　好幸、微量元素・同位体組成を用いた東北日本孤蔵王火山に共存するソレアイト・カルクアルカリ両系列の起源物質の推定、地球惑星科学関連学会合同学会 2004、幕張、千葉、2004.

柴田　知之、九州弧第四紀マグマの微量元素・同位体組成の島弧縦断方向の変化、2004 年度質量分析学会同位体比部会、山形、2004.

杉本　健，石橋秀巳，松島　健（2004）伊豆鳥島火山のマグマ供給系の進化．地球惑星科学関連

学会 2004 年合同大会

杉本　健，松島　健（2004）鳥島火山の噴気活動．日本火山学会 2004 年度秋期大会

高橋　俊郎・芳川　雅子・柴田　知之・巽　好幸、島弧ソレアイト・カルクアルカリ系列火山岩の斜長石斑晶の局所 Sr 同位体組成分析 -東北日本蔵王火山の例、2004 年度質量分析学会同位体比部会、山形、2004.

高橋俊郎・芳川雅子・柴田知之・巽好幸、東北日本蔵王火山に産するソレアイト・カルクアルカリ系列火山岩の斜長石斑晶の局所 Sr 同位体組成．地球惑星科学関連学会合同学会 2004、幕張、千葉、2004.

高橋　俊郎・芳川　雅子・柴田　知之・巽　好幸、斜長石斑晶の高精度局所 Sr 同位体比分析,日本火山学会 2003, ,福岡、2003.

高橋俊郎，芳川雅子，柴田知之，巽好幸、斜長石斑晶の高精度局所 Sr 同位体比分析、2003 年度質量分析学会同位体比部会、伊東、2003.

Takemura K.: Lake deposits: Record of volcanic activity and climatic variation. The 2nd KAGI21 International Symposium　(Beppu, November, 2004).

Takemura K., Matsuoka A. and Tsutsumi H. : Late Quaternary Activity of active faults in the Unzen Graben, western Kyushu, Japan,based on tectonic geomorphology. AGU Fall Meeting (San Francisco, USA, December 2004)

Takemura K., Inoue N., Kitada, N., Itoh, Y. and Kusumoto, S.:　Integrated study of Osaka Sedimentary Basin with geosciences- Active tectonics and basin formation -. Hokudan 2005 International Symposium on Active Faulting, Hokudan, Japan, January 17th ~ 24th, 2005

Takemura K., Matsuoka A., Tsutsumi H. and Inoue N.: Late Quaternary Activity of active faults based on tectonic geomorphology and subsurface structure in the Unzen Graben, western Kyushu, Japan. Nagasaki (Japan), Unzen Workshop 2005, (2005)

土志田　正二・岡田　篤正・竹村　恵二：堆積速度から推定する京都盆地の形成過程．地球惑星科学関連学会 2004 年合同大会（幕張メッセ，千葉，2004 年 5 月）

土志田正二・岡田篤正・竹村恵二：京都盆地における地下構造の三次元解析．日本第四紀学会 2004 年大会（山形大学，山形，2004 年 8 月）

Vaglarov, B., Shibata, T. and Yoshikawa, M. Precise Isotope Determination of Trace Amounts of Nd in Magnesium-rich Samples、2004 年度質量分析学会同位体比部会、山形、2004.

八木原寛・平野舟一郎・井口正人・為栗健・高山鉄朗・大倉敬宏・森健彦・吉川慎，諏訪之瀬島火山の火山性地震の発生位置，日本火山学会講演予稿集，2004，No.2，75-75.

山田誠・大沢信二・風早康平・安原正也，九重火山・阿蘇火山地域の湧水に含まれる炭酸成分の起源，地球惑星科学関連学会 2004 年合同大会（2004 年 5 月：幕張メッセ）

山本圭吾・井口正人・橋本武志・筒井智樹・田中聡・青木陽介・鬼澤真也・渡辺俊樹・清水洋・大倉敬宏・宮町宏樹・八木原寛・平松秀行: 2004年口永良部島火山人工地震探査データを用いた地下構造解析．防災研究所研究発表講演会 2005年2月

山本順司，火山性ヘリウム同位体比とは一噴気希ガスのソースー．火山性流体討論会，茨城県水海道市，Jun. 25-27，2004,

Yamamoto J., Occurrence of subduction-related fluid in mantle wedge-derived rocks. KAGI International Symposium Beppu, Beppu, Japan, Nov. 1-4, 2004

Yamamoto J. and Burnard P. G., Solubility controlled noble gas fractionation during magmatic degassing. Goldschmidt conference, Copenhagen, Denmark, Jun. 5-11, 2004

Yamano, M., S. Goto, H. Hamamoto, E. Gordeev, Long-term temperature monitoring in boreholes in Japan and Kamchatka, International Workshop on "New and Classical Applications of Heat Flow Studies" (Aachen, Germany), Oct. 4–7, 2004.

山野　誠，後藤秀作，濱元栄起，Evgenii Gordeev，掘削孔内温度の時間変動の観測，地球惑星科学関連学会 2004 年合同大会（千葉），May 9–13, 2004.

山野　誠，木下正高，濱元栄起，後藤秀作，藤野恵子，熊野沖南海トラフ沈み込み帯における熱流量分布，地球惑星科学関連学会 2004 年合同大会（千葉），May 9–13, 2004.

Yamano, M., S. Goto, H. Hamamoto, E. Gordeev, Long-term temperature monitoring in boreholes in Japan and Kamchatka, International Workshop on "New and Classical Applications of Heat Flow Studies" (Aachen, Germany), Oct. 4–7, 2004.

山崎一・高松信樹・網田和宏・山田誠・大沢信二・加藤尚之：別府市内を流れる河川に与える温泉の影響，（2004 年 9 月　昭和女子大学）

山崎一・高松信樹・大沢信二・網田和宏・山田誠・加藤尚之，大分県別府地域の河川に及ぼす温泉の影響，日本陸水学会（2004 年　9 月　新潟大学）

Yoshikawa, M. and Niida, K.：Sr and Nd isotopic composition of dunite channels in the Horoman peridotite complex, Hokkaido, Japan:　inference of the origin of passed melt, The 2nd KAGI21 International Symposium, Beppu, 1-4, Nov., 2004

芳川雅子・新井田清信、幌満かんらん岩体ダナイト脈の Sr-Nd 同位体組成：通過メルトの起源、日本地質学会、千葉、9 月 18-20 日, 2004.

芳川雅子・小澤一仁、早池峰 - 宮守かんらん岩体の化学・同位体組成の特徴からみた島弧下マントルでのメルト形成過程、地球惑星合同学会、幕張、2004.

吉川慎・須藤靖明　阿蘇火山中岳第一火口の温度変化と火山活動地球惑星科学関連学会 2004 年合同大会，地球惑星科学関連学会合同大会予稿集(CD-ROM)，2004 V055-P029

吉川慎・井上寛之・中坊真・須藤靖明・迫幹雄・北田直人・吉川美由紀・宇津木充・森健彦・大倉敬宏・田中良和: 阿蘇火山の水準測量　–長期間の変動–. 火山学会　秋季大会　2004年10月

吉本充宏，嶋野岳人，小山悦郎，飯田晃子，黒川　将，岡山悠子，野中美雪，安田　敦，北澤園子，小森和子，小屋口剛博，中田節也，星住英夫，石塚吉浩，古川竜太，篠原宏志，野上健治，鬼沢真也，長井雅史，新堀賢志，杉本　健（2004）浅間山 2004 年噴火の噴出物について．日本火山学会 2004 年度秋期大会

共同研究　Collaborations

国内

後藤秀作・谷口真人（総合地球環境学研究所）：都市の地下環境に残る人間活動の影響，総合地球環境学研究所プロジェクト研究

後藤秀作・山野　誠（東京大学地震研究所）：南海トラフ沈み込み帯の温度構造の研究，一般共同研究

鍵山恒臣：特別研究促進「2004 年浅間火山の噴火に関する総合的調査」（代表：東大地震研，中田節也），　熱的観測を分担

鍵山恒臣：東大地震研と霧島・三宅島・伊豆大島・浅間山・富士山の火山活動に関する電磁気学的研究を行っている.

川本竜彦：東京大学地震研究所　一般共同研究研究員

川本竜彦：愛媛大学地球深部ダイナミクス研究センター　客員研究員

川本竜彦：岡山大学固体地球研究センター　共同利用研究員

川本竜彦：スプリング８高輝度光科学研究センター　外来研究員

森健彦：京都大学防災研究所一般共同研究(16G-05)：「火山ガス放出量と爆発メカニズム」（代表：平林順一）

大沢信二　河川に及ぼす温泉水の影響評価に関する環境化学的研究，参加機関：東邦大学理学部化学科

齋藤武士：東京大学地震研究所　特定共同研究 B（プロジェクト名：活火山における噴火様式の時代的変遷と長期的噴火予知の基礎研究，研究分担課題：雲仙火山の鉄チタン酸化物の岩石磁気学的解析による溶岩ドームの噴火・崩壊機構の解明

杉本　健・中田節也，東京大学地震研究所，平成１６年度一般共同研究（研究課題：雲仙火山における噴火史の解読研究）

杉本　健・星住英夫・清水　洋，非公的共同研究（研究課題：雲仙火山眉山の火山活動史の解明）

竹村恵二：「地域地盤研究部会：地質 WG，　土質 WG」関西圏地盤研究会　関西圏地盤情報の研究協議会

竹村恵二：京都大学防災研究所一般共同研究　代表：三村　衛　（分担）：地盤データベースを活用した堆積平野地盤の高精度地質学的分析と都市地盤防災への適用に関する研究

竹村恵二：国際日本文化研究センター共同研究員

山本順司・中井俊一：東京大学地震研究所，平成１６年度一般共同研究（研究課題：ウェッジマントル起源の捕獲岩に含まれる流体から沈み込み帯の物質循環系を探る）

芳川雅子：「幌満かんらん岩体ダナイト脈の地球化学的研究」　北海道大学：新井田清信

国際

後藤秀作・大久保泰邦・内田洋平（産業技術総合研究所）・Kim Hyoung Chan（韓国地質鉱物研究院）：韓国の地下温度データを利用した気候変動復元の研究，一般共同研究

鍵山恒臣：振興調整費，雲仙火山：科学掘削による噴火機構とマグマ活動解明のための国際共同研究（代表者：産総研，宇都浩三），電磁気探査による火山体構造解析を分担

竹村恵二：「High resolution reconstruction of Holocene environmental changes from lagoonal sediments along the East Sea (the Japan Sea)」(Prof. Yu, Yonsei University, Korea)

竹村恵二：ICDP Project "Lake Biwa and Lake Suigetsu: Recorders of Global Paleoenvironments and Island Arc Tectonics"

芳川雅子，柴田知之：「斜長石とガラスを用いた阿蘇火山のマグマ供給系進化過程の解明」 京都大学大学院人間・環境学研究科：金子克哉、Institute of Earth Sciences, Academia Sinica, Taiwan: Chang-Hwa Chen

定常観測 Routine Observations

Geophysical Monitoring Under Operation at AVL

Aso Volcanological Laboratory

Permanent Stations

<u>Nakadake monitoring network</u>

Seismic Stations : HNT, PEL, KSM, SUN, KAE, KAE, KAN, UMA, TAK (microwave telemetry)
Tiltmeters : HNT (water tilt 3-comp.), SUN, KAE, NAR, UMA, KAK (on-site logging)
Extensometers : HNT (invar 3-comp.)
Microphone : HND (microwave telemetry)
Geomagnetic Stations : C1, C3, S0, W1, CS, NGD, FF1 (proton; on-site logging)
C223 (fluxgate 3-comp.; on-site), newC223 (fluxgate 3-comp.; online)
FF2 (proton; online)
Ground Temperature : KAK (boreholes of 70 and 150 m deep; microwave telemetry)

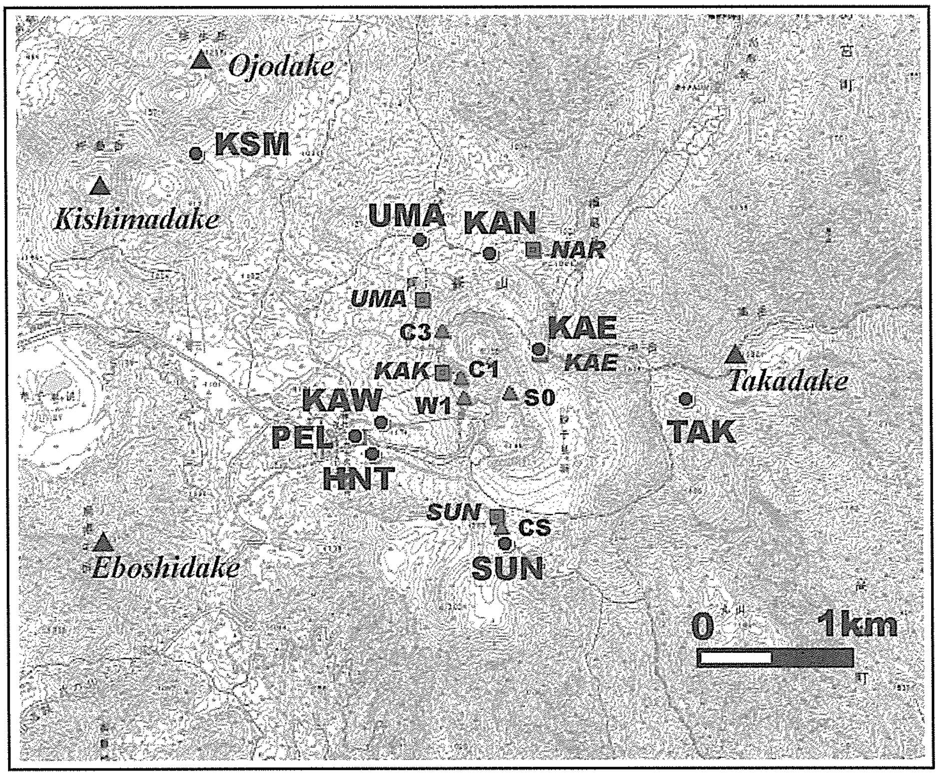

Seismic, geodetic and geomagnetic stations in the central part of Aso.

Kuju monitoring network

Seismic Stations : HNG (radio-telemetry), AKG, CJB, IOY (on-site logging)
Tiltmeters : H283, KSR (on-site logging)
Geomagnetic Stations : N2, E1, S0, SE (proton; on-site logging)

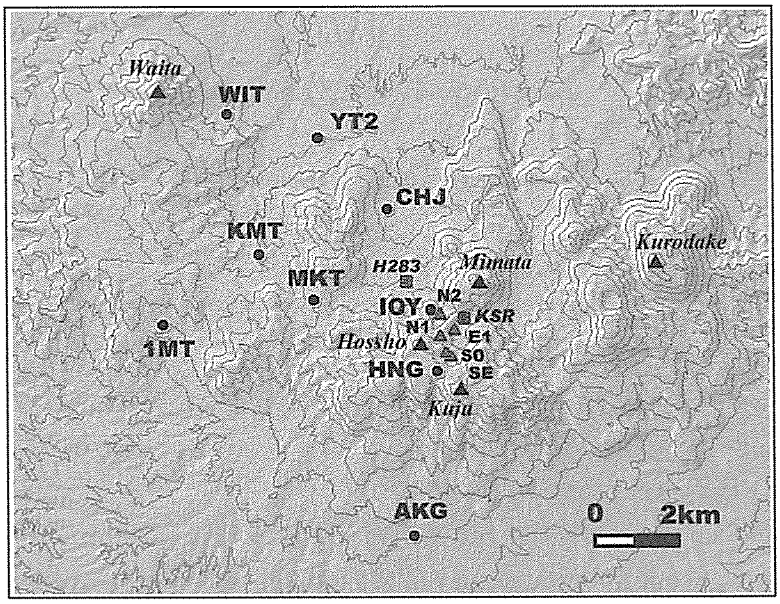

Seismic, geodetic and geomagnetic stations in Kuju area.

Central Kyushu regional network

Seismic Stations : AVL(6), MAK, NBR, MKN, HDK, TAT, MGR (online telemetry)
ASJ, HNY, SKM, KBM, TRM (dial-up)

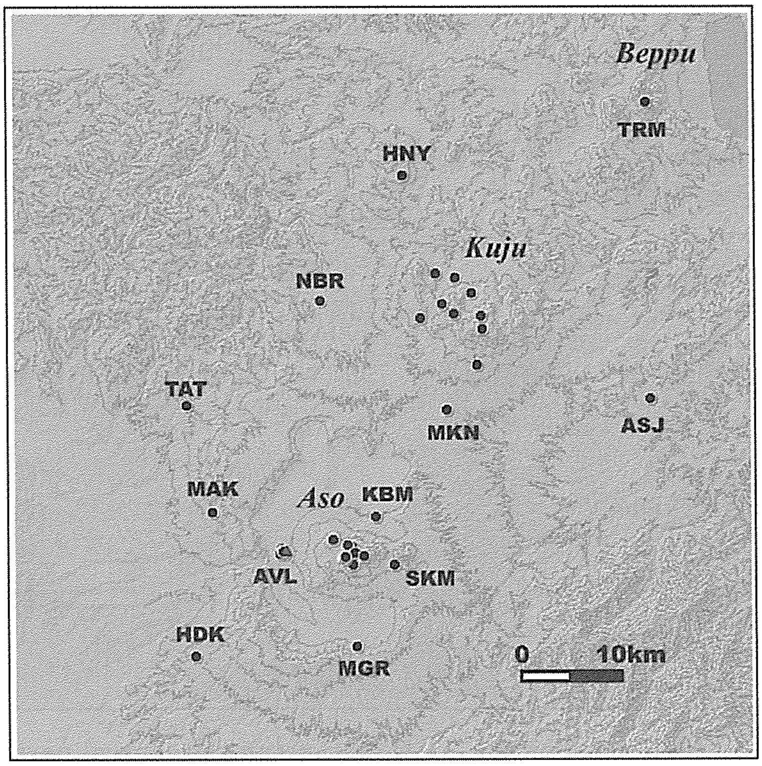

Seismic network in the central Kyushu.

装置・設備　Instruments and Facilities

装置　Instruments

【別府】

ICP 発光分光分析装置
波長分散型電子プローブマイクロアナライザー（海洋科学技術センターに貸し出し中）
エネルギー分散型電子プローブマイクロアナライザ
波長分散型蛍光 X 線分析装置
エネルギー分散型蛍光 X 線分析装置
粉末 X 線回折装置
液体シンチレーションシステム
イオンクロマトグラフ
ガスクロマトグラフ
自動滴定装置
ピストンシリンダー型高圧発生装置
ICP-MS 用レーザーアブレーション装置
四重極型 ICP-MS 装置
表面電離型質量分析装置
外熱式ダイアモンドアンビル
ラマン顕微鏡
フーリエ変換型近赤外分光光度計
赤外顕微鏡
加熱ステージ

【阿蘇】

阿蘇，九重火山連続地震観測システム
地殻変動観測坑道
孔中温度観測システム
ビデオ映像監視システム
プロトン磁力計
フラックスゲート磁力計
地磁気絶対測定システム
傾斜計
可搬型地震計（広帯域，短周期）
人工震源車
重力計
超伝導重力計
地磁気地電流測定装置（広帯域型 ULF，ELF，VLF 型）
光波測距儀
水準測量システム（自動読み）

【Beppu】

ICP emission Spectrometer
Wavelength dispersive electron microprobe (lent to JAMSTEC)
Energy dispersive electron microprobe analyzer
Wavelength dispersion type X-ray Fluorescence analyzer
Energy dispersionty type X-ray Fluorescence analyzer
Powder X-ray　diffractometer
Liquids scintillation system
Ion chromatography
Gas chromatography
Automatic titration system
Piston cylinder type high pressure apparatus
Laser ablation system
Inductively coupled plasma mass spectrometer (ICP-MS)
Thermal ionization mass spectrometer（TIMS）
Externally heated diamond anvil cell
Raman microscope
FT-NIR spectrometer
IR microscope
Heatings stage

【Aso】

Continuous seismic monitoring system for Aso and Kuju Volcanoes
Observation tunnel for ground deformation
Borehole temperature monitoring system for Aso
Video monitoring system of Aso and Kuju Volcanoes
Proton and fluxgate magnetometers
Geomagnetic absolute measurement system
Tiltmeters
Portable seismometers (broadband short period)
Car-mounted seismicsource
Gravimeters
Super-Conducting Gravimeter
Magneto-Telluric measurement system （broad-band type, ULF, ELF, VLF-band）
Electronic distance measurement system
Leveling survey system (automatic reading)

設備　Facilities

岩石粉砕・鉱物分離室

パックミル・ディスクミルによる岩石粉砕やアイソダイナミックセパレータによる鉱物分離を行う．

器具洗浄室

実験に用いる器具の洗浄を行う．クリーンドラフト1台・ドラフト1台・イオン交換筒・Milli-Qが設置されている．

クリーンルーム

ニューロファインフィルターを設置し極力金属使用を控えた設計で，クラス100のクリーン度を達成している．Sr・Nd・Pb同位体比分析のための化学処理（試料の分解・イオン交換クロマトグラフィーによる目的元素の抽出）を行っている．

地下観測坑道（阿蘇火山地殻変動観測坑道）

阿蘇中岳第一火口から南西1kmの，地下30mに設けられた，直角三角形の水平坑道で，1987年度に竣工した．現在は，水管傾斜計（25m），伸縮計（20，25m），短周期地震計，長周期地震計，広帯域、地震計、強震計、超伝導重力計が設置されている．

火山研究センター構内地震観測システム

火山研究センター構内では，従来からトリパタイトによる地震観測を行ってきたが，平成13年度に，ノイズ低減の為，約200mのボーリング孔を4本掘削し，孔底に地震計を導入した．これにより，S/N比は大幅に改善され，従来識別できなかった中岳の長周期微動が検出されるようになった．また，ボーリングコアを採取したことにより，研究センターの丘，高野尾羽根（たかのおばね）火山について地質学的に新たな知見が得られつつある．これは，阿蘇中央火口丘の噴火史を研究する上でも貴重な資料である．

An analysing system of trace element and isotopic compositions

Radiogenic isotope and trace element compositions of natural samples (e.g. rock and water, etc.) provide us important information about source materials of a sample, generating processes from the sources and age of the sample formation. Therefore isotope and trace element compositions of natural samples are important for investigating the phenomena accompanied with material transfer, such as magma genesis and mantle-crust recycling. Hence, we established an analytical method for determining trace elements by using an inductively coupled plasma mass spectrometer (Fig. 1) and for isotopic ratios of Sr, Nd and Pb: employing a thermal ionization mass spectrometer (Fig. 2) at Beppu Geothermal Research Laboratory (BGRL). The system presented here is made from collaboration with Institute for Frontier Research on Earth Evolution. The methods of chemical preparation for the each analysis were also established. All our chemical procedures are performed under a clean environment, which is basically handmade with our original design (eg. Fig. 3). The analytical methods established at BGRL realize the precise analyses of trace and isotopic compositions of ultra trace amounts of the samples (Fig. 4). Furthermore, we are developing methods to realize the mass production of the assay tests. By employing the described analytical methods, we are progressing with the study of magma genesis and material transfer in the mantle, etc.

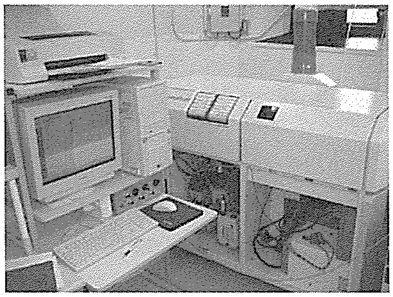

Fig. 1. Inductively coupled plasma mass spectrometer

Fig. 2. Thermal ionization mass spectrometer

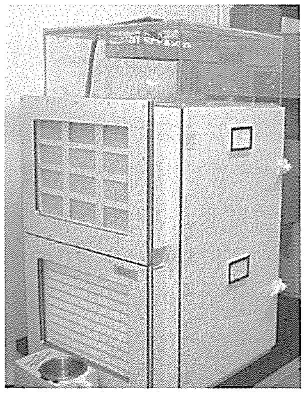

Fig. 3. Sample evaporation system under the ultra clean environment

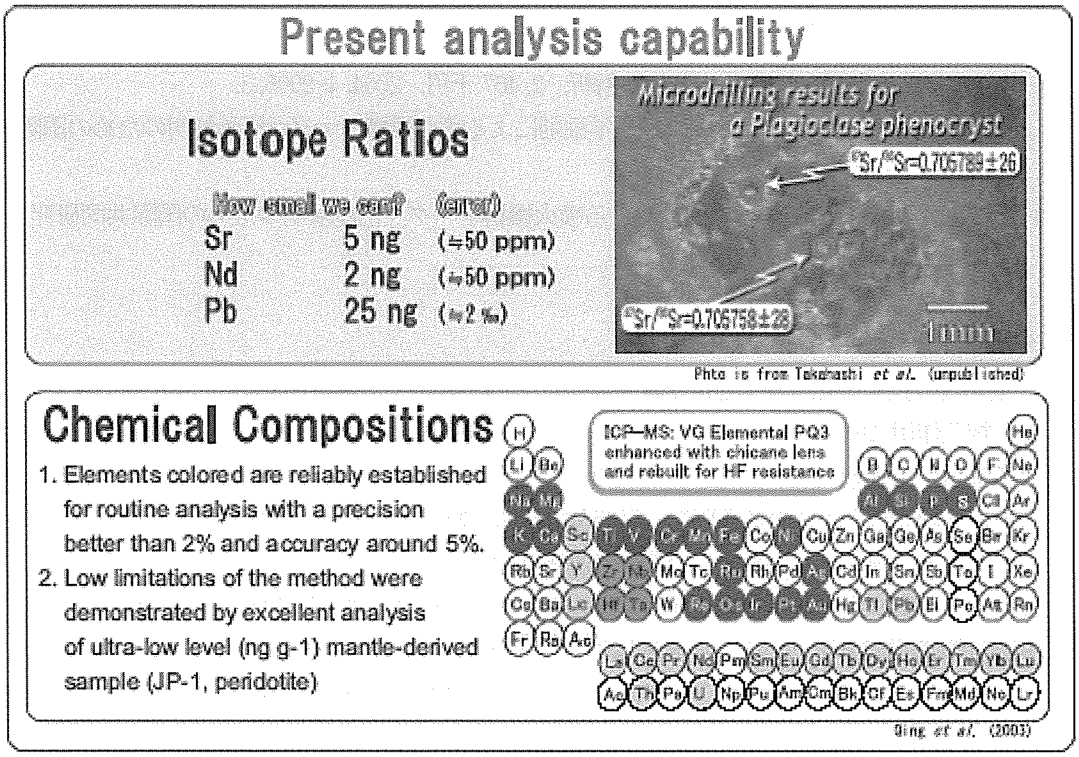

Fig. 4. Analytical method for isotopic and trace element compositions established at BGRL

研究費　Funding

科学研究費補助金

基盤研究（A）（1）大倉敬宏（分担），火山流体のモニタリングと深部マグマ上昇メカニズムの解明，研究代表者：川勝　均，H16 年度直接経費　8,700 千円

基盤研究（A）竹村恵二（分担）（代表：京都大学教授　岡田篤正），課題名：長大活断層のセグメント区分・地下構造・活動履歴の再検討と大地震予測の総合的研究．（26,650 千円/40,350 千円）

基盤研究（B）（2）　田中良和、空中磁気測量による火山性磁場変動の検出、3,800 千円

基盤研究（C）大沢信二（代表）「水文化学的手法による火山湧水からのマグマ起源二酸化炭素の流出フラックスの評価」500 千円

特定領域研究(2)・４２２　鍵山恒臣，15038204，赤外・可視映像解析による噴煙の時間変動と噴火発生場の応答時間に関する研究，1,200 千円，2004.4-2005.3.

特定領域研究（2）田中良和、火山爆発の発生場と発生過程、52,700 千円

萌芽研究　大倉敬宏(分担)，いくつかの地域で外帯低周波微動が起こらない理由，研究代表者：瀬野徹三，H16 年度直接経費　800 千円

萌芽研究　山本順司（分担），顕微ラマン分光法による流体包有物一粒からの炭素同位体比測定法の開発，研究代表者：鍵裕之，H16 年度直接経費　4,000 千円

受託研究

鍵山恒臣：科学技術振興調整費，雲仙火山：科学掘削による噴火機構とマグマ活動解明のための国際共同研究，電磁気探査による火山体構造解析，2,467 千円，2004.4-2005.3.

竹村恵二：科学技術振興調整費，雲仙火山：科学掘削による噴火機構とマグマ活動解明のための国際共同研究 1,090 千円

田中良和：科学技術振興調整費，科学掘削による噴火機構とマグマ活動解明のための国際共同研究、1,626 千円

共同研究等

大沢信二：産業総合技術研究所深部地質環境研究センター研究費「火山体水理構造と地下水 - 深部起源ガス相互作用に関する研究」2,332 千円

齋藤武士：東京大学地震研究所　特定共同研究 B（プロジェクト名：活火山における噴火様式の時代的変遷と長期的噴火予知の基礎研究，研究分担課題：雲仙火山の鉄チタン酸化物の岩石磁気学的解析による溶岩ドームの噴火・崩壊機構の解明，220 千円

柴田知之：九電産業株式会社環境部研究助成「熱水のストロンチウム同位体組成の測定」150 千円

杉本健：東京大学地震研究所，平成１６年度共同利用（一般共同研究）480 千円

竹村恵二：21 世紀 COE プログラム（代表：京都大学教授　余田成男）分担，課題名：活地球圏の変動解明

竹村恵二　京都大学防災研究所一般共同研究　（代表：三村　衛）880 千円

竹村恵二　経済産業省原子力保安院　「地表断層の形状の三次元化及び高精度化と深部起震断層との相関」（代表：岡田篤正）

田中良和：大分県温泉調査研究会、地磁気変化を利用した地熱の推移に関する研究、70 千円

田中良和：産学官連携イノベーション創生経費、空中電磁、220 万円

山本順司：東京大学地震研究所，平成１６年度共同利用（一般共同研究）320 千円

教育活動　Education

学位・授業　Academics

学位審査

鍵山恒臣　（審査員）　大久保綾子　（博士　京都大学理学研究科）
大沢信二　（審査員）　山崎　一　（修士　東邦大学理学研究科）
竹村恵二　（審査員）　服部泰久　（修士　京都大学理学研究科）
（審査員）　佐々木　亮　（修士　京都大学理学研究科）
（審査員）　戸邊勇人　（修士　京都大学理学研究科）
田中良和　（主査）　大久保綾子　（博士　京都大学理学研究科）
（審査員）　井筒　潤　（博士　京都大学理学研究科）
（審査員）　韓　徳勝　（博士　京都大学理学研究科）
（審査員）　永田大祐　（修士　京都大学理学研究科）
（審査員）　藤森　徹　（修士　京都大学理学研究科）

講義・ゼミナール

（学部）
地球惑星科学 I　竹本修三・岡田篤正・竹村恵二・久家慶子
観測地球物理学演習 A　田中良和・鍵山恒臣・須藤靖明・大倉敬宏・宇津木充・里村雄彦・藤森邦夫・西憲敬・古川善紹
観測地球物理学演習 B　竹村恵二・大沢信二・堤浩之・柴田知之・川本竜彦・山本順司
グローバルテクトニクス　田上高広・古川善紹
地球熱学　竹村恵二・鍵山恒臣・大沢信二・古川善紹
火山物理学 I　古川善紹
火山物理学 II　田中良和・須藤靖明・大倉敬宏・石原和弘・
陸水物理学　大沢信二
課題演習 D3：地下構造と活構造・地表変動　岡田篤正・竹村恵二・堤　浩之・赤松純平・福岡　浩・岩田知孝
課題研究 D4：地球熱学　古川善紹・柴田知之・川本竜彦・宇津木充・山本順司
課題研究 D6：気象学総合演習　余田成男・石岡圭一・内藤陽子・大沢信二・林泰一・石川裕彦
課題研究 D7：地球磁気圏の構造と波動現象　町田忍・家森俊彦・田中良和・亀井豊永・竹田雅彦・齋藤昭則・能勢正仁
課題研究 T8：地表変動・固体地球物理・火山物理　岡田篤正・竹村恵二・須藤靖明・堤　浩之・入倉孝次郎・佐々恭二
課題研究　地震と電磁気の関係

（大学院・修士課程）
第四紀地質学　竹村恵二
活地球固体圏特論 B　平島崇男・小畑正明・竹村恵二・古川善紹・大沢信二・中西一郎

活地球変動・結合論B　増田富士雄・竹本修三・福田洋一・竹村恵二
地球熱学・地熱流体学I　田中良和・大沢信二
地球熱学・地熱流体学II　竹村恵二・須藤靖明・古川善紹・大倉敬宏
応用地球科学ゼミナールI　岡田篤正・竹村恵二・堤浩之・小松原　琢
応用地球科学ゼミナールII　岡田篤正・竹村恵二・堤浩之・小松原　琢
地球惑星科学特殊研究（修士論文）
活地球圏科学実習

（大学院修士課程および博士後期課程）
地球熱学・地熱流体学ゼミナールI　田中良和・大沢信二・川本竜彦・柴田知之・山本順司
地球熱学・地熱流体学ゼミナールII　竹村恵二・須藤靖明・古川善紹・大倉敬宏
応用地球科学ゼミナールI　岡田篤正・竹村恵二・堤浩之・小松原　琢
応用地球科学ゼミナールII　岡田篤正・竹村恵二・堤浩之・小松原　琢
地球生物圏史セミナー　増田富士雄・前田晴良・竹村恵二・大野照文

野外実習
観測地球物理学演習A　（7月31日—8月3日）
観測地球物理学演習B　（8月4日—6日）
地質鉱物学野外実習　（3月18日—19日）

講義（他大学）ほか
鍵山恒臣　東京大学理学系研究科地球惑星科学専攻，火山科学1
鍵山恒臣　火山学・火山砂防工学集団研修講義(JICA)，火山熱学
竹村恵二　愛媛大学理学部，集中講義：地殻物質学特別講義I

セミナー　Seminars

地球熱学ゼミナール
2004年
4月　7日　竹村恵二・大沢信二・柴田知之・山本順司　21世紀COE「活地球圏の変動解明」に関する研究紹介
4月　28日　芳川雅子「早池峰・宮守かんらん岩体に記録された島弧下マントルでのメルト形成過程」
5月　26日　宮崎隆「南インド大陸下エンリッチリソスフェアマントルの形成と進化」
6月　2日　Jianguo Du　「Measurement for REE of eclogite in Dabie Mt.」
6月　23日　柴田知之　「微量元素・同位体組成を用いた東北日本孤蔵王火山に共存するソレアイト・カルクアルカリ両系列の起源物質の推定」
7月　7日　竹村・陳・柴田・中川：　阿蘇カルデラ起源火山灰の岩石学的特徴と化学組成、広域分布
7月　7日　柴田・陳・芳川・竹村：　阿蘇火砕流堆積物の同位体組成
7月　7日　由佐・柴田・芳川：　別府地域における温泉水層への海水進入
7月　7日　大沢・須藤・宇津木・馬渡・吉川・網田・山田：　阿蘇山湯溜まりの色と火山活動に関する研究
7月　7日　川本・西村・竹村：　雲仙普賢岳噴火前含水量の推定

7月　7日　竹村・大倉・古川・馬渡：　別府地域の地震
9月　24日　Jianguo Du　「My Experience in Beppu」
10月　6日　竹村恵二　「湖沼堆積物：火山活動・気候変動の記録」
10月　15日　山田誠「火山地下水システムへの深部起源CO_2付加過程に関する同位体水文学的研究」
10月　27日　頼勇「流体包有物の様々な成因と起源」
11月　12日　川本竜彦「沈み込み帯におけるケイ酸塩を溶かしこんだ水の性質の圧力変化」
11月　16日　山本順司「ヘリウムパラドックスを解いた！？」
12月　8日　網田和弘「地熱環境下における地下水流動の数値実験」
12月　22日　柴田知之「別府での同位体分析法」

2005年

1月　12日　西村光史「マグマ溜まり中の結晶沈降と再平衡化による微量元素の振る舞い」
1月　26日　斉藤武志「斉藤の研究、イントロダクション-マグネティックペトロロジーと赤熱温度測定」
1月　26日　杉本健「雲仙火山マグマ供給系の岩石学的モデル」

<u>特別セミナー・BGRLセミナー</u>

2004年

5月　19日　長谷英彰（京都大学）「阿蘇山における自然電位測定」
5月　26日　Kang Chunli「Satellite remote sensing infra-red features of strong earthquakes」
5月　28日　宇都浩三（産業技術総合研究所）「九州背弧火山活動の時空分布と雲仙科学掘削」
12月　17日　小林記之氏（京都大学）「九州中部肥後変成帯に産する高度変成岩及びミグマタイトに関する岩石学的研究」

2005年

1月　26日　平野直人　（東京工業大学）「沈み込む海洋プレート上で活動する火山ープレート屈曲と亀裂に沿ったアセノスフェア溶融物ー」
2月　9日　井上和久　（京都大学）「阿蘇火山、Aso-3火砕噴火サイクル噴出物の岩石学的性質」
3月　8日　新正裕尚（東京経済大学）「西南日本前弧の中新世火成岩についての総論と最近の展開」
3月　25日　鍵裕之（東京大学）「微量の希土類元素の存在状態と希土類元素パターン」

<u>AVLセミナー</u>

2004年

12月　14日　後藤秀作「非浮揚性熱水プルームの形成における低温熱水の寄与　ー大西洋中央海嶺TAG熱水マウンドでの例ー」
12月　21日　中坊真「九重火山の地盤変動　ー茂木モデル圧力源の移動についてー」

2005年

2月　15日　吉川美由紀「中部九州の地震波速度構造および今後の方針」
3月　15日　森健彦「二酸化硫黄放出量計測器（DOAS）の開発と実践」

学会活動　Activities in Scientific Societies

川本竜彦
Geochemical Journal 誌　Associate Editor
大倉敬宏
火山学会編集委員
大沢信二
日本温泉科学会：理事，広報・国際交流委員長
日本地熱学会：編集委員
日本水文科学会：評議員，奨励賞選考委員
竹村恵二
日本第四紀学会評議員
日本地質学会地方地質誌九州地方編集委員会委員
日本地質学会科学研究費委員会委員
日本第四紀学会論文賞受賞候補者選考委員

社会活動　Public Relations

鍵山恒臣
火山噴火予知連絡会委員
東京都三宅島活動検討委員会委員
宮崎県防災会議地震専門部会専門委員
雲仙科学掘削研究運営委員会委員
学術会議地球物理学研連火山分科委員
核燃料サイクル開発機構地殻温度構造ワーキンググループ，委員
火山噴火予知研究協議会，委員
火山噴火予知研究委員会，幹事
JICA 研修「火山学・火山砂防工学」，カリキュラム委員および講師
南九州の火山防災を考える−霧島，桜島，そして小説「死都日本」−，講演，火山観測から見た火山噴火と現代社会，宮崎, 11.06, 2004.
霧島火山群における火山砂防事業に関する検討会（国土交通省九州地方整備局宮崎河川国道事務所），講演，火山噴火と観測・情報，都城, 08.09, 2004.
霧島火山群における火山砂防事業に関する検討会（国土交通省九州地方整備局宮崎河川国道事務所），講演，御鉢の火山活動把握のむずかしさ −長期に活動を休止している火山への戦略−，宮崎, 01.29, 2004.
大沢信二
大分県温泉調査研究会理事
大分県温泉監視調査委員会委員

京都大学地球熱学研究施設一般公開講演講師

竹村恵二

『第 19 期日本学術会議地質科学総合研究連絡委員会第四紀学専門委員会』委員

文部科学省　科学技術政策研究所　科学技術動向研究センター　専門調査員

『関西国際空港（二期地区）地盤挙動調査委員会』委員

『京都府地域活断層調査委員会』委員

『地震調査研究推進本部地震調査委員会北日本活断層分科会』委員

『大阪府地下構造調査委員会』委員

『大分県地域活断層調査委員会』委員

『三重県伊勢平野地下構造調査委員会』委員

『三重県地域活断層調査委員会』委員

『科学技術振興調整費（雲仙火山:科学掘削による噴火機構とマグマ活動解明に関する調査）調査推進委員会』第二分科会委員

平成 17 年(2005) 1 月 21 日（木）別府語り部の会　講習講師「別府の温泉・火山・活断層」

平成 16 年 12 月 2 日　NZ　IGNS での講演　Takemura, K.: Recent Progress on active fault research and paleoseismology in Japan. Inst. Geology & Nuclear Sciences, Lower Hutt, New Zealand

平成 16 年(2004)　10 月 1 日（金）関西地質調査業協会講演　「近畿地方の堆積盆地の形成・堆積過程と活構造」

平成 16 年(2004)8 月 31 日（火）台湾中央研究院での講演　Takemura, K.：Recent progress on active fault research and paleoseismology in Japan after 1995 Kobe Earthquake.　Academia Sinica, Institute of Earth Sciences, Taiwan

平成 16 年(2004)8 月 17 日（木）別府語り部の会　講習講師「別府の温泉・火山・活断層」

田中良和

科学技術・学術審議会専門委員(測地学分科会)

雲仙火山：国際共同研究第二分科会委員

防災研究所研究担当

火山噴火予知研究協議会委員

科学研究費委員会専門委員

一般公開報告　Openhouse

【別府】

京都大学大学院理学研究科附属地球熱学研究施設では，平成１６年７月２８日（水）午後４時ー午後５時に研究施設に隣接するニューライフプラザ２階視聴覚室にて一般市民向け公開講義を行った．また，同日夜間（１９時ー２２時）に施設のライトアップを行い，一般市民とより親密に触れ合う場を設けた．翌日の７月２９日（木）は午前９時ー午後４時まで研究施設の一般公開を行った．公開講義には３５名の市民に来場して戴き，一般公開には９５名にお越し戴いた．

一般公開・公開講義の運営は，昨年度までと同様に当研究施設で働く職員と学生の協力を得て行い，実施形態や準備，広報，片付け，反省会なども昨年度までの方法にほぼ従った．

今年度の一般公開で新しく導入された点は，（１）最先端研究紹介コーナー設置と（２）研究施設のライトアップである．

（１）　最先端研究紹介コーナー

学会等で実際に使われたポスターなどを使って，最先端の研究を紹介するコーナーを設けた．英語で書かれたポスターも掲示されていたため一般市民に理解してもらうのは難しいものもあったが，その分，研究の最先端の雰囲気を味わってもらえたと想像している．

（２）　研究施設のライトアップ

公開講義が行われた日の夜間（１９時ー２２時），研究施設のライトアップを行った．十数人の市民に参加して戴いた．

特別講演

ニューライフプラザの２階視聴覚室を利用して，７月２８日午後４時から大沢助教授による公開講義を行った．演題は「別府地域の湧水の科学」．参加者は３５名．１時間の予定であったが，大分県民の湧水への好奇心は旺盛で，多くの質問があり予定時間を超過する事態となった．その評価はアンケート結果にも反映され，かなり高度な内容に踏み込んでいたにもかかわらず，分かり難いと答えた方はいらっしゃらなかった．

公開実験見学コース

７月２９日午前９時から午後４時まで研究施設の一般公開を行った．来場者は９５名．７時間の間，研究施設内で常に十数人の市民が観覧する状態であったため終始緊張感が漂っていたが，比較的時間をかけて展示物の解説を行うことができた．

公開，または提供した題材

- 研究施設紹介コーナー
- 石の輪廻転生
- 別府の石

- 顕微鏡で見る石の世界
- 砂地盤の液状化実験
- 最先端研究紹介コーナー
- 実験室見学コーナー
- 砂糖で作るマグマ
- マグマを顕微鏡で見る
- 地震計，サーモグラフィーの展示
- 展示ケース

アンケート集計結果（公開講義）

1 どちらからいらっしゃいましたか？

	別府市内	大分県内別府市外	大分県外	回答なし	合計
回答数	16	3	0	0	19
百分率	84.2	15.8	0.0	0.0	100

2 年代を教えて下さい

	6歳未満	6-15歳	16-19歳	20-39歳	40-59歳	60-79歳	80歳以上	合計
回答数		2		4	3	10	0	19
百分率	0.0	10.5	0.0	21.1	15.8	52.6	0.0	100

3 どのようにして今回の公開講義を知りましたか？

	ポスター	市報	新聞	テレビ	人に聞いて	その他	なし	合計
回答数	2	5	6	1	6	0	0	20
百分率	10.0	25.0	30.0	5.0	30.0	0.0	0.0	100

4 今回の公開講義の感想をお聞かせ下さい

	分かりやすかった	普通	分かりにくかった	合計
回答数	13	6	0	19
百分率	68.4	31.6	0.0	100

アンケート集計結果（一般公開）

1 どちらからいらっしゃいましたか？

	別府市内	大分県内	別府市大分県外	国外	回答なし	合計
回答数	45	13	2	2		62
百分率	72.6	21.0	3.2	3.2		100

2 年代を教えて下さい

	6歳未満	6-15歳	16-19歳	20-39歳	40-59歳	60-79歳	80歳以上	合計
回答数	3	23	1	9	10	17	0	63
百分率	4.8	36.5	1.6	14.3	15.9	27.0	0.0	100

3 どのようにして今回の一般公開を知りましたか？

	ポスター	市報	新聞	テレビ	人に聞いて	その他	なし	合計
回答数	14	13	19	0	15	1	1	63
百分率	22.2	20.6	30.2	0.0	23.8	1.6	1.6	100

4 昨年以前の一般公開にお越しになられたことがありますか？

	はい	いいえ	回答なし	合計
回答数	6	54	2	62
百分率	9.7	87.1	3.2	100

5 今回の一般公開の全体的な感想をお聞かせ下さい

	非常に良かった	良かった	普通	良くない	非常に良くない	回答なし	合計
回答数	28	25	7		1	1	62
百分率	45.2	40.3	11.3	0.0	1.6	1.6	100

6 今回の一般公開の各イベントの感想をお聞かせ下さい

		良かった	普通	良くない	覚えていない	なし	合計
別府の石	回答数	40	9	0	3	10	62
	百分率	64.5	14.5	0.0	4.8	16.1	100
石の輪廻転生	回答数	26	17	0	6	13	62
	百分率	41.9	27.4	0.0	9.7	21.0	100
砂地盤の液状化現象	回答数	42	11	0	0	9	62
	百分率	67.7	17.7	0.0	0.0	14.5	100
顕微鏡で見る石の世界	回答数	34	13	0	1	14	62
	百分率	54.8	21.0	0.0	1.6	22.6	100
砂糖で作るマグマ	回答数	39	11	0	1	11	62
	百分率	62.9	17.7	0.0	1.6	17.7	100

来年度の一般公開・公開講義において改善すべき点や提案

今年度の一般公開・公開講義の反省会において様々な意見が交わされた．議論の中心は，一般公開・公開講義を開催する意義についてであった．開催当初は一般市民にとって閉鎖的になりがちな研究施設を開放し，研究教育財源を提供して下さっている一般市民に知識の還元を行う事が目標であった．例年行っているアンケート結果を概観するとこの目標は達成されたように思われる．なぜなら，全体的な感想は概ね高い評価を得ているにもかかわらず，入場者数は年々低下しており，今年は１００人を下回っている．しかもリピーターの割合は１０％以下であり，これらの結果は，一度，当研究施設

を見学された方はある程度満足されたことを示していよう．
施設の一般公開が始まって５年目となる来年度は，一般公開と公開講義の意義を根本から問い直し，社会貢献・還元の一環としてこのような事業を続けるのであれば，一般市民の要望により適合した目標を再設定する必要があろう．

その他，反省会や事前の会議にて交わされた意見を下に記す．

- 準備期間を多く設けるため，年度初めに初会合を行う．
- 一般公開担当者ではなく担当委員会のような複数の人員を擁するチームを結成し機動力を増す．
- 一般公開前に勉強会を行い，それぞれの出し物を相互に説明できるようにするのはどうか．
- ライトアップへの参加者が少ない．別府市の祭りに組み込む等の工夫をするべき．
- 一般公開・公開講義を各一日ずつ行ったが，一日で公開講義・一般公開・ライトアップを行う事も可能であろう．時期や曜日とともに検討すべき事項であろう．
- 「研究施設一般公開・公開講義」という言葉は一般市民にとって解り難い．気楽に楽しめる催しである事が解るよう工夫するべき．
- 広報手段として，今回から導入した A0 ポスターの効果が大きかった．来年度はもう少し多くの A0 ポスターを貼り出したらどうだろうか．
- 最先端研究紹介コーナーは観衆にとって難解なものも多くあった．学会で使用したものであることや解説を充実させるべきであろう．
- 当研究施設の研究以外の実態に関する質問を多く受けた．構成員数や職，京大本学との関係など，基本的な疑問に答える場を用意したらどうだろうか．
- 一昨年度の報告書で提案された若年齢層の参加者増はかなえられなかった．教育委員会を通したポスター配布や明豊学園に向けて掲示したポスターも効果がなかったようである．中学・高校の理科教師への広報や出張講演等の努力が必要であるかもしれない．
- アンケート結果によると，温泉や火山，地震に関する関心が高いことが窺える．今年度まで，一般公開・公開講義とも建物内で行ったが，人数を絞って屋外で巡検を行うことも検討するべきではなかろうか．

一般公開・公開講義開催を告知するホームページを見て来られた方もおられた．来年度も開催日を告知するページを早めに立ち上げるべきであろう．

昨年同様，別府市教育委員会，別府市役所記者クラブ，新聞各紙，テレビ各局のご協力を戴いた．ここに御礼申し上げる．

2004 年度地球熱学研究施設（別府）一般公開・公開講義担当　山本順司

【阿蘇】

オープンハウス報告書（阿蘇）

１．目的

一般市民，特に地域住民・関係機関に，当センターの活動内容を広く知ってもらうことで，センターに対する関心・理解を得る．また，社会への学術的知識の還元・啓蒙をはかる．

２．開催日時

平成１６年１０月２３日（土）　９：３０～１６：００

３．内容

● ポスター展示（約３０点）による研究内容の紹介・火山学の一般向け解説

● 公開実験

・「地震計のデモンストレーション」

・「サーモグラフィーを使った記念撮影」

・「火山を作ろう！」

● 施設備品展示（新旧地震計等各種観測装置の展示・解説）

● 火山に関するビデオの上映

● 火山に関する書籍の閲覧供与

● パソコンによる展示

・「九州の地震活動リアルタイムモニター」

・「阿蘇火山の微動振幅レベルモニター」

● 特別講演（午前：須藤，午後：田中　各３０分）

● 見学者パンフレット（大人用，子供用）を配布

● お年寄りの来場者を考慮し休憩室を設置

４．社会告知の方法

● Ａ４・Ａ３版ポスター・チラシを配布・掲示

配布先：赤水郵便局・アゼリア・阿蘇駅・阿蘇火山防災協議会・阿蘇火山博物館・阿蘇青年の家・阿蘇山測候所・一の宮町役場・井出酒店・ウィナス・株式会社キンキ・河陽郵便局・九州東海大学・熊本大学・グリーンストック・セブンイレブン・たわら屋・地球熱学研究施設・地球物理学教室・長陽村観光協会・長陽村教育委員会・長陽村役場・東工大草津白根火山観測所・ニコニコドー・白水村役場・花阿蘇美・マグマ食堂・民宿阿蘇の湯・ルナ天文台（５０音順）

● 陽の長い一日の村美術館（長陽村秋季イベント）総合パンフレット掲載

● 阿蘇テレワークセンターメールマガジン

● 火山研究センターホームページによる公示

5．見学者に関する集計

来場者数：８７（大人６３小人２４）人

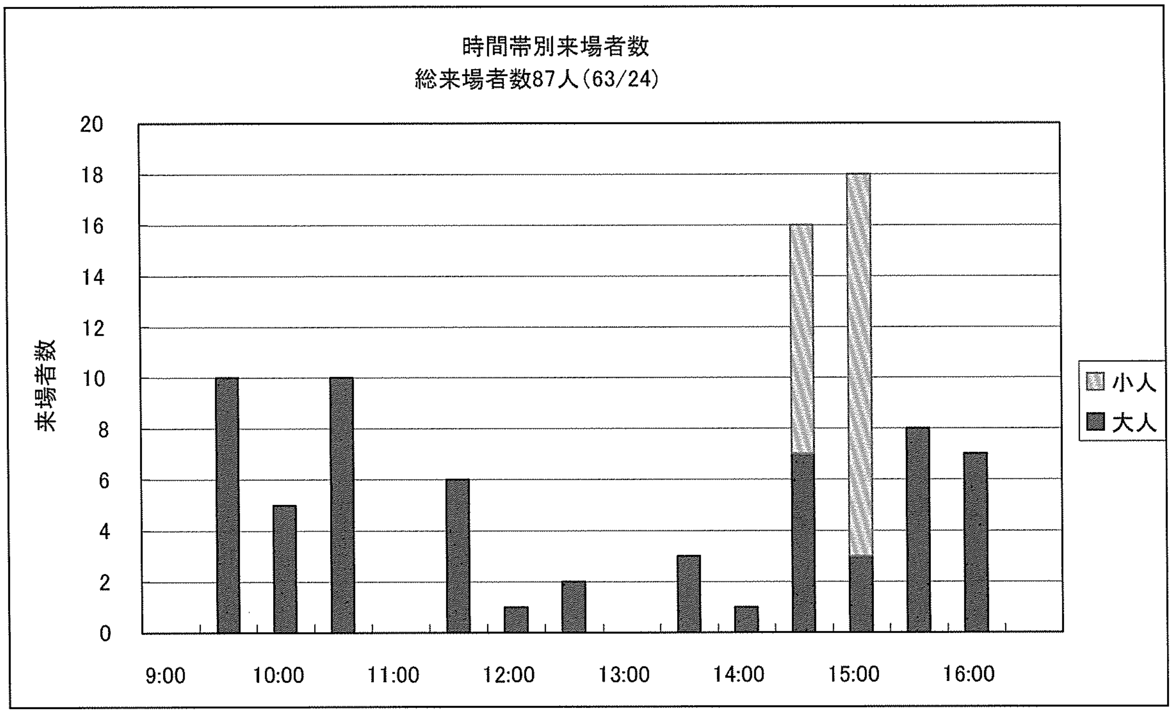

Q1．どちらからいらっしゃいましたか？

	阿蘇郡内	熊本県内阿蘇郡外	熊本県外	回答なし	合計
回答数	21	18	4	11	54
百分率	38.9%	33.3%	7.4%	20.4%	100%

Q2．年代を教えてください

	１０代	２０代	３０代	４０代	５０代	６０代以上	合計
回答数	0	16	9	17	4	7	53
百分率	0%	30.2%	17.0%	32.1%	7.5%	13.2%	100%

Q3．どのようにして今回の一般公開を知りましたか？

	友人・知人	インターネット	新聞・雑誌	ポスター	チラシ	その他	合計
回答数	29	1	2	15	2	5	54
百分率	53.7%	1.9%	3.7%	27.8%	3.7%	9.4%	100%

Q４．特別講演は面白かったですか？

	面白かった	つまらなかった	どちらでもない	聞かなかった	合計
回答数	31	0	2	23	56
百分率	55.4%	0%	3.6%	41.1%	100%

Q５．これまで火山研究センターに興味はありましたか？

	あった	なかった	どちらでもない	合計
回答数	33	14	4	51
百分率	64.7%	27.5%	7.8%	100%

Q６．一般公開に参加して火山研究センターに興味をもたれましたか？

	もった	もたなかった	どちらでもない	合計
回答数	49	0	2	51
百分率	96.1%	0%	3.9%	100%

６．まとめ

今年度も例年にならい長陽村のイベントにあわせて１０月に開催した．昨年度は、阿蘇郡内の小学校行事と日程が重なってしまい地元小学生の参加ができなかったという反省から，一般公開の日程を決定するにあたって事前調査をおこない調整をはかった．その結果，来場者８７名に対して約３割にあたる２４名の小学生（１０歳以下）に参加してもらうことができた．今年も昨年同様に火山工作をおこない，自分で作成したオリジナル火山をお土産として持ち帰ってもらった．

次に，「どのようにして今回の一般公開を知りましたか？」の問に対して，回答の半数以上が友人・知人からの情報によって今回の一般公開を知ったと回答しており，言い換えれば口コミの情報を得て来場したということになる．この現象は，当センターが一般の方々に広く認知されつつあることの現れであり、我々の掲げた目的に着実に近づいていることを示唆している．また，これまで当センターに興味のなかった方々が，今回の一般公開に参加したことで当センターに興味を持ったと回答しており，内容についても一定の評価をいただいたと認識している．

反省点として，特別講演の参加者が少なかったことがあげられる．事前に展開するポスターやチラシなどの告知の仕方に若干の修正や工夫も必要であるが，講演の時間帯に来場できない方や事前に講演の情報を知らない方にも聴いていただけるような工夫も必要である．また，アンケートの意見・要望で「パンフレットをもう少し充実してほしい」というのが一番多かった．この点については，意見を厳粛にうけとめ，次年度以降に内容の見直しが必要である．

最後にアンケートに回答していただいた方々の感想をいくつか紹介する．

- 地道な研究・観測がなされていることに感謝します．
- いつか来てみたいと思っていました．ありがとうございました．
- 色々な研究者の個性などがわかって興味深かったです．
- センターの大切さ，すごさ等すべてにビックリしました．いい勉強をさせていただきました．

・ ４０数年前，父親と一緒に見学に来たことを懐かしく思い出しました．
・ 建物が古い．もっと近代的に．
・ 重厚な建物で面白い器具があり，学生さんの説明が面白かった．
・ 阿蘇火山のことがわかって楽しかった．
・ 初心者にも易しく感じ，興味がわきました．

以上

火山研究センター　吉川　慎

来訪者　Visitors

【別府】

平成16年

4月13日一14日	北田奈緒子・伊藤浩子（地域地盤環境）
4月19日	京大理学部桑原経理掛長，河田主任
4月27日	平島崇男　ほか院生・学生5名（京大・地質学鉱物学教室）
4月28日	永川（基礎地盤コンサルタント），井上元宏（毎日新聞大分支局），古川正巳（別府市・語り部の会），松山尚典（応用地質九州）
4月30日	井上元宏（毎日新聞大分支局），秦　（佐伯建設）
5月15日一30日	康　春麗（中国地震局）
5月26日	大分市敷戸小学校長
6月2日	松山尚典（応用地質九州）ほか2名
6月 4日一7月 1日	東邦大学　山崎　一
6月25日	日野雄二（脇屋商会）
7月 9日一10日	北田奈緒子（地域地盤環境）
8月 2日一4日	観測地球物理学実習B　学生・院生17名
8月12日一13日	IFREE：巽好幸・羽生毅
8月24日一 9月 6日	東邦大学　山崎　一
8月30日一 9月 6日	東邦大学　渡邊康平・堀　真和
9月 2日一 4日	IFREE：鈴木勝彦
9月 3日一 6日	東邦大学　高松信樹
9月25日一30日	平島崇男・小林・松本（地質学鉱物学教室）
9月27日一28日	東京大学理学系研究科：鍵裕之
10月12日一22日	東邦大学　堀　真和
10月12日	JAMSTEC　坪井・鈴木勝彦ほか　１０名
10月31日一11月4日	COEKAGI２１国際シンポジウム別府　余田成男・増田富士雄・ほか約100名（外国人25名程度）
11月 3日	理学研究科長　笹尾登
11月 5日	厚坂　智（凸版印刷：修学旅行現地滞在型プラン）
11月 6日	尾池和夫総長・利根川進ほか京都大学同窓生一行27名
11月12日	台湾からの観光客3名
11月12日一24日	三根崇弘（京大地球物理）
11月13日一14日	雲仙科学掘削第2分科会集会{宇都浩三（産総研）・星住英夫（産総研）・清水　洋（九大・島原）・佐久間澄夫（東北地熱）ほか5名}
11月20日一22日	余田成男・内藤陽子ほか5名（京大地球物理学教室・気象学演習）
11月20日一22日	京都大学大学院理学研究科地球物理学教室　余田成男・他7名
11月26日	河津洋一・小林祐介（大分県土木建築部）・小野啓一・湯地三子弘（別府土木事務所）・松山尚典・ほか1名（応用地質）・末廣匡基（阪神コ

	ンサルタント）
12 月 8 日一25 日	東邦大学　山崎　一・瀧井彬彦
12 月 13 日	能登征美 他 1 名　九電産業(株)環境部　分析センター

平成１７年

1 月 12 日	巽　好幸（JAMSTEC）
1 月 21 日	平島政博（経済産業省九州，アルコール課課長）ほか 1 名，嶋田至（京大財務部契約課長），田中（理学部専門員），桑原（理学部経理）
1 月 21 日	鈴木勝彦（JAMSTEC）
1 月 26 日一28 日	東京工業大学理工学研究科：平野直人
2 月 8 日—14 日	井上氏（京都大学人間・環境学研究科 M1）
2 月 25 日	鎌田高造（文部科学省地震調査研究課）
3 月 8 日	新正裕尚（東京経済大学経営学部）
3 月 12 日	豊福氏ほか 10 名（福岡県立田川高校）
3 月 18 日—20 日	増田富士雄・下林典正・松岡廣茂・ほか京大地質学鉱物学院生・学生 13 名（京都大学地質学鉱物学実習）
3 月 21 日	林田　明（同志社大），北川浩之（名古屋大），福澤仁之（東京都立大）：湖沼掘削研究打ち合わせ
3 月 22 日	巽　好幸（JAMSTEC）
3 月 25 日一26 日	鍵裕之（東京大学理学系研究科）
3 月 25 日—28 日	上田氏（京大地質学鉱物学教室）
3 月 28 日	京大宿舎掛（中野氏ほか 1 名）
3 月 30 日一31 日	東京大学海洋研究所：佐野有司

【阿蘇】

平成 16 年

3 月 31 日—4 月 2 日	金嶋氏，高木氏（東京工業大学）
5 月 18 日	気象庁地磁気観測所鹿屋出張所　2 名
6 月 21 日—25 日	大久保綾子
6 月 22 日	気象庁阿蘇山測候所 3 名
7 月 2 日—5 日	大久保氏，松本氏，及川氏（東京大学）
7 月 7 日	江竜事務職員
7 月 20 日—23 日	金嶋氏，高木氏他 2 名（東京工業大学）
7 月 22 日—26 日	火山爆発のダイナミックス一般公開展示企画関係者（東北大学谷口宏充ほか１０名）
8 月 4 日	後藤忠典，笠谷貴史（海洋技術開発機構）
8 月 9 日	古川氏，齋藤氏，石川氏（京都大学総合人間）
8 月 11 日—14 日	古川氏，宇野氏（京都大学総合人間）
8 月 23 日—28 日	神田径、高倉伸一、日浦一（京都大学）

8月25日—27日	金嶋氏（東京工業大学）
9月13日	森川氏（中日本航空）
9月13日—14日	大久保綾子（京都大学理学研究科院生）
9月26日—29日	京都大学教員8名「課題演習Ｄ２」
10月2日—6日	産業技術総合研究所，東京工業大学，東京大学火山ガス関係者7名
10月5日—11日	北海道大学，九州大学，電力中央研究所，応用地質，ネオサイエンス他空中電磁実験関係者14名
10月11日	小山内氏ほか26名（九州大学地球惑星科学）
10月12日	気象庁阿蘇山測候所3名
10月27日	鈴木亮ほか2名（佐賀大学）
12月1日—3日	及川氏（東京大学）
12月6日—8日	川勝氏（東京大学），金嶋氏，高木氏（東京工業大学）
12月13日	石原氏ほか4名「特定領域研究会」
12月14日	PHIVOLCS Ms. Esmeralda L. Banganan，上野寛（気象庁），中内庄子（JICE）
12月16日	文部科学省，京都大学「災害復旧視察」

平成17年

2月7日	茂田氏，佐藤氏（東濃サイクル機構）
2月9日	国際電子2名
2月14日	気象庁阿蘇山測候所3名
3月1日—4日	川勝氏，山本氏（東京大学），金嶋氏，高木氏（東京工業大学）
3月15日	財団法人　砂防・地すべり技術センター総合防災部　伊藤英之他1名
3月22日	大久保氏（東京大学）
3月22日—25日	孫氏，松本氏（東京大学）